

**THE STUDIES ON CYSTATIN B
DEFICIENT MICE: NEUROCHEMICAL
AND BEHAVIOURAL ALTERATIONS
IN ANIMAL MODEL OF PROGRESSIVE
MYOCLONUS EPILEPSY
OF UNVERRICHT-LUNDBORG TYPE**

ANNIKA VAARMANN



TARTU UNIVERSITY
PRESS

Department of Pharmacology, University of Tartu, Tartu, Estonia

Supervisors: Professor Aleksander Zharkovsky,
Department of Pharmacology, University of Tartu, Estonia
Dr. Allen Kaasik,
Department of Pharmacology, University of Tartu, Estonia

Reviewers: Professor Aavo-Valdur Mikelsaar,
Department of General and Molecular Pathology,
University of Tartu, Estonia
Dr. Sulev Kõks,
Department of Physiology,
University of Tartu, Estonia

Dissertation is accepted for the commencement of the degree of Doctor of Philosophy in Neurosciences on June 6, 2007 by the Council for the Commencement of Doctoral Degree in Neurosciences

Opponent: Professor Esa R. Korpi, MD, PhD,
Institute of Biomedicine, Faculty of Medicine,
University of Helsinki, Finland

Commencement: August 30, 2007

ISSN 1736–2792
ISBN 978–9949–11–657–7 (trükis)
ISBN 978–9949–11–658–4 (PDF)

Autoriõigus Annika Vaarmann, 2007

Tartu Ülikooli Kirjastus
www.tyk.ee
Tellimus nr 248

CONTENTS

LIST OF ORIGINAL PUBLICATIONS	7
ABBREVIATIONS.....	8
INTRODUCTION.....	10
BACKGROUND OF THE STUDY.....	11
Progressive myoclonus epilepsies	11
Unverricht–Lundborg disease	11
Molecular genetic basis of EPM1	12
Histopathology	14
Clinical symptoms.....	14
Cystatin B.....	16
Mammalian model of EPM1: <i>Cstb</i> -deficient mice	18
Current pathogenetic hypothesis of EPM1	20
Tryptophan metabolism and epilepsy.....	22
Glutamate, gamma-amino butyric acid (GABA) and motor coordination.	26
AIMS OF THE STUDY	29
MATERIALS AND METHODS	30
Animals	30
High performance liquid chromatography (I, II, III, V).....	30
Chemicals.....	30
Preparation of standard solutions.....	30
Preparation of mobile phase and gradient elution.....	31
Derivatization.....	31
HPLC instrumentation	31
Generation of hydrodynamic voltammograms (HDV)	33
Behavioural testing (III, IV).....	34
Behavioural response to gentle handling	34
Inverted wire-grid test.....	34
Rotarod test	34
Blood and brain samples (II, III, V)	35
Human blood samples (II).....	35
Western blotting (IV)	35
Evaluation of neuronal density (IV).....	36
Detection of neuronal death with Fluoro-Jade staining (IV).....	37
Gene expression study (V)	37
mRNA isolation and cDNA synthesis.....	37
Quantitative real time PCR	37
Statistical analysis	38

RESULTS.....	39
HPLC-EC method for the assay of tryptophan metabolites from the biological samples.....	39
Optimisation of chromatographic conditions.....	39
Hydrodynamic voltammograms.....	42
Assay performance.....	43
Tryptophan and its metabolites in the blood of EPM1 patients and <i>Cstb</i> ^{-/-} mice.....	44
Tryptophan and its metabolites in the brain of <i>Cstb</i> ^{-/-} mice.....	45
Glutamate and GABA content in the brain of <i>Cstb</i> ^{-/-} mice.....	46
The expression levels of vesicular glutamate and GABA transporters in the brain of <i>Cstb</i> ^{-/-} mice	47
Western blotting (IV)	48
Behavioural alterations of homozygous and heterozygous <i>Cstb</i> mice	49
Neuronal loss in aged <i>Cstb</i> heterozygous mice.....	53
DISCUSSION	55
HPLC-EC method for neurochemical studies (I)	55
<i>Cstb</i> -deficiency induced changes in tryptophan metabolism (II, III).....	57
Tryptophan and its metabolites in the blood of EPM1 patients and <i>Cstb</i> ^{-/-} mice	57
Tryptophan and its metabolites in the brain of <i>Cstb</i> ^{-/-} mice and their role in the formation of EPM1-like phenotype.....	58
Changes in the excitatory–inhibitory neurotransmission in <i>Cstb</i> ^{-/-} mice cerebellum (V)	60
The effect of partial loss of <i>Cstb</i> to EPM1-like phenotype in old <i>Cstb</i> ^{+/-} mice (IV).....	61
CONCLUSIONS	63
REFERENCES.....	64
SUMMARY IN ESTONIAN	75
ACKNOWLEDGEMENTS	78
PUBLICATIONS	79

LIST OF ORIGINAL PUBLICATIONS

This thesis is based on the following articles, which are referred to in the text by their Roman numerals. Additionally, some unpublished data are presented.

- I **Vaarmann A**, Kask A, Mäeorg U. (2002) Novel and sensitive high-performance liquid chromatographic method based on electrochemical coulometric array detection for simultaneous determination of catecholamines, kynurenine and indole derivatives of tryptophan. *Journal of Chromatography B Analyt Technol Biomed Life Sci.* 769:145–153.
- II Arbatova J, D'Amato E, **Vaarmann A**, Zharkovsky A, Reeben M. (2005) Reduced serotonin and 3-hydroxyanthranilic acid levels in serum of cystatin B-deficient mice, a model system for progressive myoclonus epilepsy. *Epilepsia.* 46 (Suppl 5):49–51.
- III **Vaarmann A**, Kaasik A, Zharkovsky A. (2006) Altered tryptophan metabolism in the brain of cystatin B-deficient mice: a model system for progressive myoclonus epilepsy. *Epilepsia.* 47(10):1650–1654.
- IV Kaasik A, Kuum M, Aonurm A, Kalda A, **Vaarmann A**, Zharkovsky A. (2007) Seizures, ataxia and neuronal loss in aged cystatin B heterozygous mice. *Epilepsia.* 48:752–757.
- V **Vaarmann A**, Kruve A, Zharkovsky A. (2007) Vesicular glutamate transporter expression levels and glutamate content are altered in the brain of cystatin B-deficient mice. *Submitted.*

ABBREVIATIONS

3HOANA	3-hydroxyanthranilic acid
3HOKYN	3-hydroxykynurenine
5HIAA	5-hydroxyindoleacetic acid
5HT	serotonin, 5-hydroxytryptamine
aa	amino acid
ANA	anthranilic acid
BBB	blood-brain barrier
bp	base pair
cDNA	complementary DNA
CNS	central nervous system
CSF	cerebrospinal fluid
<i>CSTB</i> / <i>CSTB</i>	human cystatin B gene / protein
<i>Cstb</i> / <i>Cstb</i>	mouse cystatin B gene / protein
CycA	cyclophilin A
DA	dopamine
DCN	deep cerebellar nuclei
DNA	deoxyribonucleic acid
DOPAC	3,4-dihydroxyphenylacetic acid
EEG	electroencephalogram
EPM1	progressive myoclonus epilepsy type 1, Unverricht-Lundborg disease
EPM1B	Unverricht-Lundborg disease locus B
GABA	γ -aminobutyric acid
GAD	glutamate decarboxylase
Glu	glutamate
HVA	homovanillic acid
kb	kilobase
kDa	kilo Dalton, the unified atomic mass unit
KYN	kynurenine
KYNA	kynurenic acid
LOD score	logarithm of odds score
MERRF	myoclonic epilepsy with ragged-red fibers
MRI	magnet resonance imaging
MCE	2-mercaptoethanol
mRNA	messenger RNA
NA	noradrenaline
OD	optical density
OPA	<i>o</i> -phthalaldehyde
PCR	polymerase chain reaction
PCA	perchloric acid
PME	progressive myoclonus epilepsy

RNA	ribonucleic acid
RSD	relative standard deviation
RT-PCR	reverse transcriptase PCR
SEM	standard error of mean
SHS	sodium heptylsulphonate
SOS	sodium octylsulphonate
TRP	tryptophan
UTR	untranslated region
XANT	xanthurenic acid
vs	versus

INTRODUCTION

Progressive myoclonus epilepsy of Unverricht-Lundborg type (EPM1) is an autosomal recessively inherited disorder characterized by stimulus-sensitive and action related myoclonus, tonic-clonic epileptic seizures starting early in the adolescence followed by a progressive ataxia and slow deterioration in cognitive functions. The histopathological examinations in EPM1 diseased brain *post mortem* have revealed the neuronal atrophy in cerebellum, brain stem nuclei and cerebral cortex. The mutated locus for EPM1 encodes gene for the cystatin B (*CSTB*), a cysteine protease inhibitor. The main genetic defect underlying the EPM1 is a dodecamer repeat expansion in the promoter region of this gene. However, the additional seven point mutations have been described, all yielding in truncated or unfunctional protein translation. *CSTB*, a cysteine protease inhibitor, is a ubiquitously expressed tightly binding reversible inhibitor of cathepsins B, L, H and S, but its physiological function is still obscure. Despite the profound studies about cystatin B functions in neuronal homeostasis or cell death mechanisms, still the linkage of *CSTB*-deficiency on the molecular level to EPM1 phenotype has remained controversial. Nearly ten years ago, the mouse model for EPM1 was created by targeted disruption in *Cstb* gene. Homozygous *Cstb*-deficient mice similarly to EPM1 patients develop progressive ataxia, myoclonic seizures and demonstrate neuronal loss in cerebellar granule cell layer, in hippocampus and entorhinal cortex. Additionally, the considerable gliosis accompanies neuronal degeneration in both, the *Cstb*-deficient and EPM1 diseased brain. The activated glia has assumed to be as a source for neurotoxic/active substances which may contribute in the manifestation of EPM1 phenotype. The amino acid tryptophan is metabolized in brain via serotonin or kynurenine pathways. Several metabolites rising from either pathway have been related in the generation of seizures or neurological defects.

Accordingly, in the present study, we developed at first a selective analytical method for the identification of tryptophan and its serotonin and kynurenine pathway metabolites in biological samples. Further, we characterized the neurochemical state concerning the tryptophan metabolites in EPM1 diseased humans and in *Cstb*-deficient mice blood as well as in the brain of *Cstb*-deficient mice. Then we assessed *CSTB* deficiency induced behavioural and neurological defects in homozygous and heterozygous *Cstb* mice and evaluated the extent of excitatory and inhibitory activity in the brain of *Cstb*-deficient mice.

BACKGROUND OF THE STUDY

Progressive myoclonus epilepsies

Progressive myoclonus epilepsies (PMEs) are a group of rare disorders accounting for about 1% of all epilepsy cases in childhood and adolescence. These diseases share common features like tonic-clonic seizures, myoclonus, and progressive neurological dysfunction (Berkovic *et al.*, 1986; Marseille Consensus Group, 1990). PMEs differ from myoclonic epilepsy, whereas the myoclonus occurs separately from seizures. In PMEs, both symptoms tend to respond to the same drug differently, they manifest differently during the course of the disease, and they involve different consequences for the patient.

PMEs include more than a dozen different diseases, among these, the five disorders e.g. Unverricht-Lundborg disease (EPM1), Lafora disease (EPM2), sialidoses, neuronal ceroid lipofuscinoses, and myoclonic epilepsy with ragged-red fibers (MERRF) are more prevalent. All these epilepsies are inherited disorders with known genetic mutations (Table 1). Four of the five diseases have an autosomal recessive mode of inheritance while MERRF is maternally inherited in mitochondrial DNA. In Lafora disease, neuronal ceroid lipofuscinoses and sialidoses resembling progressive formation of intracellular inclusion bodies during pathogenesis have been described (Harriman *et al.*, 1955; Zeman and Albert, 1963; Carpenter *et al.*, 1974; O'Brien, 1977). While, in MERRF abnormal mitochondrial proliferation, cytochrome-c oxidase-negative fibers and ragged-red fibers appear (Nakamura *et al.*, 1995; Mancuso *et al.*, 2004; Melone *et al.*, 2004). Up to the present, any mitochondrial defects, inclusion bodies or storage material accumulation have not been identified in the case of EPM1 (Lehesjoki and Koskiniemi, 1998; Pennacchio *et al.*, 1998).

Unverricht–Lundborg disease

Unverricht–Lundborg disease, or progressive myoclonus epilepsy type 1 (EPM1, OMIM #254800, also known as Baltic or Mediterranean myoclonus epilepsy), was first described by Heinrich Unverricht in Estonia (Unverricht, 1891; Unverricht, 1895) and later by Herman Lundborg in Sweden (Lundborg, 1903). Although, this disease occurs worldwide, its prevalence is elevated in certain regions e.g. in the Mediterranean area (i.e. Italy, Southern France, Algeria, Morocco) and around the Baltic Sea. The disease is especially prevalent in Finland, where the incidence of EPM1 is about one per 17 000 births (Norio and Koskiniemi, 1979; Eldridge *et al.*, 1983; Finnish Disease Database <http://www.findis.org>), i.e. around three to four new patient diagnoses per year. At present there are approximately 200 patients known in Finland (Lehesjoki

and Koskiniemi, 1999; Finnish Disease Database <http://www.findis.org>). However, the exact numbers for prevalence or incidence of EPM1 in the Mediterranean region or worldwide are not yet available.

Molecular genetic basis of EPM1

A genome-wide search for finding the mutated gene for EPM1 was undertaken among twelve Finnish EPM1 families (Lehesjoki *et al.*, 1991). Initially, the positional cloning approach revealed significant linkage with several markers in the region of 2 million bp on the long arm of chromosome 21q22.3 (Lehesjoki *et al.*, 1991). Later, the localization was narrowed to an approximately 175 kb region on this chromosome (Virtaneva *et al.*, 1996). Following the exclusion of several candidate genes, mutations were found in locus, which encodes the previously described but unmapped protein cystatin B (CSTB) (Pennacchio *et al.*, 1996). The CSTB gene is ubiquitously expressed with a transcript of approximately 0.8 kb in Northern blot analysis (Pennacchio *et al.*, 1996). CSTB locus spans over a 2.5 kb genomic region containing three small exons which code sequences of 66 bp, 102 bp and 129 bp in length (Figure 1) (Pennacchio *et al.*, 1996), and two transcription start sites –97 bp and –108 bp upstream from the translation initiation site (Laloti *et al.*, 1997b). The 3' untranslated region is approximately 250 bp, and the introns 1422 bp and 326 bp in length (Pennacchio *et al.*, 1996).

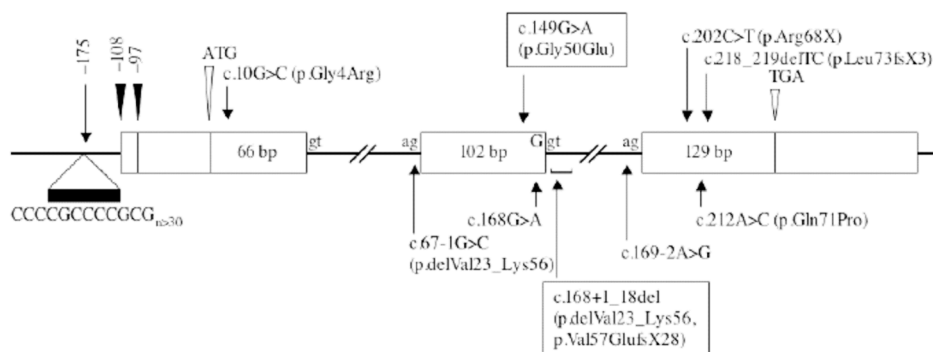


Figure 1. CSTB gene structure and EPM1-associated mutations. Abbreviations: c.– coding DNA reference sequence; del – deletion; p.– protein reference sequence; bp – base pair; standard one-letter abbreviations of nucleic acids and three letter abbreviations of amino acids. (Figure modified from Lehesjoki *et al.*, 2003 and Joensuu *et al.*, 2007)

Altogether ten EPM1 associated mutations in the CSTB gene have been described thus far. Majority of these are point mutations that account for a small proportion (less than 10%) of disease alleles worldwide. The c.67–1G>C

(Pennacchio *et al.*, 1996) c.168G>A (Kagitani-Shimono *et al.*, 2002), c.169–2A>G (Lalioi *et al.*, 1997a) affect the splice sites and the c.10G>C (Lalioi *et al.*, 1997a) c.149G>A (Joensuu *et al.*, 2007) c.212A>C (de Haan *et al.*, 2004) create amino acid changes impairing either the cathepsins binding to the CSTB protein or lead to abnormal translation products. Two mutations caused by short deletions in the CSTB gene produce either an aberrant splicing (c.168+1_18del; Joensuu *et al.*, 2007) or frame-shift (c.218_219delTC; Bessalova *et al.*, 1997) and the nonsense c.202C>T (Pennacchio *et al.*, 1996) mutation induces early termination codon resulting finally in a truncated protein.

However, the main genetic defect associated with the EPM1 is an unstable dodecamer (12 bp) or minisatellite repeat (5'-CCCCGCCCCGCG-3') expansion that is located upstream of the initiation codon of the CSTB gene (Lalioi *et al.*, 1997b; Virtaneva *et al.*, 1997; Lafrenière *et al.*, 1997). The underlying mutation is detected worldwide in about 90% and in Finland in about 98% of EPM1 affected people (Lafrenière *et al.*, 1997; Lalioi *et al.*, 1997b; Virtaneva *et al.*, 1997). In a normal CSTB gene the polymorphic 12-nucleotide repeat occurs in 2 to 3 copies, but in EPM1 associated expanded alleles the repeat copy number varies from 30 to 125 (Lalioi *et al.*, 1997b; Virtaneva *et al.*, 1997; Lalioi *et al.*, 1998). Expanded insertion probably prevents transcription of CSTB by increasing the distance between the transcription factor binding sites and the transcription initiation site (Lalioi *et al.*, 1999). No correlation between the repeat size and the age of onset or the severity of the clinical phenotype has been observed so far (Lafrenière *et al.*, 1997; Lalioi *et al.*, 1997a, 1998; Virtaneva *et al.*, 1997).

A novel locus for EPM.

During a systematic study of inherited epilepsies in Israel an inbred Arab family with a clinical pattern compatible to EPM1 was found. The disease phenotype was typical, representing progressive myoclonus and ataxia among eight affected individuals, seven of whom also had tonic-clonic epileptic seizures. Only one exception was observed, the mean age of onset was earlier than in classical EPM1 (7.3 years vs 11 years for EPM1) (Berkovic *et al.*, 2005). Surprisingly, the molecular genetic studies did not confirm the EPM1 diagnosis either. With a genome-wide screen a new locus for PME, named EPM1B, was mapped to chromosome 12 (Berkovic *et al.*, 2005). This 15-megabase region on 12p11–q13 with a maximum LOD score of 6.32 contains 47 known genes and numerous predicted genes. The locus on chromosome 12 does not contain genes known to be related to any other form of PME or genes known to be related to CSTB (Berkovic *et al.*, 2005). Identification of this new EPM1B gene may broaden the understanding about the molecular pathogenesis of EPM1.

Histopathology

Detailed neuropathological studies performed in EPM1 patients are still limited. Early autopsies of diseased humans have revealed widespread non-specific degenerative changes and in varying degrees, the loss of Purkinje cells in the cerebellum of EPM1 patients *post mortem* (Haltia *et al.*, 1969; Koskiniemi *et al.*, 1974a; Eldridge *et al.*, 1983). Later, using the MRI and proton MRS (¹H MRS) technique, the significant loss in integrity of medial thalamic and brainstem nuclei, cerebellar hemispheres and cerebral atrophy have been described in EPM1 patients brain (Mascalchi *et al.*, 2002). However, it has also been hypothesized that the neuropathological findings may partly result from anti-epileptic treatment, specially, with phenytoin, which is considered harmful due to toxic side effects (Eldridge *et al.*, 1983). Up to now, no intracellular inclusion bodies or storage material have been found (Haltia *et al.*, 1969; Koskiniemi *et al.*, 1974a; Eldridge *et al.*, 1983).

Clinical symptoms

The age of onset for EPM1 disease is between 6 and 15 years (mostly around 11 years) of age with myoclonus and/or generalized tonic-clonic epileptic seizures (Koskiniemi *et al.*, 1974a). Myoclonus manifests as a brief contraction of a muscle or group of muscles. Patients with EPM1 have myoclonic jerks associated with voluntary body movement (physical exertion) or other stimuli, such as periodic flashes of light (photoc sensitivity), noises (auditory induced myoclonus), and stress, but jerks may also occur spontaneously (Berkovic *et al.*, 1986; Marseille Consensus Group, 1990). Stimulus sensitive myoclonus is an essential feature for the diagnosis and the first symptom in approximately half of the patients (Norio and Koskiniemi, 1979; Koskiniemi, 1986; Koskiniemi, 1987). The quick myoclonic jerks may involve a single muscle, a small group of related muscles (focal), or large groups of muscles (multifocal) and may generalize to a shaking attack, to a tonic-clonic seizure attack and unconsciousness. The generalized tonic-clonic seizures are most frequent 3–7 years after the disease onset and may disappear later entirely with anticonvulsive medication (Koskiniemi *et al.*, 1974a; Norio and Koskiniemi, 1979; Koskiniemi, 1986). Clinically the disease progresses slowly, patients maintain normal cognitive functioning for a long time and decline in intelligence is not considerable, about 10 points in the IQ per decade has been reported (Koskiniemi, 1974; Koskiniemi *et al.*, 1974a; Koskiniemi, 1986). Progressive ataxia, intention tremor, incoordination and dysarthria can develop in later stages of the disorder. In addition, depression and emotional lability have been described (Lehesjoki and Koskiniemi, 1999).

Table 1. The main genetic and pathological characteristics of progressive myoclonus epilepsies.

Disease	Inheritance	Chromosome/Locus	Gene/Gene Product	Age at onset (yrs)	Pathology
Unverricht-Lundborg disease (EPM1)	AR	21q22.3/ EPM1	Cystatin B (CSTB)	6–15	Stimuli sensitive tonic- clonic seizures, photosensitivity, progressive ataxia, dysarthria, slow cognitive decline. No inclusions or storage material.
		12p11-q13/ EPM1B	Cysteine protease inhibitor; undefined gene and protein	5–10	
Lafora's disease (EPM2)	AR	6q24/ EPM2A	Laforin, a dual-specificity protein phosphatase;	10–18	Stimuli sensitive tonic- clonic seizures, myoclonus, absences, rapid cognitive decline, ataxia, progressive course, visual hallucinations. Starch-like polyglucosane masses i.e. Lafora bodies in skin, muscle, liver and brain biopsies.
		6q22/ EPM2B	Malin (NHLRC1), a single subunit E3 ubiquitin ligase		
Sialidoses type I and II	AR	6p21.3/ NEU1	Neuraminidase I i.e. lysosomal sialidase	8–15	Generalized seizures, progressive visual deficit, neuropathy, ataxia, facial myoclonus, grand mal seizures. Storage of sialidated glycopeptides and oligosaccharides.
Neuronal ceroid lipofuscinoses (NCLs)	AR	1p32/ CLN1	CLN1: palmitoyl-protein	Juvenile forms: 4–10 and 5–15 Adult form: 11–50	Progressive mental and motor retardation, visual failure, stimuli sensitive generalized or partial seizures and myoclonus, ataxia, dementia. Accumulation of autofluorescent storage material in neurons, inclusions in skin and liver.
		11p15.5/ CLN2	thioesterase-1;		
		16p12.1/ CLN3	CLN2: tripeptidyl-peptidase I;		
		13q/ CLN5	CLN3–CLN10 genes and proteins with undefined		
		15q21/ CLN6	functions, encode lysosomal or transmembrane proteins		
Myoclonic epilepsy with ragged-red fibers (MERFF)	Maternal	8p/ CLN8		Any age	Photosensitive generalized or partial seizures, neuromyopathy, dysarthria, ataxia. Ragged-red fibers on muscle biopsy.
		11p15/ CLN10			
		CLN4, CLN7, CLN9			
		mtDNA	MTTK, tRNA lysine; or other mitochondrial tRNAs		

AR-autosomal recessive; tRNA-transfer RNA; mtDNA-mitochondrial DNA; q – long arm of a chromosome; p – short arm of a chromosome (Table adapted from Delgado-Escueta *et al.*, 2001; Lehesjoki, 2003; and Shahwan *et al.*, 2005).

Electroencephalogram (EEG) is abnormal even before the symptoms appear (Koskiniemi *et al.*, 1974b; Lehesjoki and Koskiniemi, 1998) with typical spike-wave or polyspike-wave discharges (Koskiniemi *et al.*, 1974b; Koskiniemi, 1986). Sodium valproate alone or combined with clonazepam or piracetam is the most effective therapy (Iivanainen and Himberg, 1982; Somerville and Olanow, 1982; Koskiniemi, 1986; Koskiniemi *et al.*, 1998), whereas the previously used phenytoin is considered harmful due to toxic side effects (Eldridge *et al.*, 1983). Some decades ago, patients suffering the EPM1 died in young adulthood (Koskiniemi, 1986), while nowadays, due to better medication and improvement in the whole therapy regimen the life span of EPM1 patients seem to be normal (Lehesjoki, 2002). However, the myoclonus still tends to be more resistant to treatment, whereas the generalized seizures respond to anti-epileptic drug (valproate and clonazepam) therapy well.

Cystatin B

The name cystatin was adopted by Barrett (1981) for describing the protein from chicken egg white that inhibits various cysteine proteases. Human cystatin B (CSTB; also *stefin B* or Neutral Cysteine Protease Inhibitor) was first described in lymphatic tissue (Rinne, 1981; Järvinen and Rinne, 1982) and liver (Ritonja *et al.*, 1985). Later, the CSTB was classified to the family of cystatins, which are reversible inhibitors of cathepsins, a cysteine proteasis of papain superfamily (Barrett, 1986; Turk and Bode, 1991). These inhibitors are proposed to control the activities of endogenous proteases and thereby protect cells from protein degradations by endogenous proteolysis. Although, the cystatins are commonly found both intra and extracellularly, the CSTB is mostly localized intracellularly and widely distributed among different cell types and tissues. The cystatins are divided in three families: the stefins, the cystatins and the kininogens, depending on their size and structural characteristics (Barrett *et al.*, 1986). The small molecular weight CSTB protein (human 98 aa; 11kDa) is a member of the stefins family and its structure is highly conserved between species e.g. mouse, rat, and human (Ritonja *et al.*, 1985).

The crystal structures of chicken cystatin B (Bode *et al.*, 1988) and of recombinant human CSTB–papain complex (Stubbs *et al.*, 1990) have been determined. Both the chicken and human CSTB own a five-stranded β -sheet wrapped around a five-turn α -helix. The human CSTB protein consists of an additional binding site, the C-terminal strand that runs along the convex side of the sheet. CSTB interacts with papain through a tripartite wedge formed by conserved residues at the most N-terminal part of CSTB, the first hairpin loop containing the highly conserved QVVAG sequence, and the second hairpin loop (Stubbs *et al.*, 1990).

The animal studies have revealed that the *Cstb* gene is expressed in almost all tissues examined (Pennacchio *et al.*, 1996; Reymond *et al.*, 2002), while in brain *Cstb* demonstrated a differential expression pattern in several regions using *in situ* hybridization and immunohistochemical analysis. Cerebral *Cstb* expression was highest in forebrain structures, especially in the hippocampal formation and reticular thalamic nucleus (D'Amato *et al.*, 2000). Later, Riccio *et al.* (2005) demonstrated that the overall cerebellar CSTB content is slightly lower comparing to cerebral hemispheres. Expression of CSTB in different brain cell types has also been studied. Cystatin B protein is found in both, neurons and glial cells differentiated from rat neural stem cells or hippocampal cultures (Brännvall *et al.*, 2003). In primary glial cells, CSTB was expressed in progenitor and differentiated oligodendrocytes as well as in astrocytes (Riccio *et al.*, 2005). While the most neurons of developing and adult rat cerebellum do not present detectable amounts of CSTB, with the exception of the Purkinje cells and of some cells of the differentiated molecular layer (Riccio *et al.*, 2005). A very similar situation is found in man where the distribution of CSTB in cells of the cerebellum is restricted to Purkinje cells and Bergmann fibers (Riccio *et al.*, 2005). On the cellular level, the CSTB protein was initially considered to reside in the cytoplasm (Stubbs *et al.*, 1990). Later, the disposition in cytoplasmic granular structures representing either the Golgi complex or lysosomes, in a variety of cell lines was determined (Riccio *et al.*, 2001; Brännvall *et al.*, 2003). The immunofluorescence analysis has revealed the nuclear localization of the CSTB as well (D'Amato *et al.*, 2000; Riccio *et al.*, 2001; Brännvall *et al.*, 2003), an intriguing finding which lead to the idea that CSTB may participate in cellular processes other than proteolysis.

CSTB is known to inhibit several different lysosomal cysteine proteases *in vitro*, including cathepsins S, H, L and B (Ritonja *et al.*, 1985; Brömme *et al.*, 1991; Turk and Bode, 1991). Biochemical studies in EPM1 patient lymphoblastoid cell lines indicated that the CSTB inhibitory activity is significantly reduced (or absent) and correlates with increased cathepsins B, L and S activity (Rinne *et al.*, 2002), while cathepsin H activity is not significantly altered (Rinne *et al.*, 2002). These findings support the idea that the activity of these cathepsins is regulated also *in vivo* by CSTB. D'Amato *et al.* (2000) demonstrated a considerable increase in CSTB mRNA and protein expression levels 6–24 hours after kindling-induced epileptic seizures in rat forebrain neurons. Data suggest that upregulation of CSTB after seizures may counteract apoptosis by binding cathepsins and contributing the hypothesis of a neuroprotective role for CSTB (D'Amato *et al.*, 2000).

Mammalian model of EPM1: *Cstb*-deficient mice

Soon after the discovery of the mutated gene for EPM1, a mammalian model for the disease has been created by targeted disruption of the mouse *Cstb* gene (Pennacchio *et al.*, 1998). The mouse *Cstb* locus spans a 3-kb genomic region on the chromosome 10 containing 3 exons and 2 introns. The mouse sequence has an identical structure to both, the rat and human cystatin B gene, encoding a 98 amino acid polypeptide identical in length to the rat and human proteins, with 86% and 79% amino acid similarity, respectively (Pennacchio and Myers, 1996). The *Cstb* gene disruption were made by targeting vector construct containing a 1.3-kb PGK neomycin expression cassette inserted into the *EagI* site in exon 1. This disruption in *Cstb* is predicted to cause an in-frame non-sense codon after eight additional codons, truncating the protein at 15% of its normal length (Pennacchio *et al.*, 1998).

Generally, the mice lacking the *Cstb* gene have been considered as a valid model of EPM1, since mutant mice display a rather overlapping neurological phenotype and similar histopathological pattern with that described for diseased patients. The *Cstb*-deficient mice are developmentally normal and fertile, but evolve a phenotype resembling the EPM1 diseased humans, with progressive ataxia and myoclonic seizures. Originally, the spontaneous myoclonuses were described only during the sleep visible at the age of 1 month (Pennacchio *et al.*, 1998), while later, the myoclonic seizures have been observed during wakefulness as well (Houseweart *et al.*, 2003). Mild signs of ataxia became evident at 6 months of age (Pennacchio *et al.*, 1998). However, no photosensitivity and tonic-clonic seizures typical for EPM1 patients have been observed (Pennacchio *et al.*, 1998). Interestingly, in 35% of *Cstb*-deficient mice the corneal lesion developed at the age of 3–7 months (Pennacchio *et al.*, 1998), a phenomenon not seen in diseased humans. Additionally, a severe reduction in the brain (43%) and body weights (34%) of mutant mice has been found (Shannon *et al.*, 2002).

Histological analysis of mutant mice revealed apoptotic death of cerebellar granule cells at 1–12 months of age (Pennacchio *et al.*, 1998). Less marked neuronal loss was described in the hippocampal formation and entorhinal cortex in 3- to 6-month-old mice (Shannon *et al.*, 2002). General atrophy of cortical and cerebellar neurons is obvious in mutants' mice brain (Pennacchio *et al.*, 1998; Shannon *et al.*, 2002). In addition, a patchy loss of Purkinje cells accompanied by Bergmann gliosis is found in the cerebellar vermis (Shannon *et al.*, 2002). In older mice (16–20 months old), gliosis is present in the cerebral hemispheres, hippocampal formation, entorhinal cortex, neocortex and striatum. Widespread gliosis has also been detected in the white matter, which has been considered to be a secondary phenomenon.

However, the most contradictory feature of animal model concerns the seizure prone and seizure resistant phenotype of *Cstb*-deficient mice depending on the genetic background of animals. Although, the mutant mice in mixed

129Sv and C57Bl6 strain do not display myoclonic seizures, while mice in an isogenic background (129Sv) do, the ataxia and abnormal brain histopathology develop on both a mixed and isogenic background (Pennacchio *et al.*, 1998; Shannon *et al.*, 2002). These findings support the hypothesis that neuronal cell death alone, although being an important consequence of *Cstb*-deficiency, is not responsible for the establishment of epileptic phenotype.

In vitro electrophysiological studies on hippocampal slices prepared from *Cstb*-deficient mice indicated the hyperexcitability by responding to afferent stimuli with multiple population spikes (Franceschetti *et al.*, 2007). The kainate perfusion provoked the appearance of epileptic-like activity on hippocampal slices from mutant mice earlier than in wild-type mice (Franceschetti *et al.*, 2007). *In vivo*, *Cstb* mutant mice treated with kainate displayed increased susceptibility to seizures, with shorter latency to seizure onset as well as increased seizure severity accompanied by a greater degree of neuronal damage after seizures of identical grade, indicating increased sensibility to seizure-induced cell death (Franceschetti *et al.*, 2007). Additionally, in immunohistochemical studies a significant loss of GABAergic interneurons in the hippocampal CA1–CA2 region of *Cstb* knockout mice was found (Franceschetti *et al.*, 2007), proposing that disturbed GABAergic inhibition may contribute to the seizure phenotype.

Transcriptional profiling of *Cstb*-deficient mice brains has demonstrated seven genes with consistently increased transcript levels. These genes are cathepsin S, C1q B-chain of complement, β 2-microglobulin, glial fibrillary acidic protein, apolipoprotein D, fibronectin 1 and metallothionein II, which are expected to be involved in increased proteolysis, apoptosis and glial activation (Lieuallen *et al.*, 2001). The levels of cathepsins B, H and L transcripts were variable, while the cathepsin S levels were significantly increased in the absence of CSTB, proposing the feedback mechanism between the two proteins. The other transcripts found to be elevated, encode proteins that are markers of microglia activation or are known to be involved in response to neuronal damage (Lieuallen *et al.*, 2001). On the contrary to the gene expression study, no improvement of EPM1 phenotype was seen in a mouse model doubly-deficient for *Cstb* and cathepsin S (Houseweart *et al.*, 2003). However, the double mutant mice for *Cstb* and cathepsin B demonstrated the reduction in the amount of cerebellar granule cell apoptosis depending on the mouse age. Although, the ataxia and seizure phenotypes experienced by cystatin B-deficient animals were not diminished, suggesting that another molecule besides cathepsin B or other cellular pathways are also responsible for the pathogenesis.

Current pathogenetic hypothesis of EPM1

During the last two decades a lot of progress towards understanding the essence of EPM1 disease has been achieved. Although the primary genetic factor underlying the EPM1 is now identified, still, the pathogenetic mechanism by which a deficit of CSTB leads to EPM1 phenotype remains to be elucidated. Here, the present hypothesis concerning the EPM1 disease based on numeral studies performed on human and animal model of EPM1 have shortly resumed.

CSTB might have other functions than cathepsin inhibition. Since the observation that *Cstb*-deficient mice show myoclonic seizures only on an isogenic background, while developing ataxia and abnormal brain histopathology on both – a mixed and isogenic – background, the effects from modifier genes and complex cellular mechanisms of CSTB have supposed (Pennacchio *et al.*, 1998; Shannon *et al.*, 2002). Later by discovering the nuclear localization of CSTB and observing the clear differences in CSTB and cathepsins cellular distribution (i.e. majority of cystatin B does not coincide with that of cathepsins), the idea that CSTB might have a multiple function other than the inhibition of cathepsin has been raised (Riccio *et al.*, 2001). This view is also strongly supported by data obtained from mice double-deficient for *Cstb* and cathepsin B. Indeed, these animals displayed the decrease in cerebellar granule cell apoptosis, but the severity of the ataxia and seizure phenotypes remain unchanged (Houseweart *et al.*, 2003). Furthermore, the double-deficient mice for *Cstb* and cathepsin S or L did not exhibit any improvement in neurodegeneration or disease phenotype either (Houseweart *et al.*, 2003).

In addition, Di Giaimo *et al.* (2002) identified a number of proteins that are not proteases, but can interact specifically with CSTB. Among these, two proteins – the neurofilament light chain and brain β -spectrin – are expressed exclusively in cells of the nervous system, mainly in neurons, and other cytoplasmic proteins are involved in the regulation of cytoskeletal functions. Furthermore, some of these interactions with cystatin B are detectable only in the cerebellum and not in the brain hemispheres, indicating the tissue specificity of the protein complexes. In the cerebellum, these proteins are localized in different cells, depending on the age of the animal. Same proteins are in the granule cells during the cerebellar development and in the Purkinje cells in the adulthood. These results propose the possibility that a cystatin B multiprotein complex has a specific cerebellar and developmental function and that the loss of this function might contribute to the disease in EPM1 patients.

Microglia activation. Mounting evidence indicate that microglia, the resident innate immune cells in the brain, can participate as active contributors to neuron damage in neurodegenerative diseases (i.e. Alzheimer's, Parkinson's and Huntington's disease and HIV dementia), in which, the overactivation and dysregulation of microglia might result in disastrous and progressive neurotoxic consequences as well as modulate the manifestation of disease phenotype

(Block *et al.*, 2007). In the mature brain, microglia typically exists in a resting state and monitors the brain environment, but in response to certain cues such as neuronal death or damage or immunological stimuli, however, microglia is readily activated. Reactive microglia may serve diverse functions, which could be either beneficial for neuronal survival or become destructive by inducing the production of cytotoxic factors. In neurodegenerative disease, activated microglia have been shown to be present in large numbers, a condition termed microgliosis, strongly implicating these cells in disease pathology. Furthermore, microglia-mediated neurotoxicity tends to be progressive, which could contribute to the progressive nature of several neurodegenerative diseases (Block *et al.*, 2007).

Early histopathological studies have revealed that degeneration of neurons in EPM1 patients as well as *Cstb*-deficient mice brain are accompanied by marked gliosis in the cerebellum, cerebral cortex, striatum and brain stem (Haltia *et al.*, 1969; Koskiniemi *et al.*, 1974a; Shannon *et al.*, 2002). Recently, using the immunocytochemical labelling for activated microglia, the presence of a large number of activated elements in several regions of the *Cstb*-deficient mice brain, including the neocortex, the hippocampus and thalamic nuclei have been observed (Franceschetti *et al.* 2007). Likewise, the gene expression studies in *Cstb*-deficient brain show the increased expression of genetic markers which have proposed to involve in glial activation (Lieuallen *et al.*, 2001). These findings support the hypothesis that activated microglia may play a role in the formation of EPM1 phenotype, although the mechanisms by which the neuronal dysfunction is induced remains to be elusive.

Seizures beget seizures. Theory of the vicious circle revealed by Franceschetti *et al.* (2007) proposed that the onset of EPM1 may be related to a latent hyperexcitability of the EPM1 brain, and the disease progression may depend on higher susceptibility to seizure-induced damage. Whereas the treatments capable of counteracting seizures are also generally capable of diminishing the rate of disease progression, suggesting that seizure-linked excitotoxic events might play a role in determining the progression and deepening of the degenerative processes sustaining the severity of the disease. Based on authors' *in vivo* studies, one of the mechanisms underlying this hyperexcitability may be the loss of hippocampal GABA inhibition in *Cstb*-deficient mice brain or the presence of activated glia cells, which may contribute in the impairment of local excitatory/inhibitory neurotransmission.

Tryptophan metabolism and epilepsy

The essential amino acid *L*-tryptophan (TRP) is a precursor for several neurochemically active molecules that have been implicated in the pathogenesis of various neurological diseases as well as associated with seizures and myoclonic symptoms (Pintor *et al.*, 1990; Sternbach, 1991; Heyes *et al.*, 1994). In mammals, about 99% dietary TRP is metabolized via kynurenine (KYN) (Peters, 1991) pathway (Figure 2) and in peripheral tissue, less than 1% is converted to serotonin (i.e. 5-hydroxytryptamine; 5HT), a well-documented and extensively studied neurotransmitter generated via indole pathway. The kynurenine cascade is notable for the fact that it contains four neuroactive intermediates, all of which derive directly or indirectly from *L*-kynurenine (KYN), the primary major degradation product of TRP. Particularly, the quinolinic acid (QUIN) and kynurenic acids (KYNA) have been linked to the seizure events due to their opposite action on excitatory amino acid receptors. QUIN can excite neurons by acting as an agonist at the *N*-methyl-*D*-aspartate (NMDA) sensitive population of glutamate receptor (Stone and Perkins, 1981), while KYNA is the only known endogenous antagonist of NMDA receptors (Perkins and Stone, 1982) which can also block nicotinic receptors, specially presynaptic ones (Hilmas *et al.*, 2001). The 3-hydroxykynurenine (3HOKYN) and 3-hydroxyanthranilic acid (3HOANA) has shown to be oxygen free radical generators (Eastman and Guilarte, 1989; Okuda *et al.*, 1996) and, thus, can induce neuronal damage like quinolinic acid (Schwarcz *et al.*, 1983).

In mammals, TRP metabolism is highly regulated and significant differences exist in the sites (CNS, peripheral organs) and physiological control (cell type, enzymes, BBB) of serotonin vs kynurenines. In peripheral tissue, 5HT is synthesized within serotonergic neurons and neuroendocrine cells of the intestine by a two-step process involving the tryptophan hydroxylase 1 (TPH1) (Walther *et al.*, 2003) for the synthesis of the 5-hydroxytryptophan, which is then decarboxylated to 5HT. Whereas in the brain, the rate-limiting step in the synthesis of 5HT, has been catalyzed exclusively by tryptophan hydroxylase isoform 2 (TPH2) (Zhang *et al.*, 2004). The first enzymes of the KYN pathway, tryptophan 2,3-dioxygenase (TDO) and indoleamine 2,3-dioxygenase (IDO), which result in the formation of formylkynurenine, are also tissue specific. TDO is restricted almost exclusively to the liver, whereas IDO is found in most other tissues, including cells of the immune and nervous system. Kynurenine formamidase then rapidly converts formylkynurenine to KYN, which can be metabolized by three different enzymes: 1) kynureninase which forms anthranilic acid (ANA) 2) kynurenine 3-hydroxylase which forms 3HOKYN and 3) kynurenine aminotransferases (KATs) which leads to KYNA formation in the side-arm of KYN pathway. Peripheral organs contain several aminotransferases capable of forming KYNA and xanthurenic acid (XANT) from KYN and 3-HOKYN, respectively, only two such enzymes appear to exist in

the brain. Enzymes KAT I and KAT II differ substantially with regard to their pH optimum and substrate specificity. KAT I represents a pH optimum of 9.5 to 10.0 with low substrate specificity, whereas KAT II functions best at physiological pH and preferentially recognizes KYN as a substrate in the brain (Okuno *et al.*, 1991; Guidetti *et al.*, 1997). Finally, QUIN is synthesized in brain by 3-hydroxyantranilic acid oxygenase from 3HOANA, the latter generated either from 3HOKYN or ANA.

The transport of TRP and KYN across the BBB by the neutral amino acid carrier into the extracellular fluid of the CNS plays a critical role in the regulation of brain tryptophan metabolism (Fukui *et al.*, 1991). Immunocytochemical and lesion studies have revealed that glial cells, rather than neurons, harbour the enzymatic machinery for the biosynthesis of brain kynurenines (Heyes *et al.*, 1996; Guillemin *et al.*, 2001). While the IDO is enzyme under tight immunological control and can be easily activated by interferon- γ (IFN γ) as well as pro-inflammatory cytokines (Werner *et al.*, 1987; Saito *et al.*, 1991), the kynurenines seems to be a key factor in communication between nervous and immune system. Furthermore, the kynurenine 3-monooxygenase and kynurenase are also shown to be activated by IFN γ and tumour necrosis factor α (Chiarugi *et al.*, 2001). Both, astrocytes and infiltrating macrophages/microglia can pick up the TRP and KYN from extracellular fluid or CSF. However astrocytes do not appear to contain kynurenine 3-hydroxylase and therefore promote KYNA synthesis (Du *et al.*, 1992), while microglia cells seem to harbour very little KAT activity and preferentially account for QUIN branch of the pathway (Guillemin *et al.*, 2001).

Up to present, a number of comprehensive surveys have been published on disorders associated with alterations in the KYN or indole pathways of TRP (Nemeth *et al.*, 2006; Stone, 2001; Stone *et al.*, 2003), featuring recent results on various pathological states. Since the first indications that kynurenines might play a role in convulsive actions or excitotoxic processes in CNS (Lapin, 1978; Stone and Perkins, 1981; Foster *et al.*, 1984), several *in vitro* and animal studies have been published linking these compounds to epileptic or seizure events.

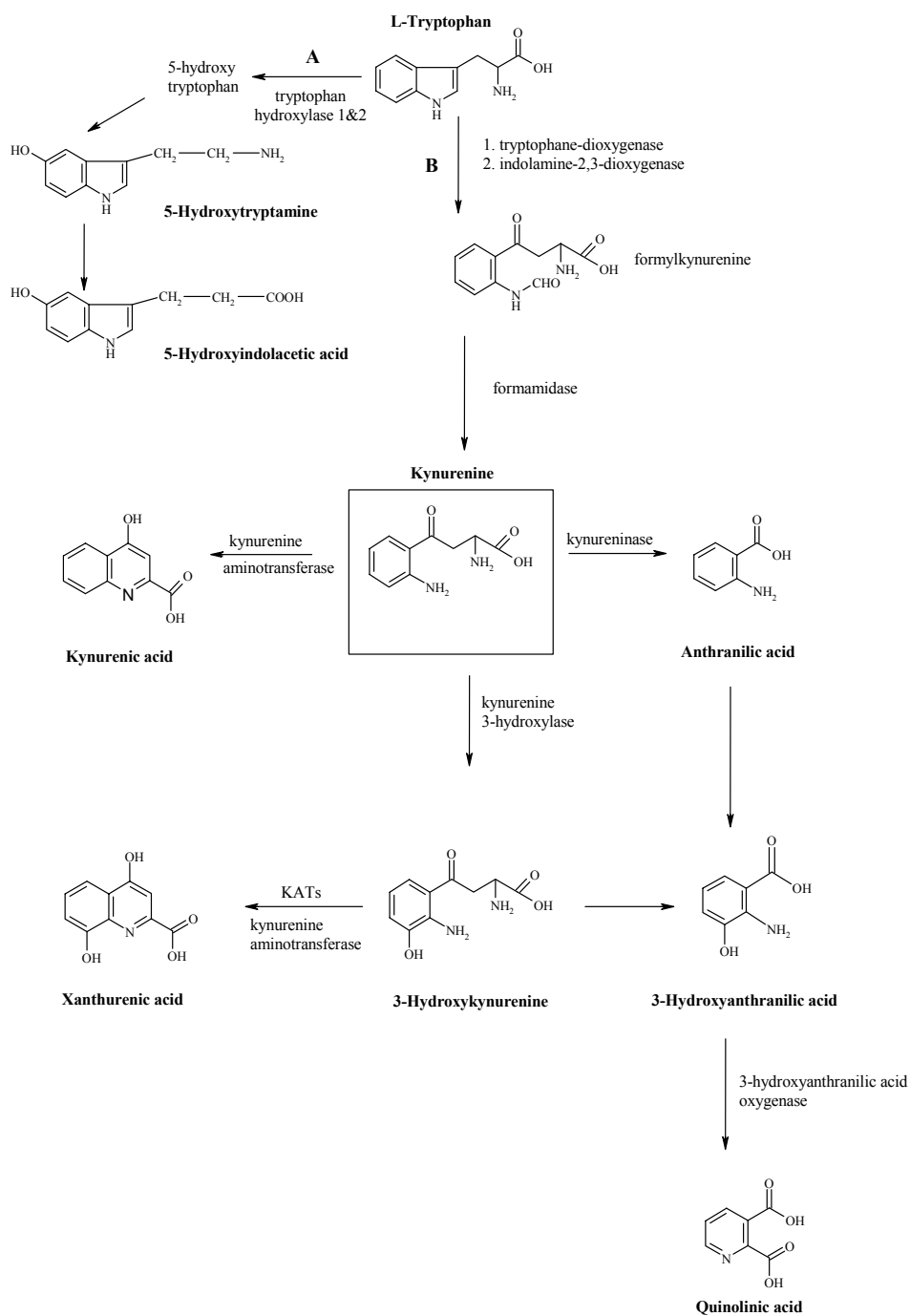


Figure 2. The tryptophan metabolism via indole (A) and kynurenine (B) pathways.

Increased amounts of QUIN (Nakano *et al.*, 1993) and up to 17-fold increase in the activity of 3-hydroxyanthranilic acid oxygenase (Nakano *et al.*, 2006) and its gene (Nakagawa *et al.*, 1998) have been reported in the brains of epileptic E1 mice. These findings, together with increased levels of KYN in these animals (Suzuki and Mori, 1992), raise the possibility of a contribution of kynurenines to their epileptic state. Furthermore, seizures are associated with a subsequent gliosis with increased cerebral activity of kynurenine metabolic enzymes (Du *et al.*, 1993). Wu and Schwarcz (1996) demonstrated in various seizure paradigms (pentylentetrazole, pilocarpine, bicuculline, kainic acid) that KYNA levels in the brain microdialysate began to rise within 1 h and gradually reached a plateau approximately 4 h after administration of the convulsants. These data indicate that an increase in extracellular KYNA may constitute a common occurrence in response to seizures and those KYNA elevations may implicate the brain's attempt to counteract seizure activity (Wu and Schwarcz, 1996). Furthermore, even low concentrations of endogenous KYNA reduce the number of hippocampal slices with spontaneous epileptiform discharge suggesting that endogenous KYNA plays an important role in the suppression of seizure-like activity (Scharfman *et al.*, 2000). In WAG/Rij rats, which are a genetic model of absence epilepsy, significantly lower concentrations of KYNA have been found in the frontal cortex than in non-epileptic controls. This indicates that selective deficits of endogenous KYNA may account for increased excitability in the frontal cortex (Kaminski *et al.*, 2003).

In human studies no differences have been reported in the concentration of QUIN in epileptic foci and non-focal areas of the human brain (Heyes *et al.*, 1990). However, the KYN and QUIN concentrations in both CSF and serum revealed to be reduced in patients with intractable complex partial seizures in both, the postictal and the interictal period (absence of seizure for > 24 h) as compared with neurologically normal control subjects (Heyes *et al.*, 1994). In people with West syndrome the reduced levels of KYNA in CSF has been observed (Yamamoto *et al.*, 1995). Likewise the concentration of KYNA has been reported to be lower than normal in the CSF of patients with infantile spasms, proposing the possibility that the motor disorder may appear due to reduced antagonism of endogenous excitants such as glutamate or QUIN (Yamamoto *et al.*, 1994). There are also differences in the diurnal rhythms of KYN excretion pattern between control subjects and patients with seizures, further differences being observed between patients with seizures of febrile and epileptic origin (Munoz-Hoyos *et al.*, 1997). However, the significance of these findings remains to be established, but may indicate a role for kynurenines in the genesis and severity of convulsant disorders.

TRP indole derivate 5HT has also proposed to involve in the seizure or myoclonus episodes. The excessive production of 5HT within CNS induces a phenomenon called serotonin syndrome with characteristic motor symptoms such as the myoclonus, hyperreflexia, tremor and coordination disturbances

(Sternbach, 1991; Bodner *et al.*, 1995). Concerning the seizures, the levels of 5HT and its intermediate metabolite 5-hydroxyindole acetic acid (5-HIAA) have shown to be higher in the focus in the temporal neocortex of patients with intractable complex partial seizures (Pintor *et al.*, 1990). While Natsume *et al.* (2003) investigated whether the metabolism of the serotonergic system in the brain, including the kynurenines, is involved in temporal lobe epilepsy (TLE). The studies of patients with intractable TLE by positron emission tomography (PET) using alpha-(11C)-methyl-L-TRP (α -MTRP) revealed a significantly increased α -MTRP uptake in the hippocampus ipsilateral to the seizure focus in patients with normal hippocampal volumes as compared with patients with hippocampal atrophy and healthy controls. Moreover, there is a significant correlation between α -MTRP uptake and the frequency of interictal spikes in patients with tuberous sclerosis complex (Fedi *et al.*, 2003).

Glutamate, gamma-amino butyric acid (GABA) and motor coordination

Brain function is tightly coupled to a fine-tuned balance between excitatory glutamatergic and inhibitory GABAergic neurotransmission. The brain areas like cerebral cortex, hippocampus and cerebellum are largely characterized by neuronal networks consisting of glutamatergic and GABAergic neurons. Glutamic acid (Glu), also referred to as glutamate (the anion) is synthesized in CNS mostly by a one-step reaction, either from glutamine provided by the glia through the action of glutaminase or through the transamination of α -ketoglutarate provided by the mitochondria. After its action on glutamate receptors, the ionotropic or metabotropic ones, glutamate can be removed from the synaptic cleft through two processes: re-uptake back into presynaptic terminals or diffusion out of synaptic cleft for uptake by glial cells. This is achieved by glutamate transporters found in neuronal and glial plasma membranes. Glutamate also serves as the precursor for the synthesis of the inhibitory GABA in GABAergic neurons. This reaction is performed either in the cytosol or on the membrane of synaptic vesicles by glutamate decarboxylase (GAD). Up to present two GAD isoforms, GAD65 and GAD67 with molecular weight 65 and 67 kDa, respectively, have been described (Erlander *et al.*, 1991). In order to differentiate excitatory pathways from inhibitory ones in the CNS, the glutamate- and GABAergic neurons can be characterized directly by transmitters, and indirectly by their synthetic enzymes and transporters. GABAergic neurons can be visualized by immunocytochemistry for GABA or for GAD and vesicular GABA transporter (vGABAT) (McIntire *et al.*, 1997). However, since glutamate is largely managed by glia cells and serves as a precursor of inhibitory transmitter GABA, the glutamate persistence in cell is

not specific only to glutamatergic neurons. Thus neither glutaminase nor plasma membrane glutamate transporters is regarded as a selective marker for glutamatergic neurons in the CNS. Nowadays, the vesicular glutamate transporters (vGLT) have considered most reliable markers for glutamatergic neurons.

Recent molecular biological studies have identified three subtypes of the vesicular glutamate transporter (Ni *et al.*, 1994; Aihara *et al.*, 2000; Gras *et al.*, 2002). In the adult brain the two predominant isoforms, vGLT1 and vGLT2, display roughly complementary expression patterns. For instance, vGLT1 predominates in the cerebral and cerebellar cortices and hippocampus, whereas vGLT2 expression is prominent in diencephalon, brainstem, and spinal cord (Freneau *et al.*, 2001; Herzog *et al.*, 2001; Varoqui *et al.*, 2002). However, none of these brain regions exclusively express one isoform, and although the majority of glutamatergic neurons express either vGLT1 or vGLT2, several studies describe coexpression of both isoforms. The third isoform, vGLT3 is less widely distributed than the other two and is expressed in neurons not classically considered glutamatergic like the 5HTergic and cholinergic neurons (Freneau *et al.*, 2002).

Commonly, the generation of epileptic and seizure activity has been associated with impaired balance of excitatory and inhibitory neurotransmission, specially, when excitatory activity surpasses inhibition in the brain. However, the disturbed excitatory/inhibitory activity may contribute to the manifestation of other neurological deficits such as ataxia, impaired motor coordination and involuntary movements as well.

The cerebellum plays an important role in controlling motor coordination, body movement and posture. The Purkinje cells have a central role in mediating highly coordinated excitatory and inhibitory signals concerned with the temporal organization of movement execution and motor coordination (Voogd and Glickstein, 1998). The cerebellar cortex forms an array of relatively simple neural networks, where the Purkinje cells receive their excitatory input from parallel fibers of glutamatergic granule cells or from climbing fiber from the inferior olivary nuclei and they form an output to the deep cerebellar nuclei (DCN) (Sotelo and Alvarado-Mallart, 1991; Voogd and Glickstein, 1998; Aizenman and Linden, 1999). This output is entirely inhibitory and mediated by the neurotransmitter GABA.

The studies where reversible deficit of glutamatergic neurotransmission have induced, the impairment of motor coordination follows, demonstrating that the granule cell glutamatergic neurotransmission is critical in controlling motor coordination (Yamamoto *et al.*, 2003). In the case of hereditary cerebellar ataxias has been hypothesized, that due to the extensive neuronal degeneration in cerebellum, the balance between excitatory and inhibitory modulation of Purkinje neuron system has been impaired (Raman *et al.*, 2000, Grusser-Cornehls and Baurle, 2001). The excitability of DCN has proposed to be

enhanced response to deterioration of Purkinje input and neurons fire spontaneously affecting motor performance at multiple levels. Accordingly, several studies with mouse models of cerebellar ataxia (i.e. Rolling mouse Nagoya, *weaver* and *lurcher* mice) have revealed the alterations in excitatory/inhibitory neurotransmission in the cerebellum of these animals. For instance, the neurochemical experiments have demonstrated reduced concentration of glutamate and an increased concentration of glycine, the inhibitory substance, in the cerebellum of Rolling mouse Nagoya (Muramoto *et al.*, 1981). Additionally, in the case of *weaver* mouse, which demonstrate a number of similarities to the *Cstb*-deficient mice phenotype (i.e. like having primary cerebellar granule and scanty Purkinje cells atrophy), the enlargement of GAD-immunopositive terminals in their cerebellar nuclei have been described (Krug *et al.*, 1995). The *lurcher* mice in which the primary event in CNS is the selective apoptotic death of Purkinje cells through a gain of function mutation of the $\delta 2$ glutamate receptor (Zuo *et al.*, 1997), have the secondary retrograde degeneration of majority of the granular cells. While cell population study in these mice cerebellum demonstrated the mild degeneration (a reduction by 20%) of large glutamatergic neurons and a more pronounced degeneration of GABAergic (by 42%) and glycinergic neurons (by 45%)(Sultan *et al.*, 2002).

AIMS OF THE STUDY

To develop a high performance liquid chromatographic (HPLC) method with electrochemical array (EC) detection enabling to selectively identify tryptophan and its serotonin and kynurenine pathway metabolites from the biological samples.

To assess whether *Cstb*-deficiency results in the alterations of tryptophan metabolism along serotonin and kynurenine pathways and further characterize the behavioural phenotype of *Cstb*-deficient mice. Specifically, to determine the changes in tryptophan metabolism in the blood of EPM1 patients and homozygous *Cstb* mice as well as in the brain of *Cstb*-deficient mice.

To evaluate the changes in the excitatory-inhibitory neurotransmission in the brain of *Cstb*-deficient mice.

To verify whether the partial loss of *Cstb* induces EPM1-like phenotype in *Cstb* heterozygous mice.

MATERIALS AND METHODS

Animals

All the experiments were performed in accordance with the guidelines established in the Principles of Laboratory Animal Care (directive 86/609/EEC) and conformed to local guidelines on the ethical use of animals. The wild-type mice (*Cstb*^{+/+}) and mice heterozygous for a disruption in the *Cstb* (*Cstb*^{+/-}) gene were purchased from The Jackson Laboratory (129SvJ strain, USA) and were further crossed to generate homozygous (*Cstb*^{-/-}) mice in our animal facilities. All animals were allowed free access to food and water and were housed in a temperature- and light-controlled environment (12 h light-dark cycles). Altogether twenty *Cstb*^{-/-} mice and same number of sex matched wild-type mice were taken for the experiments at the age of 4 to 5 months (II, III, V). In the heterozygous mice study (IV) fourteen *Cstb*^{+/-} mice and twelve *Cstb*^{+/+} mice were used at the average age of 17 months.

High performance liquid chromatography (I, II, III, V)

Chemicals

All reagents were of analytical grade and purchased from Sigma-Aldrich (MO, USA). The pure standards for tryptophan (TRP); for kynurenines: kynurenine (KYN), kynurenic acid (KYNA), anthranilic acid (ANA), 3-hydroxykynurenine (3HOKYN), 3-hydroxyanthranilic acid (3HOANA), xanthurenic acid (XANT); for indole metabolites: serotonin (5HT) and 5-hydroxyindoleacetic acid (5HIAA) and for catecholamines: dopamine (DA), noradrenaline (NA), homovanillic acid (HVA), 3,4-dihydroxyphenylacetic acid (DOPAC) and glutamate (Glu) as well as γ -aminobutyric acid (GABA) were also from Sigma-Aldrich (MO, USA). Sodium octylsulphonate (SOS) and sodium heptylsulphonate (SHS) were purchased from Fluka Chemie (Buchs, Switzerland). HPLC grade methanol (MeOH) was obtained from Merck (Darmstadt, Germany). The ultrapure water for method development was prepared with MilliQ (Millipore Corporation, Milford, MA, USA) water purification system.

Preparation of standard solutions

The primary stock standard solutions were made by dissolving a fixed amount (10–20 mg) of the component in 25 ml of 0.1–0.12 M perchloric acid (PCA). To facilitate the dissolution of kynurenine, kynurenic acid and xanthurenic acid, a few drops of 1M NaOH were added to corresponding standard solutions and

final dilutions were made with ultrapure water. All these individual concentrates were then stored in 1 ml aliquots at -80°C and thawed prior to use at 4°C . Stability of concentrated stock solutions were monitored during the six month period and no evidence for decomposition was found. Working standards in nM or μM range were prepared in 0.1–0.12 M PCA freshly before each assay.

Preparation of mobile phase and gradient elution

For HPLC analysis with EC, the stock buffer solutions of 50 mM monobasic sodium phosphate and 50 mM sodium acetate combined in a ratio of 1:1 were used as a base for most mobile phase solutions. SOS in concentrations ranging from 0.42 mM to 1.5 mM and SHS concentrations from 1 mM to 2 mM was added to influence the separation. pH of buffer solution was adjusted between 3.10 and 4.60 by titration with *ortho*-phosphoric acid. MeOH (6–12% v/v) was added to the mobile phase, which was then filtered through a $0.22\ \mu\text{m}$ pore size filter (GHP Polypropylfilters, Gelman Laboratory) and degassed under vacuum for 20 min prior to use.

For glutamate and GABA study the 100 mM acetate buffer was prepared by dissolving sodium acetate in MilliQ water. Solution pH was titrated to 6.90 by adding the acetic acid. The prepared buffer was filtered through $0.22\ \mu\text{m}$ filter and degassed under vacuum. The separation was achieved in gradient elution mode combining the MeOH and acetate buffer (0.1 M, pH=6.90). The gradient started with mobile phase composition: 15% of methanol and 85% buffer. MeOH content was then elevated to 30% in 1.5 min and kept like this for 10 min. Thereafter methanol fraction was raised to 33% within 3 min. Finally, the MeOH content was increased to 100% within 1 min and the column was eluted with methanol for 0.5 min. Altogether the program lasted 16 min.

Derivatization

For glutamate and GABA detection the pre-column derivatization was used. 27 mg of *o*-phthalaldehyde (OPA) was dissolved in 500 μl of 99% ethanol to obtain the 40 mM solution. 20 μl of 2-mercaptoethanol (MCE) and 4.5 ml of 0.4M borate buffer were taken per 5 ml of OPA solution for preparing the derivatization reagent. The autosampler was programmed to add 50 μl of the OPA-MCE reagent to 50 μl of a sample, to mix two times and to inject 10 μl onto the column after a reaction time of 1 min.

HPLC instrumentation

The HPLC analysis with EC detection was performed with an ESA model 5600 CoulArray system (Chelmsford, MA, USA) equipped with an in-line degassing unit (Jour Research, Sweden), an ESA model 582 pump, and an ESA model 540

refrigerated autosampler. The detection system consisted of two coulometric array modules, each containing four electrochemical detector cells. Initially, electrode potentials were selected over the range +50 mV to +1000 mV with 150 mV increment against palladium electrodes (exact potentials are given below). The chromatographic separation was achieved on an ESA MD-150 reversed-phase C₁₈ column (3 µm particle size, 150 × 3.0 mm ID) with a Hyper-sil C₁₈ pre-column (7.5 × 4.6 mm ID, 5 µm). The column and detectors were housed in a thermal chamber maintained at 30°C. A mobile phase flow rate 0.5 ml/min was used in all experiments and 10–20 µl of sample was injected into the column. The system was controlled and the data were acquired and processed using the CoulArray software (Version 1.04).

In HPLC studies with EC detection (I, II, III), the sample constituents were identified based on their retention time ($\pm 2\%$) as well as peak height ratios across the channels compared to corresponding values of pure standard. All peaks with ratio accuracy higher than 0.75 (standard and unknown peaks ratios matched more than 75%) and proper retention time were assessed. Ratio accuracy is the characteristic defined by the CoulArray software that describes how well the sample response ratio between two subsequent electrodes matches the corresponding standard response ratio.

The HPLC with fluorescence detection for glutamate and GABA analysis (V) contained a quaternary pump (Perkin Elmer Series 200, USA) equipped with an in-line degassing unit (Jour X-act Degasse, Jour Research, USA), autosampler (Perkin Elmer Series 200, USA) and fluorescence detector (CMA/280, USA) with fixed wavelengths (excitation: 330–365 nm and emission: 440–530 nm). The chromatographic separation was achieved on reversed-phase C₁₈ column (4.6 × 50 mm, particle size 3.5 µm; Agilent Zorbax SB-C18, USA) protected by C₁₈ pre-column (7.5 × 4.6 mm, particle size 5 µm; Alltech, USA) at room temperature. In the case of glutamate and GABA analysis, the sample constituents were identified based on their retention time ($\pm 2\%$).

Principles of HPLC-EC technology

Since the HPLC-EC method development was performed in the current study, the condensed overview of main principles and characteristics of HPLC and EC detection technology are given below. HPLC is a form of column chromatography with high separation efficiency, used frequently in biochemistry and analytical chemistry. HPLC is used to separate components of a mixture by using a variety of chemical interactions between the substance being analyzed (analyte) and the chromatography column. In isocratic HPLC the analyte is forced through a column of the stationary phase by pumping a liquid (mobile phase) at high pressure through the column. In gradient HPLC the composition of the mobile phase is changed during the separation of mixture. The sample to be analyzed is introduced in a small volume to the stream of the mobile phase

and is retarded by specific chemical or physical interactions with the stationary phase as it traverses the length of the column. The amount of retardation depends mainly on the nature of the analyte and mobile phase composition and less on the stationary phase. The time at which a specific analyte elutes (comes out of the end of the column) is called the retention time and is considered a reasonably unique identifying characteristic of a given analyte. A term called the *retention factor* k (formerly referred to as the capacity factor) is often used to describe the elution rate of an analyte on a column. The retention factor k is given as: $k = t_R - t_0 / t_0$, where t_R is the analyte retention time and t_0 is the time taken for the mobile phase to pass through the column, both times are easily obtained from a chromatogram. When an analyte's retention factor is less than one, elution is so fast that accurate determination of the retention time is very difficult. High retention factors (greater than 20) mean that elution takes a very long time. Ideally, the retention factor for an analyte is between one and five. In the case of reverse phase HPLC the nonpolar stationary phase (i.e. C₁₈ silica) interacts with analytes depending on their polarities and the retention is primarily controlled by the mobile phase. While the retention of ionic compounds in the reverse phase HPLC is complicated due to their infinite polarity, the use of ion pair reagents is required. When the organic ionic substance is added to the mobile phase, it forms an ion pair with a sample component of opposite charge and the retention of the generated neutral complex can be affected. In the case of weak organic acids and bases the alkyl- or arylsulphonate (i.e. sodium octylsulphonate, sodium heptylsulphonate) are widely used for control the retention of ionic substances. Electrochemical detection in HPLC involves the use of an electric potential to promote a chemical reaction. The electrochemical detector responds to substances that are either oxidisable or reducible. The current is an electron flow generated by a reaction that takes place at the surface of the electrodes and this current is proportional to the concentration of the analyte. The coulometric array detector consists in several electrodes placed in series. While the electrodes are made of porous graphitic carbon and the mobile phase can flow through the electrode and therefore, the electrode surface can react with electroactive compounds with nearly 100% efficiency, the detector is named coulometric as well as considered to be highly sensitive.

Generation of hydrodynamic voltammograms (HDV)

A plot of electrode potential vs peak response (i.e. height or area) describes the characteristic named hydrodynamic voltammogram, a current – potential relationship of a given analyte under defined analysis conditions. HDVs facilitate the selection of proper working electrode potentials, which are critical for the accurate, selective and sensitive measurement of sample constituents. To determine the current – potential relationships for all compounds, one electrode

was selected from an eight-electrode array and maximal potential (1100 mV vs palladium reference electrode) was applied to it. Electrode signal was allowed to equilibrate for 30 min, next, the mixture of standards was injected to column and the chromatogram was recorded as well as the peak heights were determined for all components. Then, the electrode potential was reduced 50 mV and the prior procedure was repeated step by step until 0 mV potential. The peak heights at 1100 mV potential were considered maximal and the every single peak height acquired at different electrode potential was divided by maximum value for obtaining relative peaks heights. These relative values vs electrode potentials were plotted for the generation the hydrodynamic voltammograms.

Behavioural testing (III, IV)

Behavioural response to gentle handling

For the estimation of seizure/myoclonic activity, each mouse was taken from their home cage; the mouse was gently picked up by the tail and turned in the palm of the hand from one side to the other and then placed on a flat desk for 30 seconds for evaluation. Myoclonic behaviour (i.e. brief twitching of whiskers, ears, or tail; facial spasms; shaking and jerks of limbs, head and/or torso) was assessed in a 5 step scale as follows: 0, no myoclonic activity; 1, single myoclonic jerk or frequent twitching of whiskers, ears, or tail; 2, repeated myoclonic jerks of limbs, head and/or torso; 3, frequent myoclonic seizures; 4, continuous myoclonic events during the handling.

Inverted wire-grid test

The sensomotor functions were estimated by using an inverted wire-grid test. Mice were placed on an elevated horizontal wire grid positioned 40 cm above an upholstered surface. The net was turned then to 180° and let animals to grasp and hang on the wire mesh. The latency of falling was recorded for up to 5 minutes.

Rotarod test

Motor coordination and balance of mice were measured using rotarod. All mice were pre-trained on the rotarod in order to reach a stable performance. The training consisted of seven training sessions with constant speed at 10 rpm over a 10-min period during one week. The final test (18 runs, each lasting 150 s,

and three runs per each rpm) was performed on the third day at 10, 15, 19, 22, 26 and 33 rpm.

Blood and brain samples (II, III, V)

For HPLC analysis mice were decapitated day after the behavioural testing and the brains were removed quickly on ice. Cerebellum, cerebral cortex and subcortical area, which contained hippocampus, basal ganglia, brain stem were dissected, immediately frozen and stored at -80°C until analysed.

In experiment V mice brains were dissected to cerebellum and cerebrum. The left and right hemisphere from both sections was distributed randomly between groups in order to obtain material for gene expression and biochemical studies. Thereafter, tissue was quickly placed in liquid nitrogen and stored at -80°C .

Approximately 50–100 μl of blood was collected from mouse femoral vein; centrifuged and obtained serum was instantly frozen and stored at -80°C (II, III). For HPLC studies (II, III, V) mouse brain tissue was weighted and disrupted with an ultrasonic homogenizer in an ice-cold solution of 0.1–0.12 M PCA (1:5, w/v) while to the mouse serum 1:1 (v/v) PCA was added. The homogenate or serum were then centrifuged at $13\,000 \times g$ for 10 min at 4°C , supernatant was collected and stored at -80°C until analyzed.

Human blood samples (II)

The human serum samples were obtained from Dr. Anna-Elina Lehesjoki, University of Helsinki, Finland. In all patients, EPM1 diagnosis was confirmed with a genetic test. All patients were treated with sodium valproate, other antiepileptic treatment varied. Three patients were female; two male, average age was 33 ± 5 years. Human samples were treated the same way as mouse sera for HPLC analyses.

Western blotting (IV)

Tissue proteins were isolated from frozen cerebellum using lysis buffer: 50 mM Tris-HCl (pH 7.4), 150 mM NaCl, 1% Triton X 100, and protease inhibitors. A total of 0.5 ml of the lysis buffer was added to samples, homogenized with a pellet pestle, and incubated on ice for 1 h. After centrifugation ($20,000 \times g$ for 20 min at 4°C) a supernatant was taken for further assay. The protein concentration was determined by the RC DC Protein Assay (Biorad, Hercules, CA, USA). The lysates (30 μg) were resolved by electrophoresis on 12% SDS-

polyacrylamide gel. Proteins were transferred onto polyvinylidene difluoride membranes in 0.1 M Tris base, 0.192 M glycine, and 20% (w/w) methanol using an electrophoretic transfer system. The membranes were blocked with 0.1% (w/w) Tween 20/TBS (T-TBS) containing 10% (w/w) nonfat dried milk at room temperature for 1 h. Then the membranes were incubated with 2.0 µg/ml monoclonal anti-mouse cystatin B antibodies (MAB1409, R&D System, Minneapolis, MN, USA) in T-TBS containing 10% nonfat dried milk at 4°C temperature and kept overnight. After three washes with T-TBS, the membranes were incubated with peroxidase-conjugated anti-rat antibody (Vector Laboratories, CA, USA) and diluted with 1:5,000 T-TBS at room temperature for 2 h. The membranes were then washed four times with T-TBS, and visualized using the ECL chemiluminescence system (Amersham). Immunoblots were quantified using a UVP bioimaging acquisition and image analysis system. To normalize cystatin B immunoreactivity, β -actin protein was measured on the same blot with a mouse monoclonal anti- β -actin antibody (Sigma St. Louis, MO, USA) as an internal control for loading and cystatin B/ β -actin optical density ratio was calculated.

Evaluation of neuronal density (IV)

Animals were deeply anaesthetized with chloral hydrate (400 mg/kg) and transcardially perfused with normal saline and then with 4% paraformaldehyde in a phosphate-buffered saline (PBS, 0.1 M, pH 7.4), the brain was removed and postfixed for an additional 48 h in a paraformaldehyde solution. Brains were then sectioned by vibratome (Leica VT1000, Germany) in the coronal plane at 40-µm thick sections. Each tenth section was stained by hematoxylin-eosin and neuronal density was estimated using CAST (Computer-Assisted Stereological Toolbox) Grid 2.0 software (Olympus, Denmark). Nuclei were counted in optical dissectors using systematic random sampling. Dissector dimensions were $10.9 \times 10.9 \times 20$ µm ($W \times H \times D$) for cerebellum and $22.4 \times 22.4 \times 20$ µm for cerebral cortex. Numerical density (N_v) was calculated according to the formula $N_v = "Q"/"v$ (dis), where "Q" is the number of cells counted and "v (dis)" is the volume of dissectors. The observed coefficient of error varied from 0.063 to 0.091. The volume of the specific brain structures was estimated according to Cavalieri's principle by summing up the points falling on the cross-sectional area of all sections and by multiplying the distance between two sections by the thickness of the section and by the area associated with each point. The total number of cells was calculated from the density (N_v) of the cells multiplied by the reference volume of the structure (West, 1993).

Detection of neuronal death with Fluoro-Jade staining (IV)

Fluoro-Jade staining was applied to estimate the CSTB-deficiency induced neuronal death in mice brain. Brain sections were immersed in 100% ethanol for 3 min and dehydrated through graduated alcohol solutions. Sections were then incubated in 0.06% potassium permanganate solution for 15 min, rinsed with distilled water, and incubated in a solution of 0.001% Fluoro-Jade (Histo-Chem, Jefferson, USA) in 0.1% acetic acid for 30 min. After staining, sections were rinsed in distilled water, air-dried, immersed in xylene and coverslipped.

Gene expression study (V)

mRNA isolation and cDNA synthesis

Total mRNA was isolated from frozen tissue samples (50–200 mg) using the TRIzol reagent technique according to the manufacturer's instructions (Invitrogen, France). Oligo-dT first-strand cDNA was synthesized from 2 µg of total RNA using Superscript II reverse transcriptase (Invitrogen, France).

Quantitative real-time PCR

For quantitative real-time PCR (qPCR) studies ABI PRISM 7700 Sequence Detection System equipment (PE Applied Biosystems, USA) and ABI PRISM 7000 SDS Software were used. Primers (Table 2) were designed using the Primer Express TM software (PE Applied Biosystems, USA). Forward and reverse primers (Table 2) were each designed in a different exon of the target sequence, eliminating the possibility of amplifying genomic DNA. For each set of primers, a basic local alignment search tool (BLAST) search revealed that sequence homology was obtained only for the target gene. PCR amplification was performed in a total reaction volume of 20 µl in 4 parallels. The reaction mixture consisted of 5 µl diluted template, 10 µl 2× SYBR Green PCR Master Mix (PE Applied Biosystems, USA), and 0.5 µM forward and reverse primers. Amplification specificity was controlled by a melting curve analysis and a gel electrophoresis of the PCR product. Six-fold serial dilution from one *Cstb*^{+/+} sample mRNA were analyzed for each target gene and allowed to construct linear standard curves from which the concentrations of the test sample and efficiency of reverse transcription were calculated. Results were normalized to cyclophilin A (*CycA*) transcription to compensate for variation in input RNA amounts.

Table 2. Sequences of primers used for qRT-PCR studies

Target gene		Primer sequences	PCR product size (bp)
vGABAT1	Forward	5'- GGA GAC ATT CAT TAT CAG CG -3'	220
	Reverse	5'- AAG ATG ATG AGG AAC AAC CC -3'	
GAD65	Forward	5'- GCC TTA GGG ATT GGA ACA GA -3'	176
	Reverse	5'- GCC AAG AGA GGA TCA AAA GC -3'	
vGLT1	Forward	5'- CTG CTT GTG AGT GGC TTC AT -3'	248
	Reverse	5'- ATA ATG GCC CAG AGT GGA AG -3'	
CycA	Forward	5'- GAG CAC TGG GGA GAA AGG AT -3'	259
	Reverse	5'- CTT GCC ATC CAG CCA CTC AG -3'	

vGABAT1 – vesicular GABA transporter 1; vGLT1 – vesicular glutamate transporter 1; GAD65 – glutamate decarboxylase, 65kDa; CycA – cyclophilin A.

Statistical analysis

The data are expressed as mean \pm SEM. The Student t-test was used to compare data in different groups. Least-square linear regression analyses were applied to obtain the linear regression equation for standard curves and for the calculation of analyte concentrations.

RESULTS

HPLC-EC method for the assay of tryptophan metabolites from the biological samples

Optimisation of chromatographic conditions

The validation of the analytical method for achieving the HPLC separation of thirteen substances (an exact list of components is given in Materials and methods in the Chemicals section) was started by using mobile phase containing 0.1 mM monobasic sodium phosphate-acetate buffer (pH 3.10), 10% methanol and 0.55 mM SOS. This eluent has been successfully used for the determination of catecholamines, 5HT and 5-HIAA from brain tissue homogenates in our laboratory. Whereas several catecholamines occur endogenously in many brain region and due to their relative physicochemical similarity to TRP metabolites, these compounds may disturb the selective chromatographic analysis of target analytes in biological samples. Therefore, we subjected catecholamines to the method development procedure as well. Initial detection potentials were set from 50 mV (at electrode 1) to 1000 mV (at electrode 8) with 150 mV increment vs palladium reference.

To enhance the selectivity of the former method and to separate additionally the kynurenines and TRP from the same sample, we started the chromatographic optimisation from adjustment of the composition of the mobile phase. Initially, the concentration of ion pair reagent was varied, while other constituents of eluent were held constant. An increase in the concentration of SOS from 0.4 to 1.5 mM or SHS from 1 to 2 mM predictably elevated the retention factor k values of basic (3HOKYN, NA, KYN, DA and 5HT) or neutral (TRP) compounds (Figure 3). The magnitude of this effect is dependent on ion pair agent type i.e. the length of organic chain in pairing agent as well as the retention of a compound. Later eluting basic metabolites show a greater increase in retention than earlier eluting basic substances. On the other hand, the retention times of acidic metabolites (XANT, KYNA, DOPAC, 5HIAA, ANA and HVA) slightly decrease. While the HVA and DOPAC as well as 3HOKYN and NA have very similar chromatographic behaviour at these conditions, the changes in ion pair agent content and type alone in these ranges do not give a complete resolution of all thirteen substances.

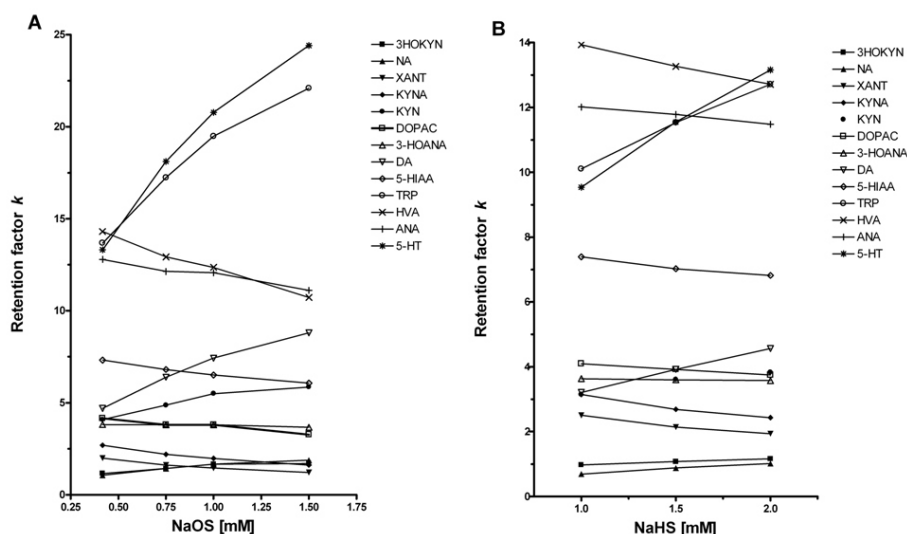


Figure 3. Effect of (A) sodiumoctylsulphonate (NaOS) and (B) sodiumheptylsulphonate (NaHS) concentration in mobile phase on retention factor of various tryptophan metabolites and catecholamines. Exact list of components is given in Materials and methods in the Chemicals section.

The influence of organic modifier (MeOH) content to retention factors was predictable. An increase in the amount of methanol from 6 to 12% decreased retention times of all components of the standard mixture, having a minor influence on elution order (data not shown). The effects of the mobile phase pH are related to the degree of ionisation of the sample molecules and are dependent on their dissociation constant values. The weak organic acids are protonated at low pH and will dissociate as the pH increases. Accordingly, raising the pH in a range of 3.10 to 4.60 preferably decrease the retention of acidic metabolites with the carboxylic group such as XANT, KYNA, DOPAC, 5HIAA, HVA, ANA and TRP (Figure 4). In the pH range used, the basic amines stay protonated and therefore their retention nearly remains invariable. Finally, we compromised between adequate resolution and sample run time and found the following mobile phase composition to be optimal: 50 mM monobasic sodium phosphate, 50 mM sodium acetate, 0.42 mM sodium-octylsulphonate, 10% (v/v) methanol, pH 4.10. As shown in Figure 5, under these conditions all thirteen substances elute from column within 20 min.

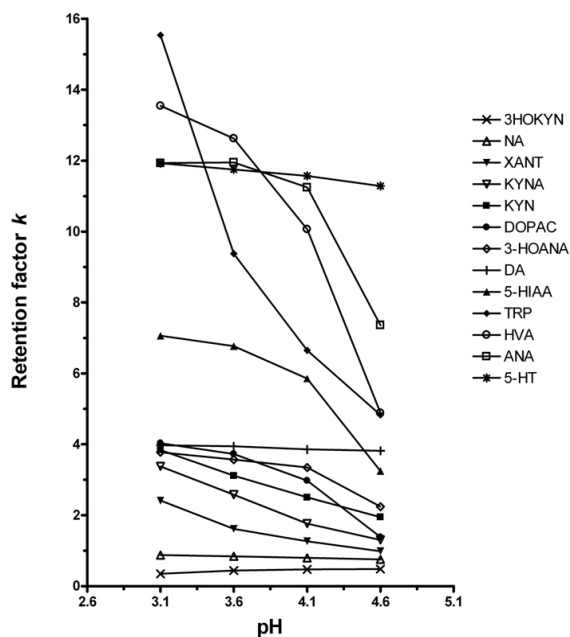


Figure 4. Effect of mobile phase pH on retention factor of various tryptophan metabolites and catecholamines. Exact list of components is given in Materials and methods in the Chemicals section.

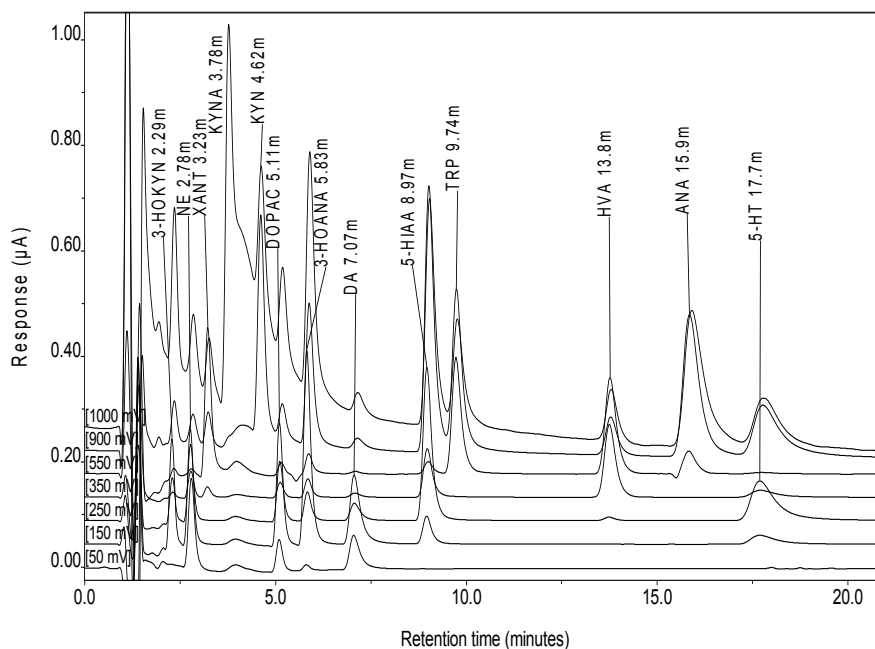


Figure 5. Typical multichannel chromatogram of a standard mixture (60 ng/ml).

Hydrodynamic voltammograms

The relative peak heights vs electrode potentials were plotted to obtain the hydrodynamic voltammograms for all standards. As can be seen in Figure 6, several compounds have more than one characteristic hill on the HDVs corresponding either to oxidizable hydroxy or amino group in their structure. For instance, 5HT and 5-HIAA show two distinct characteristic potentials; the lower is due to oxidation of the hydroxy group and the higher one from oxidation and opening the pyrrole ring of the indole structure while the KYNA, KYN and HVA represent only single maximum on current-potential plot. On the bases of HDVs, the cell potentials were selected so that each compound was detectable at two or three subsequent electrodes: the leading, dominant and consecutive channel. Thus, the suitable cell potentials were as follows: 50 mV at electrode 1, 150 mV at electrode 2, 250 mV at electrode 3, 350 mV at electrode 4, 550 mV at electrode 5, 900 mV at electrode 6, 1000 mV at electrode 7 and electrode 8 was unused.

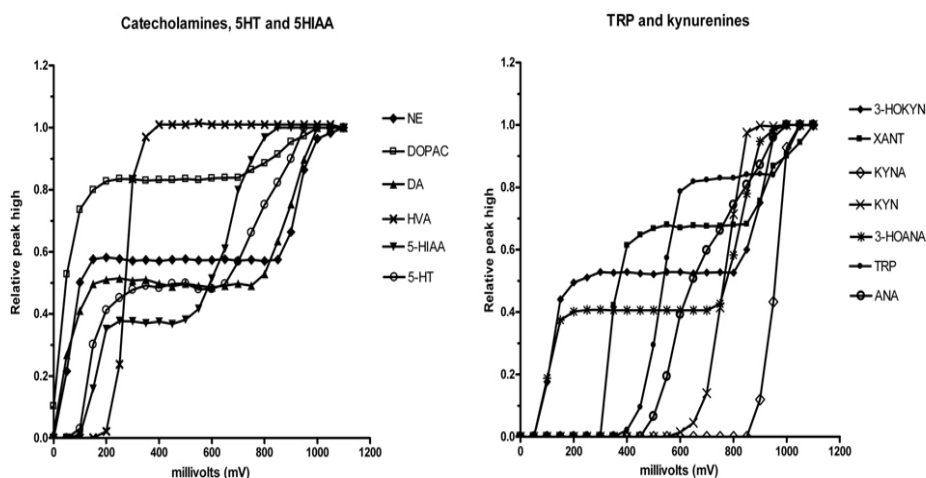


Figure 6. Hydrodynamic voltammograms obtained by plotting relative peak heights from each standard as a function of the potential (mV) applied on the working electrode. The peak heights at 1100 mV potential were considered maximal and every single peak height acquired at a different electrode potential was divided by maximum value for obtaining the relative peaks heights.

Assay performance

Assay linearity was examined by analysing the pooled standards at six concentration levels in triplicate. By least-squares regression analysis, the detector response were directly proportional with standard concentrations ($R^2 > 0.999$) for all substances, and calibration curves were linear from baseline values to 300 ng of each analyte injected. Data from assay performance are summarised in Table 3. The detection limits depended on the working potential and were between 12 and 104 pg per 20 μ l of standard injected. The repeatability was evaluated by analysing six replicates of a pooled standard. Intraday concentration variability (RSD%) ranged from 0.3% (DOPAC) to 1.7% (ANA). Variability between runs was studied by assessing standard solutions on 10 separate days. Interday variability was also excellent, changing between 0.6% (HVA) and 3.8% (KYN and KYNA). To establish the applicability of the method, the tissue homogenates of mice brain as well as serum were analysed using the newly developed HPLC–EC method.

Table 3. Chromatographic and electrochemical characteristics of analytes

Compound	Abbreviation	Retention time (min)	Dominant channel potential* (mV)	Detection limit (pg per 20 μ l injected)
3-hydroxykynurenine	3HOKYN	2.29	150	25
Noradrenaline	NA	2.78	150	13
Xanthurenic acid	XANT	3.23	550	50
Kynurenic acid	KYNA	3.78	1000	104
Kynurenine	KYN	4.62	1000	26
Dopac	DOPAC	5.11	150	12
3-Hydroxyanthranilic acid	3HOANA	5.83	150	15
Dopamine	DA	7.07	150	14
Hydroxyindoleacetic acid	5HIAA	8.97	250	23
Tryptophan	TRP	9.74	900	35
Homovanillic acid	HVA	13.80	550	17
Anthranilic acid	ANA	15.90	900	39
Serotonin	5HT	17.70	250	32

* The dominant channel potential is the electrode potential where the maximum signal occurs for a given substance.

Tryptophan and its metabolites in the blood of EPM1 patients and *Cstb*^{-/-} mice

To assess the *Cstb*-deficiency induced changes in the levels of tryptophan metabolites, we used the newly validated HPLC–EC method for the determination of concentrations of analytes in mutant mice and EPM1 patients' blood. The data on Table 4 reveal similarities as well as differences between EPM1 patients and *Cstb*^{-/-} mice with regard of tryptophan and its metabolites in their blood. In patients with EPM1 the concentration of serum TRP was significantly reduced, whereas in *Cstb*^{-/-} mice it remained unchanged as compared to control wild-type animals.

The significant decrease in 5HIAA levels and, although being non-significant, a trend toward a reduction in 5HT concentration was observed in the serum of EPM1 patients (Table 4). The concentrations of 5HT in *Cstb*^{-/-} mice were significantly reduced in comparison with *Cstb*^{+/+} mice. Despite the reduction of tryptophan the level of the first intermediate in kynurenine pathway, KYN remained unchanged, whereas the concentrations of the next metabolite 3HOANA demonstrated a clear trend toward reduction in EPM1 patients (Table 4). Since, 3HOANA concentrations were measured only in two patients the data, however, cannot be regarded as conclusive. Distinct results were obtained from *Cstb*^{-/-} mice, which demonstrated significantly lower concentration of 3HOANA as compared with control wild-type animals. Levels of the other kynurenines and catecholamines were invariable in both, the mutant mice and EPM1 patients' blood (data not shown).

Table 4. The concentrations of tryptophan (TRP) and its metabolites, serotonin (5HT), kynurenine (KYN) and 3-hydroxyanthranilic acid in the serum of EPM1 patients and *Cstb*-deficient mice. The serum was obtained from either healthy subjects (n=4) or patients with diagnosed EPM1 (n=5). +Concentrations of 3HOANA were measured in the serum obtained from two EPM1 patients only. In animal study, the serum was obtained from wild-type (*Cstb*^{+/+}) and homozygous (*Cstb*^{-/-}) mice (n=4 per group). Data are expressed as mean ± SEM. *p<0.05; **p<0.01.

Group	Tryptophan (μM)	KYN (μM)	3HOANA (nM)	5HT (nM)	5HIAA (nM)
Human study					
Control	78.8±4.4	2.4±0.5	24.2±7.1	539±260	59.8±11
EPM1	33.1±3.2**	2.6±1.3	11.8±3.9+	342±110	30.6±1.1*
Mouse study					
<i>Cstb</i> ^{+/+}	158±26	2.6±0.92	30.1±6.5	15.9±1.2	1.7±0.5
<i>Cstb</i> ^{-/-}	144±13	1.6±0.26	16.9±2.8*	9.9±1.7*	1.3±0.3

Tryptophan and its metabolites in the brain of *Cstb*^{-/-} mice

After observing the changes in TRP and 5HT levels in the blood of EPM1 patients and *Cstb*^{-/-} mice, we tested whether *Cstb*-deficiency induces impairment in TRP metabolism on mutant mice brain as well. Figure 7 shows the data of neurochemical studies from various parts of the *Cstb*^{-/-} and the *Cstb*^{+/+} mice brain. TRP concentration was significantly increased in the *Cstb*^{-/-} mice cerebellum ($34 \pm 5\%$ of increase compared to the wild-type animals) and cerebral cortex ($20 \pm 4\%$ of increase, Figure 7A), while it remained unchanged in subcortical structures as compared to wild-type mice. Levels of KYN, the first intermediate in the kynurenine pathway, were also elevated in the cerebellum of *Cstb*^{-/-} mice, but not in the cortex or subcortical structures (Figure 7B). The concentrations of KYNA, XANT and ANA were invariable in all brain regions tested (data not shown).

5HT and its metabolite 5HIAA levels in the cerebellar tissues of *Cstb*^{-/-} mice increased by more than 50% compared to corresponding values in the wild-type mice cerebellum (Figure 7C and D). An even more prominent elevation of 5HT levels was observed in the cortex of *Cstb*^{-/-} mice, where the 5HT concentration was 1501 ± 134 ng/g compared to 878 ± 95 ng/g in control animals. The levels of 5HIAA in the cortical tissues of *Cstb*^{-/-} mice were also higher than in controls. Values for 5HIAA in the cortex of *Cstb*^{-/-} mice were 292 ± 13 ng/g and in control mice 172 ± 8.7 ng/g, respectively. No changes in the levels of 5HT and its metabolite 5HIAA were observed in subcortical areas when compared with the wild-type mice brains. We also determined the concentrations of catecholamines, however, levels of these analytes remain constant throughout of the *Cstb*^{-/-} and the *Cstb*^{+/+} mice brain (data not shown).

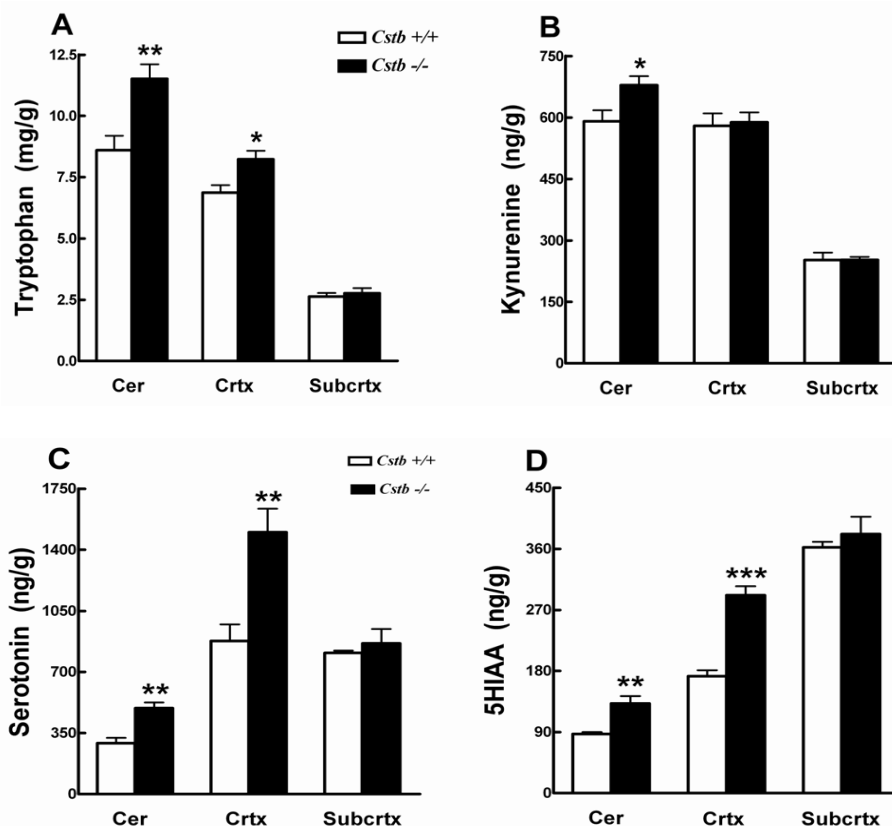


Figure 7. Levels of tryptophan and its metabolites in different regions of *Cstb*-deficient mice brain compared to the control animals. Tryptophan (A) concentrations are given in mg/g of wet weight of tissue, while kynurenine (B), serotonin (C) and 5HIAA (D) concentrations are in ng per g tissue. Data are presented as mean concentration \pm SEM (n = 6). * $p < 0.05$; ** $p < 0.01$; *** $p < 0.001$ (Student's *t* test). Abbreviations: Cer, cerebellum; Crtx, cerebral cortex; Subcrtx, subcortical structures; 5HIAA, 5-hydroxyindole acetic acid.

Glutamate and GABA content in the brain of *Cstb*^{-/-} mice

To estimate the *Cstb*-deficiency induced changes in the concentration of main excitatory and inhibitory neurotransmitters in the brain of mutant and wild-type mice, the HPLC with fluorescence detection were used. As illustrated on Figure 8, the concentration of glutamate was significantly reduced (about 15%) in *Cstb*^{-/-} mice cerebellum and cerebrum compared to those of control mice. No changes in the cerebellar GABA levels of *Cstb*^{-/-} mice, however were observed. The significant, more than 25% decrease in GABA levels was seen in the cerebrum of mutant mice.

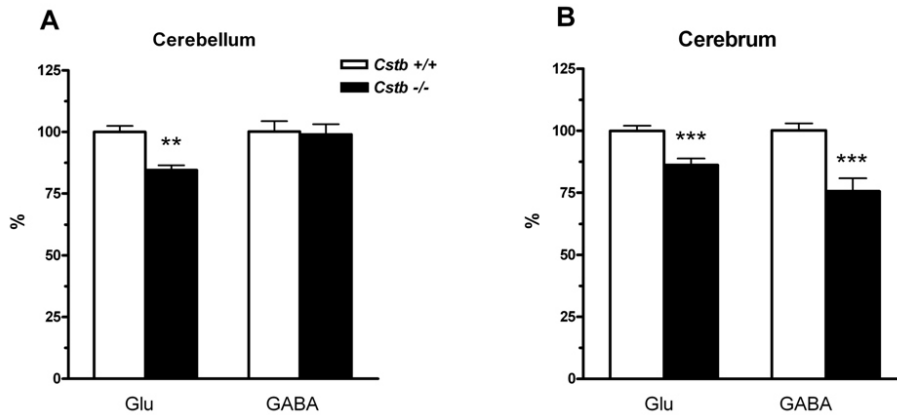


Figure 8. Glutamate (Glu) and GABA content in the *Cstb*^{-/-} cerebellum (A) and cerebrum (B). Results are given in % compared to corresponding control group; mean concentrations \pm SEM of *Cstb*^{+/+} animal group are taken 100%.** $p < 0.01$; *** $p < 0.001$ (Student's *t* test).

The expression levels of vesicular glutamate and GABA transporters in the brain of *Cstb*^{-/-} mice

Real-time quantitative PCR was used to estimate the gene expression levels of vesicular glutamate and GABA transporter, which are considered as a qualitative marker for either glutamate- or GABAergic neuronal phenotype. RT-PCR analysis revealed the significant reduction (2.4 fold) in vGLT1 gene expression in *Cstb*^{-/-} mice cerebellum (Figure 9A) as compared to wild-type animals, while the vGABAT1 transcription levels remained unchanged. Interestingly, the cerebellar GAD65 expression was elevated 1.4 times. The trend toward the reduction of vGABAT1 and vGLT1 transcript levels in *Cstb*^{-/-} mice cerebrum (Figure 9B) was observed; however these declines did not reach any statistical significance.

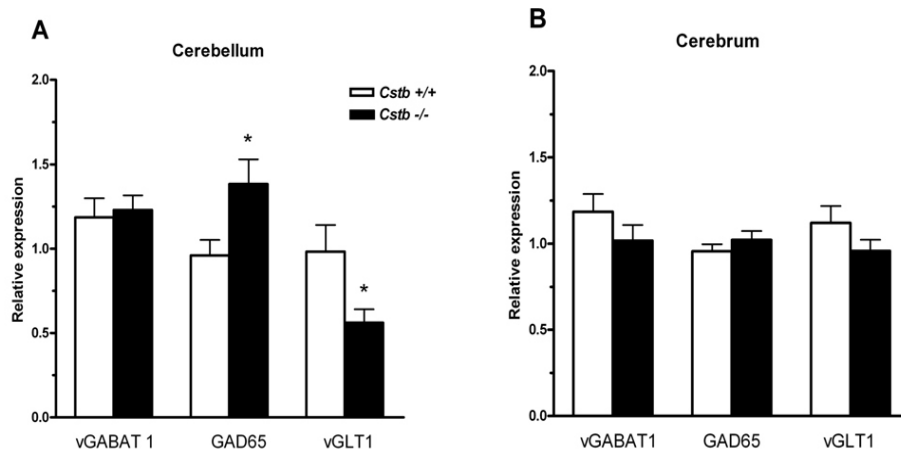


Figure 9. Real-time quantitative RT-PCR analysis of mRNA expression of vesicular GABA transporter 1 (vGABAT1), glutamic acid decarboxylase 65 kD (GAD65) and vesicular glutamate transporter 1 (vGLT1) in the *Cstb*^{-/-} mice cerebellum (A) and cerebrum (B) compared to control animals. Results are given as means \pm SEM of values normalized to cyclophilin A (CycA) transcription. * $p < 0.05$ (Student's *t* test)

Western blotting (IV)

Cystatin B protein expression in heterozygous mice cerebellum was measured by Western blot using monoclonal antibody against recombinant mouse Cstb. As expected the cerebellar Cstb protein content was found to be two times lower in heterozygous mice than their wild-type littermates (Figure 10).

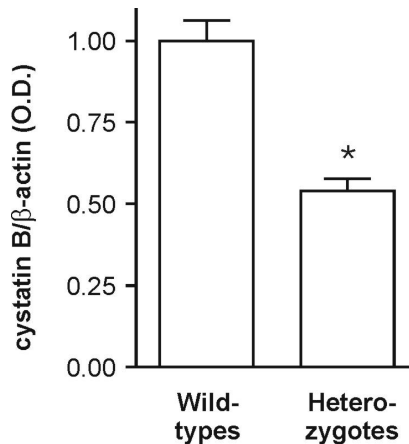


Figure 10. *Cstb* expression in wild-type and heterozygous mice. Lysates of cerebellum from three wild-type and three heterozygous adult mice were subjected to Western blotting using the anti-cystatin B and anti- β -actin antibodies. *Cstb* immunoreactivity and β -actin protein were measured on the same blot with antimouse *Cstb* antibody and anti- β -actin antibody and cystatin B/ β -actin optical density ratio was calculated. * $p < 0.05$ (Student's *t* test).

Behavioural alterations of homozygous and heterozygous *Cstb* mice

To further characterize the myoclonic phenotype of *Cstb*^{-/-} mice and evaluate whether the partial decrease in cystatin B expression in heterozygous mice could also lead to the development of EPM1 phenotype, the gentle handling, inverted wire-grid and rotarod test were performed.

Mild handling test (stimuli sensitive myoclonus). The gentle handling test revealed apparent myoclonic events during the mild handling of five-month-old *Cstb*^{-/-} mice. All animals in the *Cstb*^{-/-} group possessed at least one myoclonic episode within the short observation period and altogether gathered significantly higher myoclonus scores (1.33 ± 0.21 , $n = 6$, $p < 0.01$, Figure 11A) than wild-type mice (0.17 ± 0.16 , $n = 6$).

We tested also whether the aged heterozygous and wild-type mice are prone to handling-induced convulsions. Mild handling response were apparent in heterozygous mice and ranged from a single myoclonic jerk to repeated myoclonic jerks of limbs, head, and/or torso (Figure 12A). While the seizure rating score for all except one wild-type mouse was close to background, for half of the heterozygotes (7 of 14) it was above the background levels ($p = 0.04$; 16% variability in wild-type group and 43% in heterozygous group). Additionally, it is interesting to note that spontaneous seizures were observed in a few heterozygous mice similar to homozygous mice.

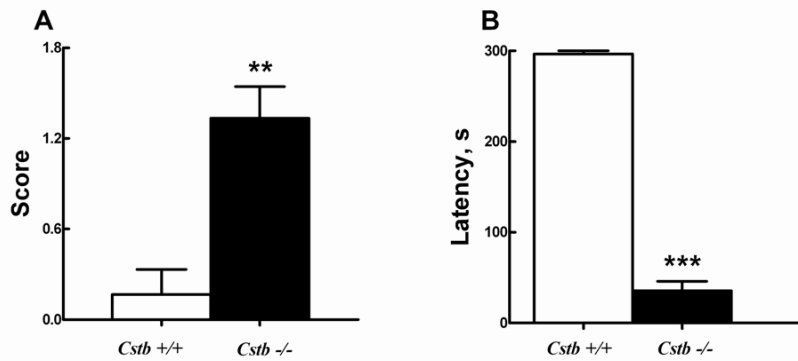


Figure 11. 5-month-old *Cstb*-deficient mice showed a myoclonic activity response to gentle handling (A) and had impaired performance in the inverted wire grid test (B). Score of myoclonic activity was recorded using a 5 step scale (see Materials and methods). Final data are expressed as the mean score \pm SEM ($n = 6$). In wire grid test (B) the latency time of falling was recorded up to 5 min. Latency time \pm SEM are presented in seconds. ** $p < 0.01$; *** $p < 0.001$ (Student's t test). Abbreviations: *Cstb* +/+, wild-type mice; *Cstb* -/-, cystatin B-deficient mice

Inverted wire-grid test. Myoclonic events described above were accompanied by a serious decline in the sensomotor performance in *Cstb*-deficient mice. In comparison with littermate controls, the *Cstb* -/- mice performance in the wire hanging test clearly deteriorated (Figure 11B, $p < 0.001$). Mutant mice had a latency time of falling, 35 ± 10 seconds, while control mice remained suspended on the grid mostly until the end of the test (297 ± 3 s).

Similar findings were obtained with heterozygous mice in the grid test. Results depicted in Figure 12B show that *Cstb* +/- mice were able to hang onto the wire for a significantly shorter period of time than age-matched wild-type animals ($p = 0.04$), although, the variability of experiments was higher in the heterozygous group (103% vs 61%). Both findings i.e. myoclonic episodes and ataxia are characteristic of EPM1 and show that *Cstb*-deficient mice had developed an EPM1-like phenotype.

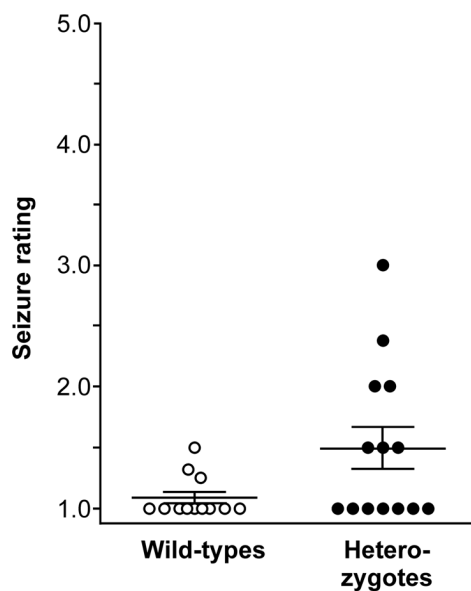


Figure 12A. Myoclonic behaviour of wild-type and heterozygous mice. Myoclonic behaviour in response to gentle handling was assessed in a 5-step scale as described in Materials and Methods.

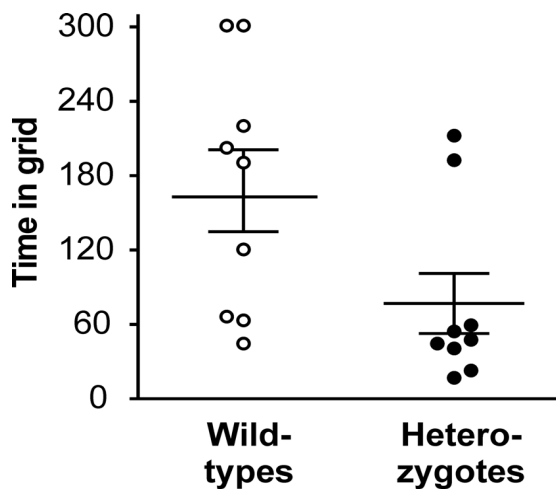


Figure 12B. Latency of falling from wire mesh. Performance of the wild-type and heterozygous mice in wire mesh was assessed as described in Methods.

The rotating rotarod test. The performance on rotating rotarod was tested only in elder *Cstb*^{+/-} mice, because the results of rotarod test for *Cstb*^{-/-} mice have been published earlier (Pennacchio *et al.*, 1998). Both wild-type and heterozygous mice performed well in the rotarod test at a rotation speed of 10 rpm or less remaining on the rod almost for the whole 300-s trial. However, when rotation speed was increased, heterozygous mice demonstrated decreased ability to stay on the rod for full trial (Figure 13A). This was most evident at 26 rpm when the majority of *Cstb*^{+/+} mice still remained on the rotating rod, while heterozygous mice were falling from the rod during the first minute ($p = 0.002$). Figure 13B shows that the overall performance of heterozygous mice in rotarod calculated by summarizing the performances at different rotarod speeds, was one-third less than in age matched wild-type animals ($p = 0.01$). Figure 13B also shows greater variability of heterozygous mice when compared with wild-type littermates (coefficient of variation 48% vs 11%). 4 out of 9 heterozygous mice showed rotarod performance similar to the wild-type mice while performance of other heterozygous mice was significantly decreased.

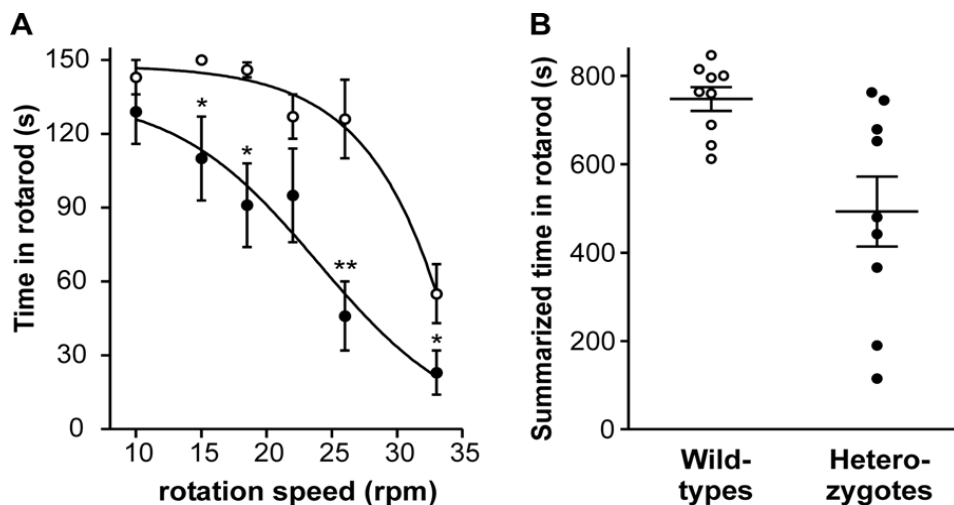


Figure 13. Rotarod performances of wild-type and heterozygous mice. (A) Average time of mice spent at rotarod at different rotation speeds (control, open circles; heterozygote, filled circles). (B) Overall performance of mice in rotarod calculated by summarizing the performances at different rotarod speeds. * $p < 0.05$, ** $p < 0.01$. (Student's *t* test)

Neuronal loss in aged *Cstb* heterozygous mice

Our experiments demonstrated strong Fluoro-Jade signal designating degenerating neurons in cerebral cortex and cerebellar granule cell layer of 9-month-old homozygote mice (Figure 14C). In heterozygous mice no visible Fluoro-Jade signal was found (Figure 14B).

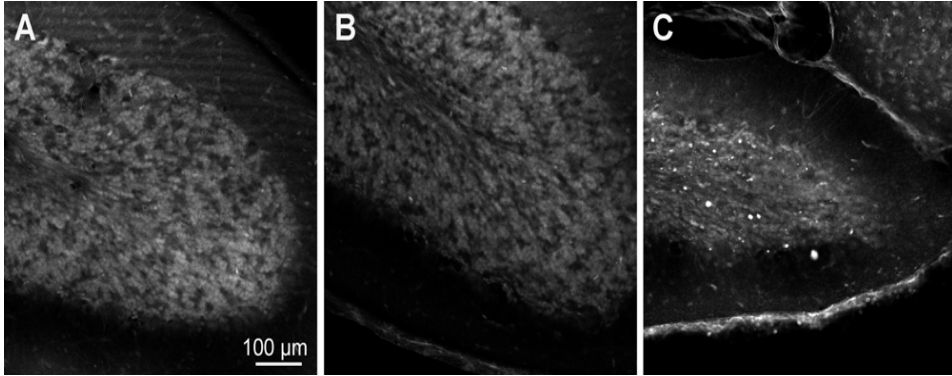


Figure 14. Fluoro-Jade staining of cerebellar sections of wild-type (A), heterozygous (B), and homozygous mice (C). Sections were processed as described in Materials and methods. Fluoro-Jade positive cells in homozygous mice cerebellum were used as positive control.

However, as slow or earlier neurodegeneration could be left undetected by visualizing only degenerating neurons, we also estimated the total neuronal numbers in these regions. Stereological analysis demonstrated no change in the cerebellar volume of heterozygous mice when compared with wild-type mice (Figure 15). However, the density of neuronal cells and also the total number of cells in cerebellar granule cell layer were significantly lower in heterozygous cystatin-B-deficient mice (Figure 15). In heterozygous mice the numerical density of cells in cerebellar granule cell layer was decreased by 19% (from $4.44 \pm 0.11 \times 10^6$ to $3.60 \pm 0.12 \times 10^6$ cells/mm³, $p = 0.0001$) and the total number of cells by 28% (from $20.8 \pm 1.3 \times 10^6$ to $14.7 \pm 0.5 \times 10^6$ cells, unilateral, $p = 0.003$). No change was also observed in the volume of cerebral cortex of heterozygous mice. Similar to cerebellum, numerical density of cells in cerebral cortex of heterozygous animals was decreased by 17% (from $0.554 \pm 0.009 \times 10^6$ to $0.459 \pm 0.009 \times 10^6$ cells/mm³, $p < 0.0001$) and the total number of cells by 19% (from $13.4 \pm 0.5 \times 10^6$ to $10.9 \pm 0.4 \times 10^6$ cells, $p = 0.001$). In contrast to behavioural experiments, the variability in these experiments was the same for the heterozygous group when compared with wild-types (for numerical density 7% vs 10% in cerebellum and 5% vs 6% in cortex and for total cell number 18% vs 10% in cerebellum and 10% vs 10% in cortex).

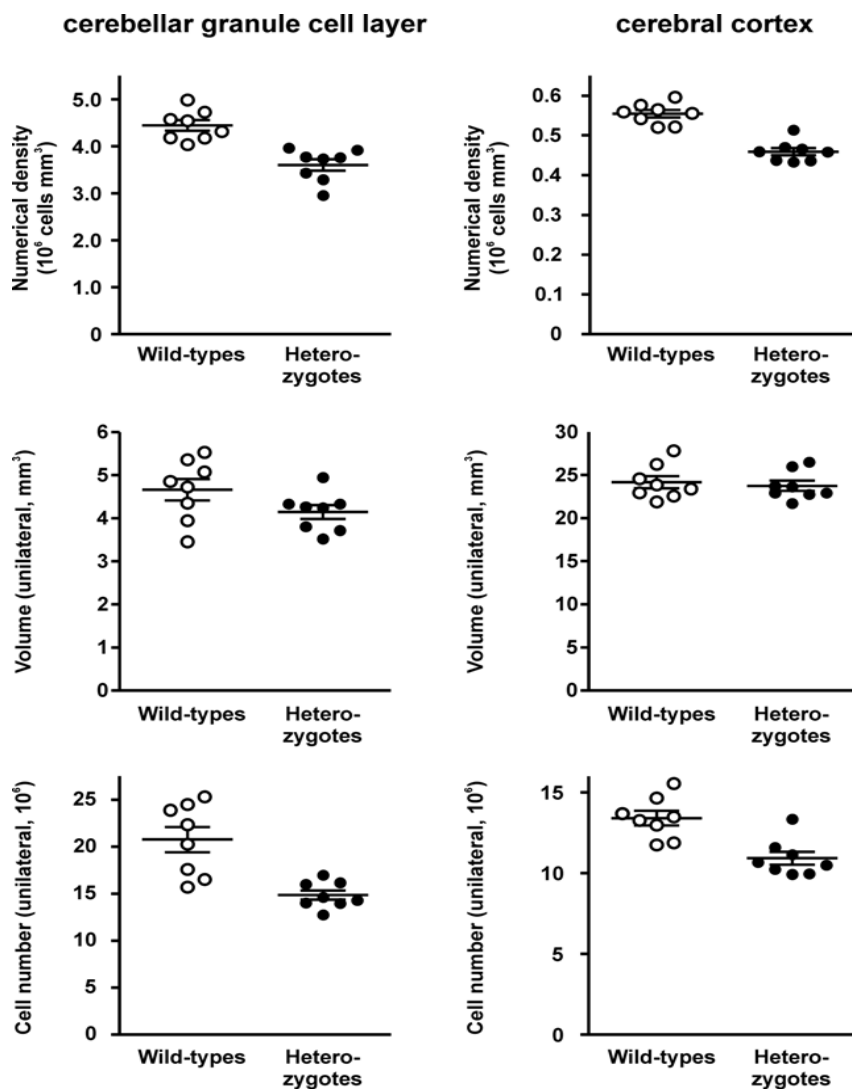


Figure 15. Numerical density of cells, volume, and total number of cells in cerebellar granule layer and cerebral cortex of control and heterozygotes. Stereological analyses were performed as described in Materials and Methods.

DISCUSSION

HPLC-EC method for neurochemical studies (I)

Up to present, several chromatographic protocols have been reported for determination of catecholamines (Lim, 1986) or individual components of tryptophan metabolism in biological fluids. Commonly used techniques are HPLC with fluorescence (Ubbink *et al.*, 1991; Shibata and 1991) or electrochemical detection (Pearson and 1991; Heyes and 1988) and lately the HPLC with mass spectrometry (Morita *et al.*, 1990; Hervé *et al.*, 1996) as well as the combinations of these three facilities (Morita *et al.*, 1990; Hervé *et al.*, 1996; Iwahashi, 1999). The sensitivity of HPLC with UV detection (Holmes, 1988; Marklová *et al.*, 2000) remains too low for biological samples. However, most of these methods are time consuming, employ gradient elution or multi-step detection and separation systems and are optimized for detection some of compounds. A frequently encountered problem during the analysis of complex samples with chromatographic techniques is the reliability of sample constituent identification. As a rule, the identification is based on the comparison of retention times of sample components and standard compounds. Reliable confirmation of peak identity generally requires additional characterisation, which can be, for example, optical or mass spectra or voltammetric responses. In our studies, we used HPLC with electrochemical array detection, where the comparison of the current–potential behaviour of standards and analytes enables to apply an extra characteristic in enhancing the specificity and selectivity of the method.

Thus, we demonstrated that the complicated goal of separation of structurally and physicochemically very similar substances from a single biological sample can be achieved by using the HPLC–EC method. An important factor in the gain of a satisfactory HPLC method was the utilization of analytes' acid-base properties in the modulation their retention. We varied ion pair reagent concentration and type in the mobile phase for assessing their capacity to affect the basic compounds retention as well as investigated the influence of buffer pH on chromatographic performance of acidic substances. The extent and potential of factors to affect the separation of every single substance were already described in detail above under the Results section. Our results indicated that separation conditions for TRP and kynurenines can be similarly affected as reported earlier for catecholamines (Bartlett, 1989; Kontur *et al.*, 1984) and when the chromatographic conditions are carefully optimized, the desired batch of compounds can be analyzed selectively in a single run.

The use of coulometric array detector for determination of catechol- and indolamines has been reported earlier (Gamache *et al.*, 1993; Tanaka and Takeda, 1997) and also the current-potential relationship of these compounds

has been studied in detail (Chi *et al.*, 1999). However, the HDVs depend strongly on chromatographic condition as well as electrodes used. Moreover, comparable information about kynurenines HDVs is insufficient (Issa *et al.*, 1994; Yamamoto *et al.*, 1995). As catecholamines and several tryptophan metabolites contain more than one oxidisable functional group, measurable in the potential range used, we constructed the oxidative hydrodynamic voltammograms for all analytes to increase the reliability and selectivity of compound identification. While the CoulArray software facilitates sample identification by using extra characteristic, ratio accuracy, generation of HDVs and careful selection of working electrodes potentials were required. Ratio accuracy is a number derived from comparison of the electrochemical profile of standard across three adjacent coulometric electrodes to that of an unknown in sample (Gamache *et al.*, 1993). This characteristic entirely bases on physical properties of an analyte in the current chromatographic condition. The greater the similarity of current-potential behaviour between standard and the unknown peak, the closer the ratio accuracy is to unity (Gamache *et al.*, 1993). Conversely, when the ratio accuracy value is low, we can be confident that the apparent peak is probably co-elution of two or more compounds or furthermore, the peak is a single compound of unknown origin (which is often the case in biological samples). In our further studies, we followed the criteria that all peaks with ratio accuracy higher than 0.75 (standard and unknown peaks ratios match more than 75%) and proper retention time ($\pm 2\%$) were assessed. Altogether, under our experimental chromatographic condition it was possible to detect KYNA sensitively and selectively at a lower potential (900 mV) than reported earlier (1060 mV) (Yamamoto *et al.*, 1995). Furthermore, the detection limits in our study (at a signal-to-noise ratio of 3), especially for kynurenines, were much lower than those published in previous reports, where they were hundreds of pg injected for electrochemical detection (Shibata and Onodera, 1991; Heyes and Quearry, 1988) or in ng range for fluorescence or UV detection (Hervé *et al.*, 1996; Marklová *et al.*, 2000). Unfortunately, we failed in the finding of electrochemical detection condition for QUIN, while this compound do not consist of the oxidizable functional group in its structure and the electrode properties did not support the reductive detection mode.

***Cstb*-deficiency induced changes in tryptophan metabolism (II, III)**

Tryptophan and its metabolites in the blood of EPM1 patients and *Cstb*^{-/-} mice

Previous clinical investigations in patients with EPM1 have demonstrated altered tryptophan metabolism in their blood and CSF (Leino *et al.*, 1980; Koskiniemi *et al.*, 1985; Pranzatelli *et al.*, 1995). However, whether these observed variations in tryptophan metabolism in EPM1 patients are related only to the CSTB deficiency induced pathological process or may appear also due to secondary factors such as, for instance, the anticonvulsant drug treatment (Pratt *et al.*, 1984), were still obscure.

Our experiments also established reduced levels of TRP in the serum of EPM1 patients in accordance with previous studies. The *Cstb*-deficient animals, however, did not demonstrate any changes in the serum tryptophan concentration and this suggests that observed reduction in TRP in humans is due to secondary abnormalities seen in EPM1 patients such as drug treatment. Sodium valproate has been shown to reduce serum tryptophan levels (Pratt *et al.*, 1984), probably, because, valproate even in therapeutic concentrations competitively inhibits L-tryptophan binding to human serum albumin (Hiraoka *et al.*, 1992). Poor adsorption of TRP from gastrointestinal tract of EPM1 patients (Koskiniemi, 1980) could also be related to valproate treatment. Despite the observed differences in serum tryptophan levels the concentration of 5HT tended to be reduced in patients with EPM1 and was significantly decreased in *Cstb*-deficient mice. The content of 5HIAA, the intermediate metabolite of serotonin, was significantly diminished in the serum of EPM1 diseased humans as well. These data suggest that disrupted 5HT metabolism is due to the deficiency in the *Cstb* gene and is not related to a decrease in the level of 5HT precursor, L-tryptophan. Abnormalities in the kynurenine pathway of tryptophan metabolism were also observed in serums of both EPM1 patients and *Cstb*-deficient mice. Despite the lack of any changes in concentrations of kynurenine, the second intermediate metabolite 3HOANA was reduced in *Cstb*-deficient mice and a similar trend toward reduction was observed in EPM1 patients. This might indicate that the utilization of 3HOANA along the kynurenine pathway is enhanced. Since 3HOANA is an immediate precursor of quinolinic acid, known as a strong excitotoxin and convulsant (Lapin, 1978), one can propose that production of quinolinic acid is increased in EPM1. Taken together, our data allow us to conclude that cystatin B deficiency can promote the impairment of tryptophan metabolism along 5HT- and kynurenine pathways. Whereas several kynurenines have been implicated as active contributors in the pathogenesis of various neurodegenerative diseases as well

as associated with seizures and myoclonic symptoms, further studies directed toward better understanding of the role of tryptophan metabolism in EPM1 are required.

Tryptophan and its metabolites in the brain of *Cstb*^{-/-} mice and their role in the formation of EPM1-like phenotype

Progressive ataxia, myoclonus and generalized clonic/tonic seizures are characteristic symptoms commonly observed in EPM1 patients. The phenotype of *Cstb*^{-/-} mice also resembles the symptoms found in EPM1 diseased humans. Initial behavioural studies, regarding these mice, have described the development of myoclonus and seizures only during sleep (Pennacchio *et al.*, 1998), however, later the occurrence of myoclonus in *Cstb*^{-/-} mice during wakefulness has also been reported (Houseweart *et al.*, 2003). In accordance with previous studies, *Cstb*^{-/-} mice, in our experiments, demonstrated ataxia, but we also observed that myoclonic events in *Cstb*^{-/-} mice could be induced by handling and lifting of the animal. This corresponds well with the features of myoclonus seen in EPM1 patients, which could be induced by touch, light or other sensory stimulation.

Our neurochemical data demonstrate that the myoclonic phenotype of *Cstb*^{-/-} mice is associated with a constitutively increased TRP metabolism along the serotonin and kynurenine pathways. This was reflected by increased levels of 5HT and its metabolite 5HIAA in the cortex and cerebellum, structures where the most abundant cellular atrophy is found (Shannon *et al.*, 2002). These obtained results are, in some respects, in contrast with the neurochemical changes observed in EPM1 patients. Previous studies have shown the reduction of TRP and 5HIAA concentration in the serum and CSF of patients diagnosed with EPM1 (Airaksinen and Leino, 1982; Pranzatelli *et al.*, 1995). Furthermore, our analysis of the *Cstb*^{-/-} mice serum revealed a reduction of 5HT concentration, while TRP and KYN levels remain unchanged compared to control animals. The discrepancy, concerning the opposite findings in 5HT levels in blood and brain tissues of *Cstb*^{-/-} mice (paper II), suggests that serum serotonin levels do not reflect 5HT levels in the brain tissue. 5HT has a poor blood-brain-barrier permeability and the production, as well as metabolism of 5HT in the brain and peripheral organs, is independent. This might be also explained by the fact that tryptophan hydroxylase isoforms (TPH1 & TPH2), which catalyse the rate-limiting step in the synthesis of 5-hydroxytryptamine from TRP, have a diverse distribution pattern. TPH1 is mainly expressed in the periphery (Walther *et al.*, 2003), while TPH2 are exclusively intrinsic to the brain (Zhang *et al.*, 2004). It cannot be excluded that these two isoforms are differentially affected in some pathologies that may also include EPM1. Indeed, opposite changes in blood and brain 5HT levels have been reported earlier with reference to a convulsive background (Uluittu *et al.*, 1986), suggesting some

connection between seizure events and differential 5HT production and metabolism in the periphery and CNS, phenomena which could be induced by alteration in the TPH1 and/or TPH2 activity.

Although a causal relationship between the phenotype of *Cstb*^{-/-} mice and increased 5HT turnover in cortex and cerebellum remains to be determined we propose that observed alteration of 5HT turnover could, at least, in part contribute to myoclonus and ataxia seen in *Cstb*^{-/-} mice and in patients with EPM1. With regard of myoclonus, however, the role of serotonergic neurotransmission remains controversial. It is well documented that excessive stimulation of serotonergic neurotransmission in the brain induced by the administration of 5HT precursors l-tryptophan or 5-hydroxytryptophan, or high doses of 5HT re-uptake inhibitors, induce serotonin syndrome featuring by myoclonus and ataxia in both rodents and humans (Sternbach, 1991; Bodner *et al.*, 1995; Sporer, 1995). On the other hand, in some pathological conditions such as postanoxic intention myoclonus a decreased level of 5HT and its metabolite were found. This type of myoclonus showed improvement following treatment with 5HT precursors TRP or 5-hydroxytryptophan (Van Woert *et al.*, 1976). In the case of EPM1, the myoclonic events are proposed to have a cortical origin (Karhu *et al.*, 1994; Valzania *et al.*, 1999), the area where the most prominent 5HT turnover was determined. In contrast to other conditions associated with myoclonus, EPM1 patients did not respond with improvement following treatment with 5HT precursors (Pranzatelli *et al.*, 1995). Further pharmacological analysis of the sensitivity of myoclonus in *Cstb*^{-/-} mice to the drugs affecting serotonergic neurotransmission is needed before final conclusions could be drawn.

The deregulated TRP metabolism along the 5HT and kynurenine pathways in the cerebellum of *Cstb*^{-/-} mice may also modulate the manifestation of ataxia. It is well documented that ataxia develops as a symptom of serotonin-syndrome (Lane and Baldwin, 1997) Furthermore, an increased 5HT turnover was observed in the cerebellum of several murine models of cerebellar ataxia: *reeler*, *stagerer*, *weaver*, cerebellar cell degeneration mutants and, Nieman-Pick disease (Ohsugi *et al.*, 1986; Yadid *et al.*, 1998). In addition, to the enhanced serotonin turnover, our data demonstrate an increased levels of KYN in the cerebellum of *Cstb*^{-/-} mice. Several kynurenines have been shown to exhibit excitatory, convulsing or toxic properties (Stone and Perkins, 1981; Stone, 1993). There are numerous data demonstrating a role of quinolinic acid in the pathogenesis of neurodegenerative and epileptic disorders (for review, see Stone, 2001). Whether increased levels of KYN indicate the pathogenetic role of excitotoxic kynurenines in the neurodegeneration and other symptoms underlying the phenotype of *Cstb* deficiency remains to be studied. In conclusion, the data reported here provide a strong argument for the view that *Cstb* deficiency can induce a secondary enhancement of tryptophan metabolism

in CNS along the 5HT and KYN pathways, which may contribute to the observed phenotype of *Cstb*^{-/-} mice.

Changes in the excitatory–inhibitory neurotransmission in *Cstb*^{-/-} mice cerebellum (V)

Our experiment demonstrated that *Cstb* deficiency induced neuronal loss is accompanied by significant alterations in glutamate and GABA content as well as the disturbed expression of vesicular glutamate and GABA transporters in *Cstb*^{-/-} mice brain. The vesicular glutamate transporters have been demonstrated to define a glutamatergic phenotype of neurons (Bellocchio *et al.*, 2000; Takamori *et al.*, 2000; McIntire *et al.*, 1997) as well as glutamate decarboxylases and GABA transporter on vesicular membrane are considered to have GABAergic characteristics (Saito *et al.*, 1974; Borden 1996; Chaudhry *et al.*, 1998).

Observed decrease in vGLT1 expression levels and glutamate content in mutant mice cerebellum fits well with histological findings reported earlier, where selective loss of excitatory granule cells in the cerebellum of *Cstb*^{-/-} mice have been demonstrated (Shannon *et al.*, 2002). Our data are also consistent with a recent experiment, where impairment in motor coordination was attained by inducing the reversible deficit of glutamatergic neurotransmission in mice cerebellum (Yamamoto *et al.*, 2003), and suggest that excitatory activity of the granule cell is critical in controlling motor coordination. Similarly, a reduced glutamate or glutamate-immunolabelled cell numbers have been described in the cerebellum of various mouse models of cerebellar ataxia like *Purkinje cell degeneration* mutants, *lurcher* and *weaver* mutants (McBride and Ghetti, 1988; Grusser-Cornehls and Baurle., 2001; Sultan *et al.*, 2002). Although different neuronal populations are affected in these neurodegenerative diseases the final outcome results in disturbances of excitatory/inhibitory circuits. Thus, in *Purkinje cell degeneration* and *lurcher* mutants virtually all Purkinje cells are being destroyed (Mullen *et al.*, 1976; Swisher and Wilson, 1977), proposing that the excitability of deep cerebellar nuclei is altered in response to deterioration of Purkinje input. In *weaver* mutants, similarly to *Cstb*^{-/-} mice, the vast majority of granule cells are lost (Rakic and Sidman, 1973), suggesting the diminished excitatory modulation of Purkinje cell activity. However, our data concerning unchanged GABA content and vGABAT1 gene expression levels propose that inhibitory GABAergic circuits are relatively conserved in the cerebellum of *Cstb*^{-/-} mice. Additionally, we observed increase in the expression of GAD65 gene, which product glutamate decarboxylase mediates the GABA synthesis from glutamate in GABAergic nerve endings. The augmentation in GAD65 mRNA levels may be

regarded as a compensatory reaction directed toward the maintenance of functional GABA levels in the conditions where glutamate pool in *Cstb*-deficient mice cerebellum is diminished.

The signs of alterations in the excitatory and inhibitory neurotransmission were also found in the cerebrum of *Cstb*^{-/-} mice. Both, GABA and glutamate levels were diminished in the cerebrum of *Cstb*^{-/-} mice and although being nonsignificant, a trend toward reduction in the expression levels of vGLT1 and vGABAT1 were observed in the cerebrum as well. Recently, Franceschetti *et al.* (2007) demonstrated that density of GABA-immunoreactive cells is reduced in the hippocampus of *Cstb*^{-/-} mice proposing the impairment in GABAergic inhibition in mutant mice brain. Our data concerning the decreased GABA content in *Cstb*-deficient mice cerebrum partly support the view of failed inhibitory activity of mutant mice. The parallel decrease in the levels of excitatory neurotransmitter glutamate in the brain of *Cstb*^{-/-} mice, however, does not allow us to make any conclusion about possible alterations in excitatory and inhibitory neurotransmission in the cerebrum of *Cstb*^{-/-} mice.

Taken together, the data reported here demonstrate that *Cstb* deficiency is accompanied with the disturbed glutamatergic and GABAergic activity in the cerebellum of *Cstb*^{-/-} mice, which might contribute to the ataxia phenotype seen in this model of human EPM1.

The effect of partial loss of *Cstb* to EPM1-like phenotype in old *Cstb*^{+/-} mice (IV)

Our study with heterozygous *Cstb*^{+/-} mice revealed that partial loss of cystatin B in mice could also induce an EPM1-like phenotype, but with milder symptoms. Although heterozygous carriers are generally asymptomatic, earlier studies in Finnish EPM1 families have reported minor symptoms together with slight changes in the EEG recordings also in near relatives of patients (Koskiniemi *et al.* 1974, Norio and Koskiniemi 1979). Recently Rinne *et al.* (2002) found that a decrease in the levels of cystatin B was accompanied by a slight increase in general cathepsin activity in lymphoblastoid cells in asymptomatic heterozygous carriers of mutated cystatin B gene.

Indeed, our experiments demonstrate neuronal loss by 20–30% in the cerebellum and cerebral cortex of cystatin B heterozygotic mice. The mild neurodegeneration was accompanied by mild ataxia, motor incoordination, and myoclonus upon handling. Still the observed symptoms were significantly milder than those that were observed in homozygous cystatin-B-deficient mice. Our data also demonstrate that although all heterozygous mice have signs of neurodegeneration, only part of them develop mild behavioural symptoms characteristic for EPM1-like phenotype. These observations are supported by

earlier studies in Finnish EPM1 families reporting milder symptoms of EPM1 in some heterozygous carriers of the disease allele (Koskiniemi, 1974; Norio and Koskiniemi, 1979). The observed phenomenon of semidominance (i.e., milder phenotype expression compared with homozygotes), with partial penetrance of EPM1-like symptoms (seizures, ataxia) has also been described for several other diseases (Thomas *et al.*, 2001). Most probably the cystatin B level in heterozygous mice is close to the threshold needed to fulfil its cellular functions. The question why the observed neurodegeneration is not always associated with the EPM1 phenotype, however, remains open. The possibility that a certain level of neurodegeneration has to be achieved to see the ataxia or convulsions seems unlikely. The extent of neurodegeneration was similar in all heterozygous mice, despite greater variability of the symptoms. No difference in the level of neurodegeneration was observed in symptomatic and non symptomatic heterozygous mice. Our study corroborates the findings by Shannon *et al.* (2002) who showed that neuronal atrophy is an important consequence of cystatin B deficiency independent from seizure events. Our data show that heterozygous cystatin-B-deficient mice can have subtle symptoms of EPM1 when compared with age-matched wild-type mice.

CONCLUSIONS

The developed high performance liquid chromatographic method with electrochemical array detection allows selective separation and sensitive quantification of catecholamines, tryptophan and its serotonin and kynurenine pathway metabolites from a single biological sample. Reliable detection of substances is achieved by using the current-potential characteristic constructed from an array of electrodes.

Tryptophan levels are significantly decreased in the serum of EPM1 diseased humans, but stay invariable in the serum of *Cstb*^{-/-} mice. These data confirm the hypothesis that reduction in tryptophan concentration is probably a secondary effect of an antiepileptic treatment and is not related to the *Cstb* deficiency. However, the *Cstb* deficiency provokes disturbances in the intermediate metabolism of tryptophan along serotonin and kynurenine pathways in both *Cstb*-deficient mice and EPM1 patients.

The behavioural alterations seen in *Cstb*-deficient mice are accompanied by enhanced tryptophan metabolism along kynurenine and serotonin pathways in the cerebellum and cerebral cortex of *Cstb*-deficient mice. The observed changes in preconvulsive tryptophan metabolites might have a causal impact to the formation of EPM1-like phenotype in *Cstb*-deficient mice.

The inhibitory GABAergic circuits are relatively conserved in cerebellum of *Cstb*^{-/-} mice. *Cstb* deficiency provokes impairment in glutamatergic neuronal circuits in the cerebellum of *Cstb*^{-/-} mice, which might, at least partly, contribute to the ataxia phenotype seen in this model of human EPM1.

Heterozygous *Cstb* mice develop the EPM1 phenotype, although much later in their lifetime and in a milder form than the homozygous *Cstb* mice do. Even a partial decrease in neuronal cystatin B levels can induce neuronal loss in the cerebellum and cerebral cortex of heterozygous mutants. Mild handling can provoke myoclonic seizures in elder *Cstb*^{+/-} mice and significant impairment in balance and motor coordination skills manifest in heterozygous mutants as well.

REFERENCES

- Aihara Y, Mashima H, Onda H, Hisano S, Kasuya H, Hori T, Yamada S, Tomura H, Yamada Y, Inoue I, Kojima I, Takeda J (2000) Molecular cloning of a novel brain-type Na(+)-dependent inorganic phosphate cotransporter. *J Neurochem* 74:2622–2625.
- Airaksinen EM and Leino E (1982) Decrease of GABA in the cerebrospinal fluid of patients with progressive myoclonus epilepsy and its correlation with the decrease of 5HIAA and HVA. *Acta Neurol Scand* 66:666–672.
- Aizenman CD and Linden DJ (1999) Regulation of the rebound depolarization and spontaneous firing patterns of deep nuclear neurons in slices of rat cerebellum. *J Neurophysiol* 82:1697–1709.
- Barrett AJ (1981) Cystatin, the egg white inhibitor of cysteine proteinases. *Methods Enzymol* 80:771–778.
- Barrett AJ (1986) The cystatins, a diverse superfamily of cysteine peptidase inhibitors. *Biomed Biochim Acta* 45:1363–1373.
- Barrett AJ, Fritz H, Grubb A, Isemura S, Jarvinen M, Katunuma N, Machleidt W, Muller-Esterl W, Sasaki M, Turk V (1986) Nomenclature and classification of the proteins homologous with the cysteine-proteinase inhibitor chicken cystatin. *Biochem J* 236:312.
- Bartlett WA (1989) Effects of mobile phase composition on the chromatographic and electrochemical behaviour of catecholamines and selected metabolites. Reversed-phase ion-paired high-performance liquid chromatography using multiple-electrode detection. *J Chromatogr* 493:1–14.
- Bellocchio EE, Reimer RJ, Freneau RT Jr, Edwards RH (2000) Uptake of glutamate into synaptic vesicles by an inorganic phosphate transporter. *Science* 289:957–960.
- Berkovic SF, Andermann F, Carpenter S, Wolfe LS (1986) Progressive myoclonus epilepsies: specific causes and diagnosis. *N Engl J Med* 315:296–305.
- Berkovic SF, Mazarib A, Walid S, Neufeld MY, Manelis J, Nevo Y, Korczyn AD, Yin J, Xiong L, Pandolfo M, Mulley JC, Wallace RH (2005) A new clinical and molecular form of Unverricht-Lundborg disease localized by homozygosity mapping. *Brain* 128:652–658.
- Bespalova IN, Adkins S, Pranzatelli M, Burmeister M (1997) Novel cystatin B mutation and diagnostic PCR assay in an Unverricht-Lundborg progressive myoclonus epilepsy patient. *Am J Med Genet* 74:467–471.
- Block ML, Zecca L, Hong JS (2007) Microglia-mediated neurotoxicity: uncovering the molecular mechanisms. *Nat Rev Neurosci* 8:57–69.
- Bode W, Engh R, Musil D, Thiele U, Huber R, Karshikov A, Brzin J, Kos J, Turk V (1988) The 2.0 Å X-ray crystal structure of chicken egg white cystatin and its possible mode of interaction with cysteine proteinases. *EMBO J* 7:2593–2599.
- Bodner RA, Lynch T, Lewis L, Kahn D (1995) Serotonin syndrome. *Neurology* 45:219–223.
- Borden LA (1996) GABA transporter heterogeneity: pharmacology and cellular localization. *Neurochem Int* 29:335–356.
- Brännvall K, Hjelm H, Korhonen L, Lahtinen U, Lehesjoki A-E, Lindholm D (2003) Cystatin-B is expressed by neural stem cells and by differentiated neurons and astrocytes. *Biochem Biophys Res Commun* 308:369–374.

- Brömme D, Rinne R, Kirschke H (1991) Tight-binding inhibition of cathepsin S by cystatins. *Biomed Biochim Acta* 50:631–635.
- Carpenter S, Karpati G, Andermann F, Jacob JC, Andermann E (1974) Lafora's disease: peroxisomal storage in skeletal muscle. *Neurology* 24:531–538.
- Chaudhry FA, Reimer RJ, Bellocchio EE, Danbolt NC, Osen KK, Edwards RH, Storm-Mathisen J (1998) The vesicular GABA transporter, VGAT, localizes to synaptic vesicles in sets of glycinergic as well as GABAergic neurons. *J Neurosci* 18:9733–9750.
- Chi JD, Odontiadis J, Franklin M (1999) Simultaneous determination of catecholamines in rat brain tissue by high-performance liquid chromatography. *J Chromatogr B Biomed Sci Appl* 731:361–367.
- Chiarugi M, Calvani E, Meli E, Traggiai Moroni F (2001) Synthesis and release of neurotoxic kynurenine metabolites by human monocyte-derived macrophages. *J Neuroimmunol* 120:190–198.
- Consensus Group Marseille (1990) Classification of progressive myoclonus epilepsies and related disorders. *Ann Neurol* 28:113–116.
- D'Amato E, Kokaia Z, Nanobashvili A, Reebe M, Lehesjoki AE, Saarma M, Lindvall O (2000) Seizures induce widespread upregulation of cystatin B, the gene mutated in progressive myoclonus epilepsy, in rat forebrain neurons. *Eur J Neurosci* 12:1687–1695.
- de Haan GJ, Halley DJ, Doelman JC, Geesink HH, Augustijn PB, Jager-Jongkind AD, Majoie M, Bader AJ, Leliefeld-Ten Doeschate LA, Deelen WH, Bertram E, Lehesjoki AE, Lindhout D (2004) Univerricht-Lundborg disease: underdiagnosed in the Netherlands. *Epilepsia* 45:1061–1063.
- Delgado-Escueta AV, Ganesh S, Yamakawa K (2001) Advances in the genetics of progressive myoclonus epilepsy. *Am J Med Genet* 106:129–138.
- Di Giaimo R, Riccio M, Santi S, Galeotti C, Ambrosetti DC, Melli M (2002) New insights into the molecular basis of progressive myoclonus epilepsy: a multiprotein complex with cystatin B. *Hum Mol Genet* 11:2941–2950.
- Du F, Schmidt W, Okuno E, Kido R, Kohler C, Schwarcz R (1992) Localization of kynurenine aminotransferase immunoreactivity in the rat hippocampus. *J Comp Neurol* 321:477–487.
- Du F, Williamson J, Bertram E, Lothman E, Okuno E, Schwarcz R (1993) Kynurenine pathway enzymes in a rat model of chronic epilepsy: immunohistochemical study of activated glial cells. *Neuroscience* 55:975–989.
- Eastman CL and Guilarte TR (1989) Cytotoxicity of 3-hydroxykynurenine in a neuronal hybrid cell line. *Brain Research* 495:225–231.
- Eldridge R, Iivanainen M., Stern R, Koerber T, Wilder BJ (1983) “Baltic” myoclonus epilepsy: hereditary disorder of childhood made worse by phenytoin. *Lancet* 2:838–842.
- Erlander MG, Tillakaratne NJK, Feldblum S, Patel N; Tobin AJ (1991) Two genes encode distinct glutamate decarboxylases. *Neuron* 7:91–100.
- Finnish Disease Database. This database is developed and maintained by the Department of Medical Genetics, University of Helsinki and the Department of Molecular Medicine, National Public Health Institute, Finland. Available at: <http://www.findis.org>. Accessed June 11, 2007.

- Foster AC, Vezzani A, French ED, Schwarcz R (1984) Kynurenic acid blocks neurotoxicity and seizures induced in rats by the related brain metabolite quinolinic acid. *Neurosci Lett* 48:273–278.
- Franceschetti S, Sancini G, Buzzi A, Zucchini S, Paradiso B, Magnaghi G, Frassoni C, Chikhladze M, Avanzini G, Simonato M (2007) A pathogenetic hypothesis of Unverricht-Lundborg disease onset and progression. *Neurobiol Dis* 25:675–685.
- Freneau RT Jr, Burman J, Qureshi T, Tran CH, Proctor J, Johnson J, Zhang H, Sulzer D, Copenhagen DR, Storm-Mathisen J, Reimer RJ, Chaudhry FA, Edwards RH (2002) The identification of vesicular glutamate transporter 3 suggests novel modes of signaling by glutamate. *Proc Natl Acad Sci USA* 99:14488–14493.
- Freneau RT Jr, Troyer MD, Pahner I, Nygaard GO, Tran CH, Reimer RJ, Bellocchio EE, Fortin D, Storm-Mathisen J, Edwards RH (2001) The expression of vesicular glutamate transporters defines two classes of excitatory synapse. *Neuron* 31:247–260.
- Fukui S, Schwarcz R, Rapoport SI, Takada Y, Smith QR (1991) Blood–brain barrier transport of kynurenines: implications for brain synthesis and metabolism. *J Neurochem* 56:2007–2017.
- Gamache P, Ryan E, Svendsen C, Murayama K, Acworth IN (1993) Simultaneous measurement of monoamines, metabolites and amino acids in brain tissue and microdialysis perfusates. *J Chromatogr* 614:213–220.
- Gras C, Herzog E, Bellenchi GC, Bernard V, Ravassard P, Pohl M, Gasnier B, Giros B, El Mestikawy S (2002) A third vesicular glutamate transporter expressed by cholinergic and serotonergic neurons. *J Neurosci* 22:5442–5451.
- Grusser-Cornehls U and Baurle J (2001) Mutant mice as a model for cerebellar ataxia. *Prog Neurobiol* 63:489–540.
- Guidetti P, Okuno E, Schwarcz R (1997) Characterization of rat brain kynurenine amino-transferases I and II. *J Neurosci Res* 50:457–465.
- Guillemin GJ, Kerr SJ, Pemberton LA, Smith DG, Smythe GA, Armati PJ, Brew BJ (2001) IFN-beta1b induces kynurenine pathway metabolism in human macrophages: potential implications for multiple sclerosis treatment. *J Interferon Cytokine Res* 21:1097–1101.
- Haltia M, Kristensson K, Sourander P (1969) Neuropathological studies in three Scandinavian cases of progressive myoclonus epilepsy. *Acta Neurol Scand* 45:63–77.
- Harriman DG, Millar JH, Stevenson AC (1955) Progressive familial myoclonic epilepsy in three families: its clinical features and pathological basis. *Brain* 78:325–349.
- Herve C, Beyne P, Jamault H, Delacoux E (1996) Determination of tryptophan and its kynurenine pathway metabolites in human serum by high-performance liquid chromatography with simultaneous ultraviolet and fluorimetric detection. *J Chromatogr B Biomed Appl* 675:157–161.
- Herzog E, Bellenchi GC, Gras C, Bernard V, Ravassard P, Bedet C, Gasnier B, Giros B, El Mestikawy S (2001) The existence of a second vesicular glutamate transporter specifies subpopulations of glutamatergic neurons. *J Neurosci* 21:RC181.
- Heyes MP, Achim CL, Wiley CA, Major EO, Saito K, Markey SP (1996) Human microglia convert l-tryptophan into the neurotoxin quinolinic acid. *Biochem J* 320:595–597.

- Heyes MP, Quearry BJ (1988) Quantification of 3-hydroxykynurenine in brain by high-performance liquid chromatography and electrochemical detection. *J Chromatogr* 428:340–344.
- Heyes MP, Saito K, Devinsky O, Nadi NS (1994) Kynurenine pathway metabolites in cerebrospinal fluid and serum in complex partial seizures. *Epilepsia* 35:251–257.
- Heyes MP, Wyler AR, Devinsky O, Yerger JA, Markey SP, Nadi NS (1990) Quinolinic acid concentrations in brain and cerebrospinal fluid of patients with intractable complex partial seizures. *Epilepsia* 31:172–177.
- Hilmas C, Pereira EF, Alkondon M, Rassoulpour A, Schwarcz R (2001) The brain metabolites kynurenic acid inhibits $\alpha 7$ -nicotinic receptor activity and increases non- $\alpha 7$ nicotinic receptor expression. *J Neurosci* 21:7463–7473.
- Hiraoka A, Miura I, Sato M, Tominaga I, Hattori M (1992) Effects of anti-epileptic drugs on the L-tryptophan binding to human serum albumin. *Chem Pharm Bull (Tokyo)* 40:1629–1630.
- Holmes EW (1988) Determination of serum kynurenine and hepatic tryptophan dioxygenase activity by high-performance liquid chromatography. *Anal Biochem* 172:518–525.
- Houseweart MK, Pennacchio LA, Vilaythong A, Peters C, Noebels JL, Myers RM (2003) Cathepsin B but not cathepsins L or S contributes to the pathogenesis of Unverricht–Lundborg progressive myoclonus epilepsy (EPM1). *J Neurobiol* 56:315–327.
- Iivanainen M and Himberg JJ (1982) Valproate and clonazepam in the treatment of severe progressive myoclonus epilepsy. *Arch Neurol* 39:236–238.
- Issa F, Gerhardt GA, Bartko JJ, Suddath RL, Lynch M, Gamache PH, Freedman R, Wyatt RJ, Kirch DG (1994) A multidimensional approach to analysis of cerebrospinal fluid biogenic amines in schizophrenia: I. Comparisons with healthy control subjects and neuroleptic-treated/unmedicated pairs analyses. *Psychiatry Res* 52:237–249.
- Iwahashi H (1999) 3-Hydroxyanthranilic acid-derived compounds formed through electrochemical oxidation. *J Chromatogr B Biomed Sci Appl* 736:237–245.
- Järvinen M and Rinne A (1982) Human spleen cysteineproteinase inhibitor. Purification, fractionation into isoelectric variants and some properties of the variants. *Biochim Biophys Acta* 708:210–217.
- Joensuu T, Kuronen M, Alakurtti K, Tegelberg S, Hakala P, Aalto A, Huopaniemi L, Aula N, Michellucci R, Eriksson K, Lehesjoki AE (2007) Cystatin B: mutation detection, alternative splicing and expression in progressive myoclonus epilepsy of Unverricht–Lundborg type (EPM1) patients. *Eur J Hum Genet* 15:185–193.
- Kagitani-Shimono K, Imai K, Okamoto N, Ono J, Okada S (2002) Unverricht–Lundborg disease with cystatin B gene abnormalities. *Pediatr Neurol* 26:55–60.
- Kaminski RM, Zielinska E, Dekundy A, van Luijckelaar G, Turski W (2003) Deficit of endogenous kynurenic acid in the frontal cortex of rats with a genetic form of absence epilepsy. *Pol J Pharmacol* 55:741–746.
- Karhu J, Hari R, Paetau R, Kajola M, Mervaala E (1994) Cortical reactivity in progressive myoclonus epilepsy. *Electroencephalogr Clin Neurophysiol* 90:93–102.
- Kontur P, Dawson R, Monjan A (1984) Manipulation of mobile phase parameters for the HPLC separation of endogenous monoamines in rat brain tissue. *J Neurosci Methods* 11:5–18.

- Koskiniemi M (1974) Psychological findings in progressive myoclonus epilepsy without Lafora bodies. *Epilepsia* 15:537–545.
- Koskiniemi M (1975) Findings in routine laboratory examination in progressive myoclonus epilepsy. *Acta Neurol Scand* 51:12–20.
- Koskiniemi M (1987) Baltic myoclonus. *Ann Clin Res* 19:311–312.
- Koskiniemi M, Donner M, Majuri H, Haltia M, Norio R (1974a) Progressive myoclonus epilepsy. A clinical and histopathological study. *Acta Neurol Scand* 50:307–332.
- Koskiniemi M, Laakso J, Kuurne T, Laipio M, Harkonen M (1985) Indole levels in human lumbar and ventricular cerebrospinal fluid and the effect of L-tryptophan administration. *Acta Neurol Scand*. 71:127–132.
- Koskiniemi M, Toivakka E, Donner M (1974b) Progressive myoclonus epilepsy. Electroencephalographical findings. *Acta Neurol Scand* 50:333–359.
- Koskiniemi M, Van Vleymen B, Håkämies L, Lamusuo S, Taalas J (1998) Piracetam relieves symptoms in progressive myoclonus epilepsy: a multicentre, randomised, double blind, crossover study comparing the efficacy and safety of three dosages of oral piracetam with placebo. *J Neurol Neurosurg Psychiatry* 64:344–348.
- Koskiniemi ML (1980) Deficient intestinal absorption of L-tryptophan in progressive myoclonus epilepsy without Lafora bodies. *J Neurol Sci* 47:1–6.
- Koskiniemi ML (1986) Baltic myoclonus. *Adv Neurol* 43:57–64.
- Krug F, Baurle J, Grusser-Cornehls U (1995) Enlargement of GAD-immunopositive terminals in the lateral vestibular nucleus (LVN) of weaver mutant mice. *Histol Histopathol* 10:105–109.
- Lafrenière RG, Rochefort DL, Chrétien N, Rommens JM, Cochius JI, Kälviainen R, Nousiainen U, Patry G, Farrell K, Söderfeldt B, Federico A, Hale BR, Cossio OH, Sørensen T, Pouliot MA, Kmiec T, Uldall P, Janszky J, Pranzatelli MR, Andermann F, Andermann E, Rouleau GA (1997) Unstable insertion in the 5' flanking region of the cystatin B gene is the most common mutation in progressive myoclonus epilepsy type 1, EPM1. *Nat Genet* 15:298–302.
- Lalioi MD, Mirotsoy M, Buresi C, Peitsch MC, Rossier C, Ouazzani R, Baldy-Moulinier M, Bottani A, Malafosse A, Antonarakis SE (1997a) Identification of mutations in cystatin B, the gene responsible for the Unverricht-Lundborg type of progressive myoclonus epilepsy (EPM1). *Am J Hum Genet* 60:342–351.
- Lalioi MD, Scott HS, Antonarakis SE (1999) Altered spacing of promoter elements due to the dodecamer repeat expansion contributes to reduced expression of the cystatin B gene in EPM1. *Hum Mol Genet* 8:1791–1798.
- Lalioi MD, Scott HS, Buresi C, Rossier C, Bottani A, Morris MA, Malafosse A, Antonarakis SE (1997b) Dodecamer repeat expansion in cystatin B gene in progressive myoclonus epilepsy. *Nature* 386:847–851.
- Lalioi MD, Scott HS, Genton P, Grid D, Ouazzani R, M'Rabet A, Ibrahim S, Gouider R, Dravet C, Chkili T, Bottani A, Buresi C, Malafosse A, Antonarakis SE (1998) A PCR amplification method reveals instability of the dodecamer repeat in progressive myoclonus epilepsy (EPM1) and no correlation between the size of the repeat and age at onset. *Am J Hum Genet* 62:842–847.
- Lane R and Baldwin D (1997) Selective serotonin reuptake inhibitor-induced serotonin syndrome: review. *J Clin Psychopharmacol* 17:208–221.

- Lapin IP (1978) Stimulant and convulsive effects of kynurenines injected into brain ventricles in mice. *J Neural Transm* 42:37–43.
- Lehesjoki AE (2002) Clinical features and genetics of Unverricht-Lundborg disease. *Adv Neurol* 89:193–197.
- Lehesjoki AE (2003) Molecular background of progressive myoclonus epilepsy. *EMBO J* 22:3473–3478.
- Lehesjoki AE and Koskiniemi M (1998) Clinical features and genetics of progressive myoclonus epilepsy of the Unverricht-Lundborg type. *Ann Med* 30:474–480.
- Lehesjoki AE and Koskiniemi M (1999) Progressive myoclonus epilepsy of Unverricht-Lundborg type. *Epilepsia* 40:23–28.
- Lehesjoki AE, Koskiniemi M, Sistonen P, Miao J, Hastbacka J, Norio R, de la Chapelle A (1991) Localization of a gene for progressive myoclonus epilepsy to chromosome 21q22. *Proc Natl Acad Sci USA* 88:3696–3699.
- Leino E, MacDonald E, Airaksinen MM, Riekkinen PJ (1980) Homovanillic acid and 5-hydroxyindoleacetic acid levels in cerebrospinal fluid of patients with progressive myoclonus epilepsy. *Acta Neurol Scand* 62:41–54.
- Lieuallen K, Pennacchio LA, Park M, Myers RM, Lennon GG (2001) Cystatin B-deficient mice have increased expression of apoptosis and glial activation genes. *Hum Mol Genet* 10:1867–1871.
- Lim CK. HPLC of small molecules: practical approach. IRL Press Limited, Oxford, 1986, Ch.3.
- Lundborg H (1903) Die progressive Myoklonusepilepsie (Unverricht's Myoklonie). Uppsala: Almqvist and Wiksell (pub.) 8:567–570.
- Mancuso M, Filosto M, Mootha VK, Rocchi A, Pistolesi S, Murri L, DiMauro S, Siciliano G (2004) A novel mitochondrial tRNA^{Phe} mutation causes MERRF syndrome. *Neurology* 62:2119–2121.
- Marklová E, Makovickova H, Krakorova I (2000) Screening for defects in tryptophan metabolism. *J Chromatogr A* 870:289–293.
- Mascalchi M, Michelucci R, Cosottini M, Tessa C, Lolli F, Riguzzi P, Lehesjoki AE, Tosetti M, Villari N, Tassinari CA (2002) Brainstem involvement in Unverricht-Lundborg disease (EPM1): An MRI and (1)H MRS study. *Neurology* 58:1686–1689.
- McBride WJ and Ghetti B (1988) Changes in the content of glutamate and GABA in the cerebellar vermis and hemispheres of the Purkinje cell degeneration (pcd) mutant. *Neurochem Res* 13:121–125.
- McIntire SL, Reimer RJ, Schuske K, Edwards RH, Jorgensen EM (1997) Identification and characterization of the vesicular GABA transporter. *Nature* 389:870–876.
- Melone MA, Tessa A, Petrini S, Lus G, Sampaolo S, di Fede G, Santorelli FM, Cotrufo R (2004) Revelation of a new mitochondrial DNA mutation (G12147A) in a MELAS/MERFF phenotype. *Arch Neurol* 61:269–272.
- Morita I, Kawamoto M, Hattori M, Eguchi K, Sekiba K, Yoshida H (1990) Determination of tryptophan and its metabolites in human plasma and serum by high-performance liquid chromatography with automated sample clean-up system. *J Chromatogr* 526:367–374.
- Mullen RJ, Eicher EM, Sidman RL (1976) Purkinje cell degeneration, a new neurological mutation in the mouse. *P Natl Acad Sci USA* 73:208–212.

- Munoz-Hoyos A, Molina-Carballo A, Rodriguez-Cabezas T, Uberos-Fernandez J, Ruiz-Cosano C, Acuna-Castroviejo D (1997) Relationships between methoxyindole and kynurenine pathway metabolites in plasma and urine in children suffering from febrile and epileptic seizures. *Clin Endocrinol (Oxf)* 47:667–677.
- Muramoto O, Kanazawa I, Ando K (1981) Neurotransmitter abnormality in Rolling mouse Nagoya, an ataxic mutant mouse. *Brain Res* 215:295–304.
- Nakagawa Y, Asai H, Miura T, Kitoh J, Mori H, Nakano K (1998) Increased expression of 3-hydroxyanthranilate 3,4-dioxygenase gene in brain of epilepsy-prone El mice. *Brain Res Mol Brain Res* 58:132–137.
- Nakamura M, Nakano S, Goto Y, Ozawa M, Nagahama Y, Fukuyama H, Akiguchi I, Kaji R, Kimura J (1995) A novel point mutation in the mitochondrial tRNA(Ser(UCN)) gene detected in a family with MERRF/MELAS overlap syndrome. *Biochem Biophys Res Commun* 214:86–93.
- Nakano K, Asai H, Kitoh J (2006) Abnormally high activity of 3-hydroxyanthranilate 3,4-dioxygenase in brain of epilepsy-prone El mice. *Brain Res* 572:1–4.
- Nakano K, Takahashi S, Mizobuchi M, Kuroda T, Masuda K, Kitoh J (1993) High levels of quinolinic acid in brain of epilepsy-prone El mice. *Brain Res* 619:195–198.
- Natsume J, Kumakura Y, Bernasconi N, Soucy JP, Nakai A, Rosa P, Fedi M, Dubeau F, Andermann F, Lisbona R, Bernasconi A, Diksic M (2003) Alpha-[11C] methyl-L-tryptophan and glucose metabolism in patients with temporal lobe epilepsy. *Neurology* 60:756–761.
- Nemeth H, Toldi J, Vecsei L (2006) Kynurenines, Parkinson's disease and other neurodegenerative disorders: preclinical and clinical studies. *J Neural Transm Suppl* 70:285–304.
- Ni B, Rostock PR Jr, Nadi NS, Paul SM (1994) Cloning and expression of a cDNA encoding a brain-specific Na(+)-dependent inorganic phosphate cotransporter. *Proc Natl Acad Sci USA* 91:5607–5611.
- Norio R and Koskiniemi M (1979) Progressive myoclonus epilepsy: genetic and nosological aspects with special reference to 107 Finnish patients. *Clin Genet* 15:382–398.
- O'Brien JS (1977) Neuraminidase deficiency in the cherry red spot-myoclonus syndrome. *Biochem Biophys Res Commun* 79:1136–1141.
- Ohsugi K, Adachi K, Ando K (1986) Serotonin metabolism in the CNS in cerebellar ataxic mice. *Experientia* 42:1245–1247.
- Okuda S, Nishiyama N, Saito H, Katsuki H (1996) Hydrogen peroxide-mediated neuronal cell death induced by an endogenous neurotoxin, 3-hydroxykynurenine. *Proc Natl Acad Sci USA* 93:12553–12558.
- Okuno E, Nakamura M, Schwarcz R (1991) Two kynurenine aminotransferases in human brain. *Brain Res* 542:307–312.
- Pearson SJ and Reynolds GP (1991) Determination of 3-hydroxykynurenine in human brain and plasma by high-performance liquid chromatography with electrochemical detection. Increased concentrations in hepatic encephalopathy. *J Chromatogr* 565:436–440.
- Pennacchio LA and Myers RM (1996) Isolation and characterization of the mouse cystatin B gene. *Genome Res* 6:1103–1109.

- Pennacchio LA, Bouley DM, Higgins KM, Scott MP, Noebels JL, Myers RM (1998) Progressive ataxia, myoclonic epilepsy and cerebellar apoptosis in cystatin B-deficient mice. *Nat Genet* 20:251–258.
- Pennacchio LA, Lehesjoki AE, Stone NE, Willour VL, Virtaneva K, Miao, J, D'Amato E, Ramirez L, Faham M, Koskiniemi M, Warrington JA, Norio R, de la Chapelle A, Cox DR, Myers RM (1996) Mutations in the gene encoding cystatin B in progressive myoclonus epilepsy (EPM1). *Science* 271:1731–1734.
- Perkins MN and Stone TW (1982) An iontophoretic investigation of the actions of convulsant kynurenes and their interaction with the endogenous excitant quinolinic acid. *Brain Res* 247:184–187.
- Peters JC (1991) Tryptophan nutrition and metabolism: an overview. *Adv Exp Med Biol* 294:345–358.
- Pintor M, Mefford IN, Hutter I, Pocotte SL, Wyler AR, Nadi NS (1990) Levels of biogenic amines, their metabolites, and tyrosine hydroxylase activity in the human epileptic temporal cortex. *Synapse* 5:152–156.
- Pranzatelli MR, Tate E, Huang Y, Haas RH, Bodensteiner J, Ashwal S, Franz D (1995) Neuropharmacology of progressive myoclonus epilepsy: response to 5-hydroxy-L-tryptophan. *Epilepsia* 36:783–791.
- Pratt JA, Jenner P, Johnson AL, Shorvon SD, Reynolds EH (1984) Anticonvulsant drugs alter plasma tryptophan concentrations in epileptic patients: implications for antiepileptic action and mental function. *J Neurol Neurosurg Psychiatry* 4:1131–1133.
- Rakic P and Sidman RL (1973) Organization of cerebellar cortex secondary to deficit of granule cells in weaver mutant mice. *J Comp Neurol* 152:133–161.
- Raman IM, Gustafson AE, Padgett D (2000) Ionic currents and spontaneous firing in neurons isolated from the cerebellar nuclei. *J Neurosci* 20:9004–9016.
- Reymond A, Marigo V, Yaylaoglu MB, Leoni A, Ucla C, Scamuffa N, Caccioppoli C, Dermitzakis ET, Lyle R, Banfi S, Eichele G, Antonarakis SE, Ballabio A (2002) Human chromosome 21 gene expression atlas in the mouse. *Nature* 420:582–586.
- Riccio M, Di Giaimo R, Pianetti, S, Palmieri PP, Melli M, Santi S (2001) Nuclear localization of cystatin B, the cathepsin inhibitor implicated in myoclonus epilepsy (EPM1). *Exp Cell Res* 262:84–94.
- Riccio M, Santi S, Dembic M, Di Giaimo R, Cipollini E, Costantino-Ceccarini E, Ambrosetti, D, Maraldi NM, Melli M (2005) Cell-specific expression of the *epml* (cystatin B) gene in developing rat cerebellum. *Neurobiol Dis* 20:104–114.
- Rinne A, Järvinen M, Martikainen J, Alavaikko M, Räsänen O (1981) Über das Vorkommen des epidermalen SH-Protease-Inhibitors im lymphatischen Gewebe. *Verb Anat Ges* 75:573–574.
- Rinne R, Saukko P, Järvinen M, Lehesjoki AE (2002) Reduced cystatin B activity correlates with enhanced cathepsin activity in progressive myoclonus epilepsy. *Ann Med* 34:380–385.
- Ritonja A, Machleidt W, Barrett AJ (1985) Amino acid sequence of the intracellular cysteine proteinase inhibitor cystatin B from human liver. *Biochem Biophys Res Commun* 131:1187–1192.
- Saito K, Markey SP, Heyes MP (1991) Chronic effects of gamma-interferon on quinolinic acid and indoleamine-2,3-dioxygenase in brain of C57BL6 mice. *Brain Res* 546:151–154.

- Scharfman HE, Goodman JH, Schwarcz R (2000) Electrophysiological effects of exogenous and endogenous kynurenic acid in the rat brain: studies in vivo and in vitro. *Amino Acids* 19:283–297.
- Schwarcz R, Whetsell WO Jr., Mangano R M (1983) Quinolinic acid: an endogenous metabolite that produces axon-sparing lesions in rat brain. *Science* 219:316–318.
- Shahwan A, Farrell M, Delanty N (2005) Progressive myoclonic epilepsies: a review of genetic and therapeutic aspects. *Lancet Neurol* 4:239–248.
- Shannon P, Pennacchio LA, Houseweart MK, Minassian BA, Myers RM (2002) Neuropathological changes in a mouse model of progressive myoclonus epilepsy: cystatin B deficiency and Unverricht-Lundborg disease. *J Neuropathol Exp Neurol* 61:1085–1091.
- Shibata K and Onodera M (1991) High-performance liquid chromatographic determination of 3-hydroxykynurenine with fluorimetric detection; comparison of preovulatory phase and postovulatory phase urinary excretion. *J Chromatogr* 570:13–18.
- Somerville ER and Olanow CW (1982) Valproic acid. Treatment of myoclonus in dyssynergia cerebellaris myoclonica. *Arch Neurol* 39:527–528.
- Sotelo C and Alvarado-Mallart RM (1991) The reconstruction of cerebellar circuits. *Trends Neurosci* 14:350–355.
- Sporer KA (1995) The serotonin syndrome. Implicated drugs, pathophysiology and management. *Drug Safety* 13:94–104.
- Sternbach H (1991) The serotonin syndrome. *Am J Psych* 148:705–713.
- Stone TW (1993) Neuropharmacology of quinolinic and kynurenic acids. *Pharmacol Rev* 45:309–379.
- Stone TW (2001) Kynurenines in the CNS: from endogenous obscurity to therapeutic importance. *Prog Neurobiol* 64:185–218.
- Stone TW and Perkins MN (1981) Quinolinic acid: a potent endogenous excitant at amino acid receptors in CNS. *Eur J Pharm* 72:411–412.
- Stone TW, Mackay GM, Forrest CM, Clark CJ, Darlington LG (2003) Tryptophan metabolites and brain disorders. *Clin Chem Lab Med* 41: 852–859.
- Stubbs MT, Laber B, Bode W, Huber R, Jerala R, Lenarcic B, Turk V (1990) The refined 2.4 Å X-ray crystal structure of recombinant human stefin B in complex with the cysteine proteinase papain: a novel type of proteinase inhibitor interaction. *EMBO J* 9:1939–1947.
- Sultan F, König T, Mock M, Thier P (2002) Quantitative organization of neurotransmitters in the deep cerebellar nuclei of the Lurcher mutant. *J Comp Neurol* 452:311–323.
- Suzuki S and Mori A (1992) Regional distribution of tyrosine, tryptophan, and their metabolites in the brain of epileptic El mice. *Neurochem Res* 17:693–698.
- Swisher DA and Wilson DB (1977) Cerebellar histogenesis in the lurcher (Lc) mutant mouse. *J Comp Neurol* 173:205–218.
- Takamori S, Rhee JS, Rosenmund C, Jahn R (2000) Identification of a vesicular glutamate transporter that defines a glutamatergic phenotype in neurons. *Nature* 407:189–194.
- Tanaka S and Takeda N (1997) Biogenic Monoamines in the Brain and the Corpus Cardiacum Between Albino and Normal Strains of the Migratory Locust, *Locusta*

- migratoria – Degradation pathways of biogenic amines in insect nervous tissue. *Comp Biochem Physiol* 117: 221–227.
- Thomas PQ, Dattani MT, Brickman JM, McNay D, Warne G, Zacharin M, Cameron F, Hurst J, Woods K, Dunger D, Stanhope R, Forrest S, Robinson IC, Beddington RS (2001) Heterozygous HESX1 mutations associated with isolated congenital pituitary hypoplasia and septo-optic dysplasia. *Hum Mol Gen* 10:39–45.
- Turk V and Bode W (1991) The cystatins: protein inhibitors of cysteine proteinases. *FEBS Lett* 285:213–219.
- Ubbink JB, Vermaak WJ, Bissbort SH (1991) High-performance liquid chromatographic assay of human lymphocyte kynureninase activity levels. *J Chromatogr* 566:369–375.
- Uluittu M, Chis R, Petec G (1986) The influence of auditory and lithium stimulation on blood and brain serotonin in the normal rat and in that susceptible to audiogenic convulsions. *Physiologie* 23:167–176.
- Unverricht H (1891) Die Myoclonie. Berlin: Franz Deuticke (pub.).
- Unverricht H (1895) Ueber familiaere Myoclonie. *Dtsch Z Nervenheilk* 32–67.
- Valzania F, Strafella AP, Tropeani A, Rubboli G, Nasseti SA, Tassinari CA (1999) Facilitation of rhythmic events in progressive myoclonus epilepsy: A transcranial magnetic stimulation study. *Clin Neurophysiol* 110:152–157.
- Van Woert MH, Jutkowitz R, Rosenbaum D, Bowers MB Jr (1976) Serotonin and myoclonus. *Monogr Neural Sci* 3:71–80.
- Varoqui H, Schafer MK, Zhu H, Weihe E, Erickson JD (2002) Identification of the differentiation-associated Na⁺/PI transporter as a novel vesicular glutamate transporter expressed in a distinct set of glutamatergic synapses. *J Neurosci* 22:142–155.
- Virtaneva K, D'Amato E, Miao J, Koskiniemi M, Norio R, Avanzini G, Franceschetti S, Michelucci R, Tassinari CA, Omer S, Pennacchio LA, Myers RM, Dieguez-Lucena JL, Krahe R, de la Chapelle A, Lehesjoki AE (1997) Unstable minisatellite expansion causing recessively inherited myoclonus epilepsy, EPM1. *Nat Genet* 15:393–396.
- Virtaneva K, Miao J, Träskelin AL, Stone N, Warrington JA, Weissenbach J, Myers RM, Cox DR, Sistonen P, de la Chapelle A, *et al.*, (1996) Progressive myoclonus epilepsy EPM1 locus maps to a 175-kb interval in distal 21q. *Am J Hum Genet* 58:1247–1253.
- Voogd J and Glickstein M (1998) The anatomy of the cerebellum. *Trends Neurosci* 21:370–375.
- Walther DJ, Peter JU, Bashammakh S, Hortnagl H, Voits M, Fink H, Bader M (2003) Synthesis of serotonin by a second tryptophan hydroxylase isoform. *Science* 299:76.
- Werner ER, Bitterlich G, Fuchs D, Hausen A, Reibnegger G, Szabo G, Dierich MP, Wachter H (1987) Human macrophages degrade tryptophan upon induction by interferon-gamma. *Life Sci* 41:273–280.
- West MJ (1993) New stereological methods for counting neurons. *Neurobiol Aging* 14:275–285.
- Wu HQ and Schwarcz R (1996) Seizure activity causes elevation of endogenous extracellular kynurenic acid in the rat brain. *Brain Res Bull* 39:155–162.

- Yadid G, Sotnik-Barkai I, Tornatore C, Baker-Cairns B, Harvey-White J, Pentchev PG, Goldin E (1998) Neurochemical alterations in the cerebellum of a murine model of Niemann-Pick type C disease. *Brain Res* 799:250–256.
- Yamamoto H, Murakami H, Horiguchi K, Egawa B (1995) Studies on cerebrospinal fluid kynurenic acid concentrations in epileptic children. *Brain Dev* 17:327–329.
- Yamamoto H, Shindo I, Egawa B, Horiguchi K (1994) Kynurenic acid is decreased in cerebrospinal fluid of patients with infantile spasms. *Pediatr Neurol* 10:9–12.
- Yamamoto M, Wada N, Kitabatake Y, Watanabe D, Anzai M, Yokoyama M, Teranishi Y, Nakanishi S (2003) Reversible suppression of glutamatergic neurotransmission of cerebellar granule cells in vivo by genetically manipulated expression of tetanus neurotoxin light chain. *J Neurosci* 23:6759–6767.
- Zeman W and Albert M (1963) On the Nature of the “Stored” Lipid Substances in Juvenile Amaurotic Idiocy (Batten-Spielmeyer-Vogt). *Ann Histochem* 22:255–257.
- Zhang X, Beaulieu JM, Sotnikova TD, Gainetdinov RR, Caron MG (2004) Tryptophan hydroxylase-2 controls brain serotonin synthesis. *Science* 305:217.
- Zuo J, De Jager PL, Takahashi KA, Jiang W, Linden DJ, Heintz N (1997) Neurodegeneration in Lurcher mice caused by mutation in delta2 glutamate receptor gene. *Nature* 388:769–773.

SUMMARY IN ESTONIAN

TSÜSTATIIN B PUUDULIKKUSEGA KAASNEVATE NEUROKEEMILISTE NING KÄITUMUSLIKE MUUTUSTE UURIMUS UNVERRICHT-LUNDBORGI TÜÜPI PROGRESSERUVA MÜOKLOONILISE EPILEPSIA LOOMMUDELIS

Unverricht-Lundborgi tüüpi progresseeruv müoklooniline epilepsia (EPM1, OMIM254800) on harvaesinev autosomaalne retsessiivne neuroloogiline haigus. EPM1 haigusjuhte on kirjeldatud kogu maailmas, kuid sagedamini esineb seda epilepsia vormi Vahemere ning Läänemere piirkonnas. Unverricht-Lundborgi haigus avaldub lapsepõlves (6.–15. eluaastani) stiimulile tundlike müokloonuste ja/või generaliseerunud toonilis-klooniliste krampidega. Haiguse süvenedes lisanduvad ataksia ning aeglane intellekti langus. Histopatoloogilised uuringud näitavad EPM1 haigetel laiaulatuslikke degeneratiivseid muutusi ajukoos, ajutüves ning väikeajus. Peamine haigust põhjustav mutatsioon on dodekameerse (12-lülilise) korduse kasv tsüstatiin B (CSTB) valku kodeeriva geeni promootoralas. CSTB on üks tsüstatiinidest, mis arvatavalt kaitsevad rakke valkude endogeense proteolüüsi eest, inhibeerides mitmeid katepsiinide perekonda kuuluvaid lüsoomaalseid tsüsteiini proteaase. Sarnaselt EPM1 haigetega kujunevad CSTB geeni puudulikkusega hiirtel (*Cstb*–/–) välja haigusele iseloomulikud müokloonused, progresseeruv ataksia ning neurodegeneratiivsed muutused väikeajus ja suurajukoos. Siiani on selgusetu, mil viisil CSTB puudulikkus raku tasandil viib müokloonuste ja krampide avaldumiseni EPM1 haiguspildis. Üha enam arvatakse, et esmane CSTB puudulikkus, soodustades neuronite suremist spetsiifilistes ajupiirkondades, vallandab omakorda rea sekundaarseid protsesse, mis on vastutavad EPM1-le iseloomuliku fenotüübi kujunemisel. Mitmed uuringud on näidatud, et neuronaalse atroofiaga kaasneb nii EPM1 haigete kui *Cstb*–/– hiirte ajus märkimisväärne astrogliosis ning mikroglia aktivatsioon. Astro- ja mikroglia peetakse oluliseks neurokeemiliselt aktiivsete ainete allikaks, millede vabanemine võib indutseerida neuronaalset rakusurma või osaleda krampide tekkes. Aminohappe trüptofaani metabolismeerumisel ajus vabanevad kinureniinid ning indoolühendid on just seetõttu kujunenud intensiivselt uuritavaks ainete rühmaks. Kinoliin- ja kinureniinhape on teadaolevalt ainukesed endogeensed ühendid, mis on võimelised selektiivselt mõjutama erutusmediaatorite suhtes tundlikke *N*-metüül-*D*-aspartaadi (NMDA) retseptoreid. KNS-s allub mõlema ühendi süntees rangele füsioloogilisele kontrollile, sõltudes immuunoloogilistest faktoritest ning raku tüübist (astrotsüüdid vs mikroglia).

Töö eesmärgid

Valideerida kõrgefektiivne vedelikkromatograafiline meetod elektrokeemilise jada detekteerimisega (HPLC–EC), mis võimaldaks selektiivselt samast bioloogilisest proovist korraga analüüsida trüptofaani kahe (kinureniini ja serotoniini) metabolismiraja komponente.

Uurida, kas CSTB puudulikkusega kaasnevad muutused trüptofaani metaboliitide sisalduses EPM1 haigete veres ning CSTB geeni puudulikkusega hiirte veres ja ajus. Samuti kirjeldada täiendavalt *Cstb*–/– hiirte fenotüüpi.

Selgitada võimalikke muutusi erutus(glutamaat)- ja pidurdus(GABA)närvingetes CSTB geeni puudulikkusega hiirte ajus.

Uurida, kas osaline CSTB puudulikkus kutsub esile EPM1-le iseloomuliku haiguse fenotüübi heterosügootsetel (*Cstb*+/-) CSTB geeni puudulikkusega hiirtel.

Töö tulemused ja järeldused

Kolmeteistkümne struktuurilt ja füsikokeemiliselt väga sarnase ühendi kromatograafiline lahutamine saavutati liikuva faasi pH ning ionpaarreagendi tüübi ja sisalduse varieerimisega. Selline lähenemine võimaldas selektiivselt mõjutada trüptofaani metaboliitide retentsiooni lähtuvalt nende happelis-aluselistest omadustest ning hinnata võimalike endogeensete ainete segavat mõju. Proovi komponentide usaldusväärseks detekteerimiseks analüüsiti kõikide ühendite voolu-pinge sõltuvuskõveraid, et valida sobivaimad detektori elektroodidele rakendatavad potentsiaalid. HPLC–EC meetodi valideerimise tulemused näitasid, et trüptofaani kinureniini ja serotoniini metabolismiraja komponente on võimalik kvantifitseerida samaaegselt ühest proovimaatriksist.

EPM1 haigetel on vereseerumis langenud trüptofaani kontsentratsioon samas kui homosügootsetel CSTB geeni kahjustusega hiirtel on trüptofaani tase võrreldes metsiktüüpi isenditega muutumatu. Need tulemused kinnitavad hüpoteesi, et trüptofaani sisalduse langus EPM1 haigete veres on tõenäoliselt antiepileptilisest ravist tingitud sekundaarne efekt, mis esineb CSTB puudulikkusest sõltumatult. Siiski, CSTB puudulikkus põhjustab nii EPM1 patsientide kui *Cstb*–/– hiirte veres olulise languse indoolühendite ning kinoliinhappe vahetu eellasühendi, 3-hüdroksüantraniilhappe sisalduses. EPM1-le iseloomuliku sümptomaatikaga hiirte aju neurokeemilistest uuringutest selgus, et oluliselt on tõusnud trüptofaani metabolismi kinureniini ning serotoniini metabolismirajas suurajukoores ja väikeajus. Trüptofaani metabolismi aktivatsioon neis ajupiirkondades võib mõjutada EPM1-le iseloomuliku fenotüübi väljakujunemist *Cstb*–/– hiirtel.

Neurokeemilised ning geeniekspressiooni uuringud näitasid, et GABA-ergiline süsteem on *Cstb*–/– hiirte väikeajus suhteliselt hästi säilinud. Samas

mõjutab CSTB geeni väljalülitamine oluliselt glutamaatergilist süsteemi homosügootsete hiirte väikeajus. Need tulemused on heas kooskõlas varasemate histoloogiliste uuringutega, mis näitasid, et CSTB puudulikkusega hiirte väikeajus degenerereeruvad selektiivselt glutamaatergilised granulaarrakud. Võib oletada, et erutus (glutamaat)- ja pidurdus(GABA)närviringete omavahelise tasakaalu häirumine *Cstb*^{-/-} hiirte väikeajus võib osaliselt soodustada EPM1-le iseloomuliku tasakaalu- ja koordinatsioonihäire avaldumist CSTB puudulikkusega hiirtel.

Sarnaselt homosügootsetele CSTB puudulikkusega hiirtele kujuneb ka heterosügootsetel hiirtel välja EPM1-le iseloomulik fenotüüp. *Cstb*^{+/-} hiirtel on oluliselt langenud sooritusvõime rotaroodi ja võrel rippumise testis ning sensorsete stiimulite mõjul vallanduvad neil müokloonused. Osaline (50%-ne) CSTB valgu ekspressiooni langus on piisav, et esile kutsuda neurodegeneratiivseid muutusi 17 kuu vanuste *Cstb*^{+/-} hiirte väikeajus ning suurajukoores.

ACKNOWLEDGEMENTS

This study was carried out at the Department of Pharmacology, University of Tartu and was funded by grants from Estonian Science Foundation and European Union 5th Framework Program.

I would like to express my deepest gratitude to everyone who have helped me or have contributed to my thesis during these years.

In particular, my sincere thanks to:

My supervisor Professor Aleksander Zharkovsky, for guiding me through this thesis project and for his never-failing enthusiasm. Thank you for allowing me to work independently for such a long time.

My co-supervisor Dr. Allen Kaasik, for his constant support and willingness to teach, especially, for providing me the opportunity to educate myself in RT-PCR methodology as well as French spirit.

My former supervisor Dr. Ants Kask, who first opened the door and introduced me to the fascinating field of neurosciences.

All my colleagues at the Department of Pharmacology for their help and kindness and for friendly atmosphere.

All my companions at the neuroschool, especially Maarika, who made the 1st year studies so enjoyable with her spicy humor and inspiring conversations.

Küll, Kersti and Kristina, thank you for your friendship. I haven't ever succeeded without our joint gourmet dinners where we could discuss our fascination and frustration with science and life as well as for all other adventurous activities throughout these years for keeping the body and mind open to the pleasures of life.

My deepest gratitude and respect goes to:

My parents Aini and Otu, for creating an open and mental atmosphere in my childhood home and for their continuous support, encouragement and infinite belief in me during these long years.

My dear children, Annette and Gustav, for their sincere love and patience, for keeping me in contact with simple everyday pleasures and putting things into perspective.

And last but not least, I am most beholden to my friend and soul mate Gert for his love and understanding. This thesis would have never been completed without your firm support.

PUBLICATIONS

Vaarmann A, Kask A, Mäeorg U. (2002) Novel and sensitive high-performance liquid chromatographic method based on electrochemical coulometric array detection for simultaneous determination of catecholamines, kynurenine and indole derivatives of tryptophan. *Journal of Chromatography B Analyt Technol Biomed Life Sci.* 769:145–153.

Arbatova J, D'Amato E, **Vaarmann A**, Zharkovsky A, Reeben M. (2005)
Reduced serotonin and 3-hydroxyanthranilic acid levels in serum
of cystatin B-deficient mice, a model system for progressive
myoclonus epilepsy. *Epilepsia*. 46 (Suppl 5):49–51.

Vaarmann A, Kaasik A, Zharkovsky A. (2006)
Altered tryptophan metabolism in the brain
of cystatin B-deficient mice: a model system
for progressive myoclonus epilepsy.
Epilepsia. 47(10):1650–1654.

Kaasik A, Kuum M, Aonurm A, Kalda A, **Vaarmann A**, Zharkovsky A.
(2007) Seizures, ataxia and neuronal loss in aged cystatin
B heterozygous mice. *Epilepsia*. 48:752–757.

V

Vaarmann A, Kruve A, Zharkovsky A. (2007) Vesicular glutamate transporter expression levels and glutamate content are altered in the brain of cystatin B-deficient mice. *Manuscript submitted to Epilepsy Research.*

Vesicular glutamate transporter expression levels and glutamate content are altered in the cerebellum of *cystatin B*-deficient mice

Annika Vaarmann^a, Anneli Kruve^b and Alexander Zharkovsky^{a*}

^aDepartment of Pharmacology, University of Tartu, Ravila 19, 51014 Tartu, ESTONIA

^bDepartment of Chemistry, University of Tartu, Jakobi 2, 51014 Tartu, ESTONIA

Corresponding author:

Prof. A. Zharkovsky

Department of Pharmacology

University of Tartu

Ravila 19

Tartu 51014

ESTONIA

Fax +372 737 4352

Phone +372 737 4351

aleksander.zarkovski@ut.ee

Keywords: EPM1; cystatin B; ataxia; glutamate; GABA; GAD65; RT-PCR

ABSTRACT

Progressive myoclonus epilepsy of the Unverricht–Lundborg type is a rare disorder associated with mutations in gene encoding the cystatin B, an inhibitor of cysteine proteases. Cystatin B knockout mice share phenotype with human disease demonstrating similarly the myoclonic seizures, progressive ataxia and neuronal atrophy in hippocampus and cerebellum. We used liquid chromatographic and real time PCR techniques to determine whether glutamate and GABA content as well as vesicular glutamate transporter 1, vesicular GABA transporter 1 and glutamic acid decarboxylase (GAD65) gene expression levels are disturbed in mutant mice brain. We found the significant decrease in glutamate content and vesicular glutamate transporter 1 gene expression levels as well as the increase in GAD65 expression levels while the GABA transporter gene and GABA concentrations remain unchanged in

cerebellum of cystatin B deficient mice. These results demonstrate that primary loss of excitatory granule cells in the cerebellum of cystatin B knockout mice may induce impairment in cerebral excitatory/inhibitory circuits, which may underlie in the progression of ataxia phenotype in cystatin B deficient mice.

1. INTRODUCTION

Cystatin B deficient mice (*Cstb*^{-/-}) represent a genetic model of Unverricht–Lundborg disease, a progressive myoclonus epilepsy type 1 (EPM1, OMIM #254800). EPM1 is characterized by tonic-clonic seizures, stimulus sensitive myoclonus starting early in adolescents, followed by progressive ataxia, and slow deterioration of cognitive functions (Koskiniemi et al., 1974). In most patients, the disease is caused by expansions of a dodecamer repeat in the cystatin B (*Cstb*) gene promoter region (Laloti et al., 1997; Virtaneva et al 1997; Pennacchio et al., 1996). Mutation probably prevents proper transcription of locus by increasing the distance between the transcription factor binding sites and the transcription initiation site thereby reducing or terminating the protein translation. *Cstb* acts as an intracellular inhibitor of cysteine proteases and are likely to protect the cells from endogenous proteolysis (Barrett, 1986; Turk and Bode, 1991). Despite the numerous studies about *Cstb* functions in neuronal homeostasis or cell death mechanisms (Lieuallen et al., 2001; Shannon et al., 2002; Houseweart et al., 2003), still the linkage of *Cstb* deficiency on the molecular level to EPM1 phenotype remains unclear. *Cstb*^{-/-} mice own a number of similarities to the phenotype of EPM1 in humans including myoclonic seizures, progressive ataxia, and incoordination (Pennacchio et al., 1998). Histological studies have revealed neuronal loss in cerebellar granule cell layer, in hippocampal formation and cerebellar atrophy in these mice (Pennacchio et al., 1998; Shannon et al., 2002). These findings are in line with studies in EPM1 patients brains, where cerebral atrophy as well as significant loss in cerebellar hemispheres and Purkinje cells have been described (Haltia et al., 1969; Mascalchi et al., 2002).

The cerebellum plays an important role in controlling motor coordination, body movement and posture. The Purkinje cells, having central role within cerebellar neural circuits and networks, mediate highly coordinated excitatory and inhibitory signals concerned with the temporal organization of movement execution and motor coordination (Voogd and Glickstein, 1998). Cerebellar Purkinje neurons receive their excitatory input from parallel fibers of glutamatergic granule cells or from climbing fiber of the inferior olivary nuclei, and they form single output modulated by GABAergic inhibition system to the deep cerebellar nuclei (DCN) (Sotelo and Alvarado-Mallart, 1991; Aizenman and Linden, 1999). The deficit of glutamatergic neurotransmission induces impairment of motor coordination demonstrating that the granule cell

glutamatergic neurotransmission is critical in controlling motor coordination (Yamamoto et al., 2003). It is hypothesised, that the development of cerebellar ataxia due to the extensive neuronal degeneration in cerebellum leads to the impaired balance between excitatory and inhibitory modulation of Purkinje neuron system (Raman et al., 2000; Grusser-Cornehls and Baurle, 2001).

The aim of our study was to elucidate whether neuronal loss seen in the brain of *Cstb*^{-/-} mice results in the impairment of the glutamatergic and GABAergic neurotransmission. The vesicular glutamate transporter 1 (vGLT1) has been demonstrated to define the glutamatergic phenotype of neurons (Bellocchio et al., 2000; Takamori et al., 2000) whereas vesicular GABA transporter 1 (vGABAT1) as well as the glutamate decarboxylase (GAD65), an enzyme catalysing the production of GABA from glutamate on the vesicular membrane (Kaufman et al., 1991; McIntire et al., 1997) define GABAergic phenotype. Therefore, we assessed the expression of these transporters and GAD65 genes in *Cstb*^{-/-} mice brain by using the quantitative RT-PCR as well as the glutamate and GABA content in *Cstb*^{-/-} mice brain.

2. MATERIALS AND METHODS

2.1. Animals

All the experiments were performed in accordance with the guidelines established in the Principles of Laboratory Animal Care (directive 86/609/EEC) and conformed to local guidelines on the ethical use of animals. The wild type mice (*Cstb*^{+/+}) and mice heterozygous for a disruption in the *Cstb* gene were purchased from The Jackson Laboratory (129SvJ strain, USA) and were further crossed to generate homozygous (*Cstb*^{-/-}) mice in our animal facility. All animals were allowed free access to food and water and were housed in a temperature- and light-controlled environment (12 h light-dark cycles). Eight male 5-month-old *Cstb*^{-/-} mice and six age and sex matched *Cstb*^{+/+} mice were used for study. After decapitation brains were dissected to cerebellum and cerebrum. The left and right hemisphere from both sections was distributed randomly between groups in order to obtain material for gene expression and biochemical studies. Tissue was quickly placed in liquid nitrogen and stored at -80°C.

2.2. Chemicals

All standards and reagents were of analytical grade and purchased from Sigma-Aldrich (MO, USA). HPLC grade methanol (MeOH) was obtained from Merck (Darmstadt, Germany). The ultrapure water for HPLC study was prepared with MilliQ (Millipore Corporation, Milford, MA, USA) water purification system.

2.3. Quantitative RT-PCR

Total mRNA was isolated from frozen tissue samples (50–200 mg) using the TRIzol reagent technique according to the manufacturer's instructions (Invitrogen, Cergy Pontoise, France). Oligo-dT first-strand cDNA was synthesized from 2 µg of total RNA using Superscript II reverse transcriptase (Invitrogen).

For quantitative real-time PCR (qPCR) studies ABI PRISM 7700 Sequence Detection System equipment (PE Applied Biosystems, USA) and ABI PRISM 7000 SDS Software were used. Primers for mouse vGABAT1, GAD65 and vGLT1 (Table 1) were designed using the Primer Express™ software (PE Applied Biosystems, USA). PCR amplification was performed in a total reaction volume of 20 µL in 4 parallels. The reaction mixture consisted of 5 µL diluted template, 10 µL 2x Master SYBR Green PCR Master Mix (PE Applied Biosystems, USA), and 0.5µM forward and reverse primers. Amplification specificity was controlled by a melting curve analysis and a gel electrophoresis of the PCR product. Six fold serial dilution from one wild type sample total RNA were analyzed for each target gene and allowed to construct linear standard curves from which the concentrations of the test sample and efficiency of PCR reaction were calculated. Results were normalized to cyclophilin A (CycA) transcription to compensate for variation in input RNA amounts.

Table 1. Sequences of primers used for qRT-PCR studies

Target gene		Primer sequences	PCR product size (bp)
vGABAT1	Forward	5'- GGA GAC ATT CAT TAT CAG CG -3'	220
	Reverse	5'- AAG ATG ATG AGG AAC AAC CC -3'	
GAD65	Forward	5'- GCC TTA GGG ATT GGA ACA GA -3'	176
	Reverse	5'- GCC AAG AGA GGA TCA AAA GC-3'	
vGLT1	Forward	5'- CTG CTT GTG AGT GGC TTC AT -3'	248
	Reverse	5'-ATA ATG GCC CAG AGT GGA AG -3'	
CycA	Forward	5'- GAG CAC TGG GGA GAA AGG AT-3'	259
	Reverse	5'- CTT GCC ATC CAG CCA CTC AG-3'	

vGABAT1 – vesicular GABA transporter 1; vGLT1 – vesicular glutamate transporter 1; GAD65 – glutamate decarboxylase, 65kDa; CycA – cyclophilin A

2.4. Biochemical studies

Glu and GABA content were assayed by HPLC with fluorescence detection. The mouse brain tissues were homogenized with Bandelin Sonoplus ultrasonic homogenizer (Bandelin Electronic, Germany) in ice cold solution of 0.1 M perchloric acid (1:5, w/v) for 15s. The homogenate was then centrifuged at 13000g for 15 min at 4°C. For pre-column derivatization 50 µl of o-phthalaldehyde (OPA)-mercaptoethanol reagent was added to 50 µl of sample. The chromatography system consisted of a quaternary pump (Perkin Elmer Series 200, USA) equipped with an in-line degassing unit (Jour X-act Degasse, Jour Research, USA), autosampler (Perkin Elmer Series 200, USA) and fixed wavelength fluorescence detector (CMA/280, USA). The chromatographic separation was achieved on reversed-phase C₁₈ column (4.6x50 mm, particle size 3.5 µm; Agilent Zorbax SB-C18, USA) protected by C₁₈ pre-column (7.5x4.6 mm, particle size 5 µm; Alltech, USA) at room temperature. 10 µl of the derivatized sample was injected into the column. The separation was performed in gradient elution mode combining the methanol (MeOH) and acetic buffer (0.1M, pH=6.90). The gradient started with mobile phase composition: 15% of methanol and 85% buffer. MeOH content was then elevated to 30% in 1.5 min and kept like this for 10 min. Thereafter methanol fraction was raised to 33% within 3 min. Finally, the MeOH content was increased to 100% within 1 min and the column was eluted with methanol for 0.5min. Altogether the program last 16 min. Excitation wavelength was between 330 and 365 nm and detection wavelength between 440 and 530 nm. For data analyses Kromex 32S (Akrom-EX OÜ, Estonia) software was used.

3. RESULTS

Real-time quantitative PCR analysis revealed a significant reduction (2.4 fold) in vGLT1 gene expression in the cerebellar tissue of *Cstb*^{-/-} mice (Fig.1 A) as compared to wild type animals, while the vGABAT1 transcription levels remained unchanged. The changes in the vGLT1 transcript were accompanied by reduced levels of Glu in cerebellum. By contrast, the cerebellar GAD65 expression was elevated 1.4 times. No changes in the cerebellar GABA levels of *Cstb*^{-/-} mice, however was observed (Fig. 2A).

The trend toward the reduction of vGABAT1 and vGLT1 transcript levels in *Cstb*^{-/-} mice cerebrum (Fig.1 B) was observed; however these declines did not reach the statistical significance. As illustrated on Fig.2, the concentrations of glutamate and GABA were significantly reduced in *Cstb*-deficient mice cerebrum compared to those of control mice.

4. DISCUSSION

Our results demonstrate reduced level of glutamate and decreased expression of vesicular glutamate transporter in the cerebellum of *Cstb*^{-/-} mice. In addition, an enhanced expression of GAD65 gene without any changes in the levels of GABA was detected in the cerebellum of mutant mice.

Observed decrease in vGLT1 expression levels and glutamate content in mutant mice cerebellum fits well with histological findings reported earlier, where selective loss of excitatory granule cells in cerebellum of *Cstb*^{-/-} mice have been demonstrated (Shannon et al, 2002). Our data are also consistent with recent experiment, where impairment in motor coordination was attained by inducing the reversible deficit of glutamatergic neurotransmission in mice cerebellum (Yamamoto et al., 2003), and suggest that excitatory activity of the granule cell is critical in controlling motor coordination. Similarly, a reduced glutamate or glutamate-immunolabelled cell numbers have been described in the cerebellum of various mouse models of cerebellar ataxia like *Purkinje cell degeneration* mutants, *lurcher* and *weaver* mutants (McBride and Ghetti, 1988; Grusser-Cornehls and Baurle, 2001; Sultan et al., 2002). Although different neuronal populations are affected in these neurodegenerative diseases the final outcome results in disturbances of excitatory/inhibitory circuits. Thus, in *Purkinje cell degeneration* and *lurcher* mutants virtually all Purkinje cells are being destroyed (Mullen et al., 1976; Swisher and Wilson, 1977), proposing that the excitability of deep cerebellar nuclei is altered in response to deterioration of Purkinje input. In *weaver* mutants, similarly to *Cstb*^{-/-} mice, the vast majority of granule cells are lost (Rakic and Sidman, 1973), suggesting the diminished excitatory modulation of Purkinje cell activity. However, our data concerning unchanged GABA content and vGABAT1 gene expression levels propose that inhibitory GABAergic circuits are relatively conserved in cerebellum of *Cstb*^{-/-} mice. Additionally, we observed increase in expression of GAD65 gene, which product glutamate decarboxylase mediates the GABA synthesis from glutamate in GABAergic nerve endings. The augmentation in GAD65 mRNA levels may be regarded as a compensatory reaction directed toward the maintenance of functional GABA levels in the conditions where glutamate pool in *Cstb*-deficient mice cerebellum is diminished.

The signs of alterations in the excitatory and inhibitory neurotransmission were also found in the cerebrum of *Cstb*^{-/-} mice. Both, the GABA and glutamate levels were diminished in the cerebrum of *Cstb*^{-/-} mice and although being nonsignificant, a trend toward a reduction in the expression levels of vGLT1 and vGABAT1 were observed in the cerebrum as well. Recently, Franceschetti *et al.* (2007) demonstrated that density of GABA-immunoreactive cells is reduced in the hippocampus of *Cstb*^{-/-} mice proposing the impairment in GABAergic inhibition in mutant mice brain. Our data concerning the decreased GABA content in *Cstb*-deficient mice cerebrum

partly support the view of failed inhibitory activity of mutant mice. The parallel decrease in the levels of excitatory neurotransmitter glutamate in brain of *Cstb*^{-/-} mice, however, does not allow us to make any conclusion about a possible alterations in excitatory and inhibitory neurotransmission in the cerebrum of *Cstb*^{-/-} mice.

Taken together, the data reported here demonstrate that *Cstb* deficiency is accompanied with the disturbed glutamatergic and GABAergic activity in the cerebellum of *Cstb*^{-/-} mice, which might contribute to the ataxia phenotype seen in this model of human EPM1.

5. REFERENCES

- Aizenman, C.D., Linden, D.J., 1999. Regulation of the rebound depolarization and spontaneous firing patterns of deep nuclear neurons in slices of rat cerebellum. *J. Neurophysiol.* 82, 1697–1709.
- Barrett, A.J., 1986. The cystatins, a diverse superfamily of cysteine peptidase inhibitors. *Biomed. Biochim. Acta.* 45, 1363–1373.
- Bellocchio, E.E., Reimer, R.J., Freneau, R.T. Jr, Edwards, R.H., 2000. Uptake of glutamate into synaptic vesicles by an inorganic phosphate transporter. *Science* 289, 957–960.
- Franceschetti, S., Sancini, G., Buzzi, A., Zucchini, S., Paradiso, B., Magnaghi, G., Frassoni, C., Chikhladze, M., Avanzini, G., Simonato, M., 2007. A pathogenetic hypothesis of Unverricht-Lundborg disease onset and progression. *Neurobiol. Dis.* 25, 675–685.
- Grusser-Cornehls, U., Baurle, J., 2001. Mutant mice as a model for cerebellar ataxia. *Prog. Neurobiol.* 63, 489–540.
- Haltia, M., Kristensson, K. Sourander, P., 1969. Neuropathological studies in three Scandinavian cases of progressive myoclonus epilepsy. *Acta Neurol. Scand.* 45, 63–77.
- Houseweart, M.K., Pennacchio, L.A., Vilaythong, A., Peters, C., Noebels, J.L., Myers, R.M., 2003. Cathepsin B but not cathepsins L or S contributes to the pathogenesis of Unverricht-Lundborg progressive myoclonus epilepsy (EPM1). *J. Neurobiol.* 56, 315–327.
- Kaufman, D.L., Houser, C.R., Tobin, A.J., 1991. Two forms of the gamma-aminobutyric acid synthetic enzyme glutamate decarboxylase have distinct intraneuronal distributions and cofactor interactions. *J Neurochem.* 56, 720–723.
- Koskineniemi, M., Donner, M., Majuri, H., Haltia, M., Norio, R., 1974. Progressive myoclonus epilepsy. A clinical and histopathological study. *Acta Neurol. Scand.* 50, 307–332.
- Lalioti, M.D., Mirotsoy, M., Buresi, C., Peitsch, M.C., Rossier, C., Ouazzani, R., Baldy-Moulinier, M., Bottani, A., Malafosse, A., Antonarakis, S.E., 1997. Identification of mutations in cystatin B, the gene responsible for the Unverricht-Lundborg type of progressive myoclonus epilepsy (EPM1). *Am. J. Hum. Genet.* 60, 342–351.

- Lieuallen, K., Pennacchio, L.A., Park, M., Myers, R.M., Lennon, G.G., 2001. Cystatin B-deficient mice have increased expression of apoptosis and glial activation genes. *Hum. Mol. Genet.* 10, 1867–1871.
- Mascalchi, M., Michelucci, R., Cosottini, M., Tessa, C., Lolli, F., Riguzzi, P., Lehesjoki, A.E., Tosetti, M., Villari, N., Tassinari, C.A., 2002. Brainstem involvement in Unverricht-Lundborg disease (EPM1): An MRI and (1)H MRS study. *Neurology* 58, 1686–1689.
- McBride, W.J., Ghetti, B., 1988. Changes in the content of glutamate and GABA in the cerebellar vermis and hemispheres of the Purkinje cell degeneration (pcd) mutant. *Neurochem. Res.* 13, 121–125.
- McIntire, S.L., Reimer, R.J., Schuske, K., Edwards, R.H., Jorgensen, E.M., 1997. Identification and characterization of the vesicular GABA transporter. *Nature* 389, 870–876.
- Mullen, R.J., Eicher, E.M., Sidman, R.L., 1976. Purkinje cell degeneration, a new neurological mutation in the mouse. *P Natl Acad Sci U S A.* 73, 208–212.
- Pennacchio, L.A., Bouley, D.M., Higgins, K.M., Scott, M.P., Noebels, J.L., Myers, R.M., 1998. Progressive ataxia, myoclonic epilepsy and cerebellar apoptosis in cystatin B-deficient mice. *Nat. Genet.* 20, 251–258.
- Pennacchio, L.A., Lehesjoki, A.E., Stone, N.E., Willour, V.L., Virtaneva, K., Miao, J., D'Amato, E., Ramirez, L., Faham, M., Koskiniemi, M., Warrington, J.A., Norio, R., de la Chapelle, A., Cox, D.R., Myers, R.M., 1996. Mutations in the gene encoding cystatin B in progressive myoclonus epilepsy (EPM1). *Science* 271, 1731–1734.
- Rakic, P., Sidman, R.L., 1973. Organization of cerebellar cortex secondary to deficit of granule cells in weaver mutant mice. *J. Comp. Neurol.* 152, 133–161.
- Raman, I.M., Gustafson, A.E., Padgett, D., 2000. Ionic currents and spontaneous firing in neurons isolated from the cerebellar nuclei. *J. Neurosci.* 20, 9004–9016.
- Shannon, P., Pennacchio, L.A., Houseweart, M.K., Minassian, B.A., Myers, R.M., 2002. Neuropathological changes in a mouse model of progressive myoclonus epilepsy: cystatin B deficiency and Unverricht-Lundborg disease. *J. Neuropath. Exp. Neur.* 61, 1085–1091.
- Sotelo, C., Alvarado-Mallart, R.M., 1991. The reconstruction of cerebellar circuits. *Trends Neurosci.* 14, 350–355.
- Sultan, F., König, T., Möck, M., Their, P., 2002. Quantitative organization of neurotransmitters in the deep cerebellar nuclei of the Lurcher mutant. *J. Comp. Neurol.* 452, 311–323.
- Swisher, D.A., Wilson, D.B., 1977. Cerebellar histogenesis in the lurcher (Lc) mutant mouse. *J. Comp. Neurol.* 173, 205–218.
- Takamori, S., Rhee, J.S., Rosenmund, C., Jahn, R., 2000. Identification of a vesicular glutamate transporter that defines a glutamatergic phenotype in neurons. *Nature* 407, 189–194.
- Turk, V., Bode, W., 1991. The cystatins: protein inhibitors of cysteine proteinases. *FEBS Lett.* 285, 213–219.
- Virtaneva, K., Miao, J., Träskelin, A.L., Stone, N., Warrington, J.A., Weissenbach, J., Myers, R.M., Cox, D.R., Sistonen, P., de la Chapelle, A., 1996. Progressive myoclonus epilepsy EPM1 locus maps to a 175-kb interval in distal 21q. *Am. J. Hum. Genet.* 58, 1247–1253.

- Voogd, J., Glickstein, M., 1998. The anatomy of the cerebellum. *Trends Neurosci.* 21, 370–375.
- Yamamoto, M., Wada, N., Kitabatake, Y., Watanabe, D., Anzai, M., Yokoyama, M., Teranishi, Y., Nakanishi, S., 2003. Reversible suppression of glutamatergic neurotransmission of cerebellar granule cells in vivo by genetically manipulated expression of tetanus neurotoxin light chain. *J Neurosci.* 23, 6759–6767.

FIGURES

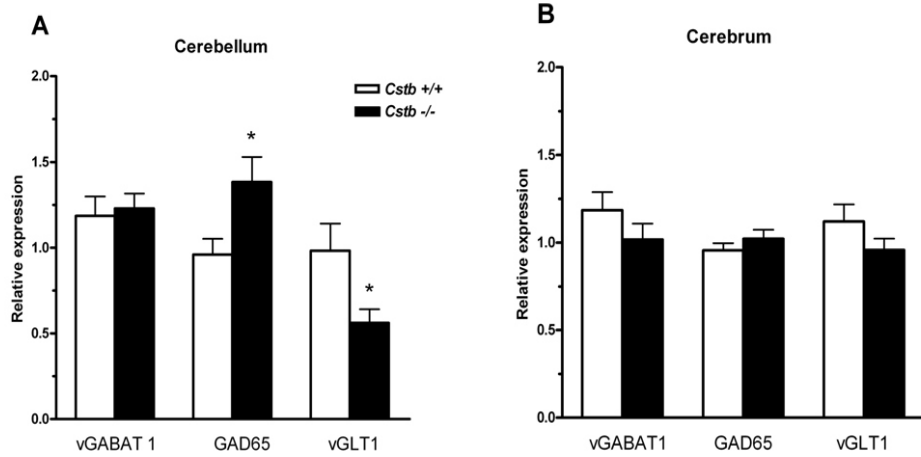


Figure 1. Real-time quantitative RT-PCR analysis of mRNA expression of vesicular GABA transporter 1, glutamic acid decarboxylase 65 kD (GAD65) and vesicular glutamate transporter 1 (vGLT1) in the *Cstb*^{-/-} mice cerebellum (A) and cerebrum (B) compared to control animal. Results are given as means \pm S.E.M. of values normalized to cyclophilin A (CycA) transcription. * $p < 0.05$ (Student's *t* test)

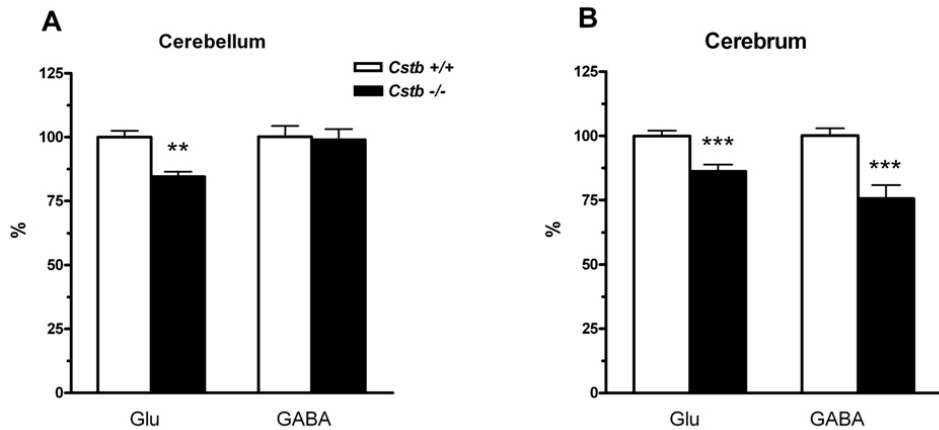


Figure 2. Glutamate (Glu) and GABA content in the *Cstb*^{-/-} cerebellum (A) and cerebrum (B). Results are given in % compared to corresponding control group; mean concentrations \pm S.E.M. of *Cstb*^{+/+} animal group are taken 100%. $P < 0.01$; *** $p < 0.001$ (Student's *t* test)

CURRICULUM VITAE

Annika Vaarmann

Citizenship: Estonian
Date and place of birth: February 3, 1975 in Tallinn, Estonia
Address: Ravila Str 19, 51014, Tartu, Estonia
Phone: +372 737 4354
e-mail: annika.vaarmann@ut.ee

Education

1982–1993 Tallinn Secondary School No 54
1993–1999 University of Tartu, Faculty of Physics and Chemistry, Department of Chemistry, BSc
1999–2001 University of Tartu, Faculty of Physics and Chemistry, Department of Chemistry, Chair of Organic Chemistry, MSc
2003–2007 University of Tartu, Faculty of Medicine, PhD studies in neurosciences

Special courses

2006 – “Behavioral Studies in Drug Research II”, Pühajärve and Tartu, Estonia
2004 – RT-PCR training, Department of Pharmacy, Université Paris-Sud, INSERM U446, France
2004 – QPCR Course, The Centre of Molecular and Clinical Medicine, Faculty of Medicine, University of Tartu, Estonia
2003 – Practical course in Confocal Microscopy, The Centre of Molecular and Clinical Medicine, Faculty of Medicine, University of Tartu, Estonia
2000 – HPLC methods for determination of amino acids, The Department of Physiology and Pharmacology, Karolinska Institutet, Sweden

Honours

2006 Scholarship of Hilda and Harri Mägi Foundation
2006 IBRO CEERC Committee Scholarship

Professional employment

1999–2002 Senior laboratory assistant at the Department of Pharmacology, Faculty of Medicine, Tartu University
2002– Research Fellow at the Department of Pharmacology, Faculty of Medicine, Tartu University

Professional organizations

Estonian Society of Pharmacology

Scientific work

The main scientific interests have focused on the neurochemistry of neurological and psychiatric disorders and processes affecting the neuronal mitochondrial biogenesis. 11 scientific publications.

CURRICULUM VITAE

Annika Vaarmann

Kodakondsus: Eesti
Sünniaeg- ja koht: 3. veebruar 1975, Tallinn
Aadress: Ravila 19, 51014, Tartu
Telefon: +372 737 4354
e-mail: annika.vaarmann@ut.ee

Haridus

1982–1993 Tallinna 54. Keskkool
1993–1999 Tartu Ülikool, Füüsika-keemiateaduskond, keemia eriala, BSc
1999–2001 Tartu Ülikool, Füüsika-keemiateaduskond, orgaanilise keemia õppetool, MSc
2003–2007 Tartu Ülikool, Arstiteaduskond, neuroteaduste doktoriõpe, doktorant

Erialane enesetäiendus

2006 – “Behavioral Studies in Drug Research II”, Pühajärve ja Tartu
2004 – RT-PCR koolitus, Lõuna-Pariisi Ülikooli Farmaatsia teaduskond, INSERM labor U446, Prantsusmaa
2004 – QPCR kursus, Molekulaarse ja Kliinilise Meditsiini Tippkeskus, Tartu
2003 – Practical course in Confocal Microscopy, Molekulaarse ja Kliinilise Meditsiini Tippkeskus, Tartu
2000 – HPLC meetodika koolitus aminohapete määramiseks mikrodialüsaatidest, Füsioloogia ja farmakoloogia osakond, Karolinska Instituut, Rootsi

Tunnustused

2006 Hilda ja Harri Mägi stipendium
2006 IBRO CEERC Committee Stipend

Erialaorganisatsioonid

Eesti Farmakoloogia Seltsi liige

Teenistuskäik

1999 – 2002 Tartu Ülikool, Farmakoloogia instituut, vanemlaborant
alates 2002 Tartu Ülikool, Farmakoloogia instituut, farmakoloogia teadur

Teadustöö

Teadustöö on seotud afektiivsete häirete ning neurodegeneratiivsete haiguste neurokeemilise iseloomustamise, farmakonide toimemehhanismide selgitamise ning mitokondrite biogeneesi mõjutavate protsesside uurimisega. Rahvusvahelise levikuga eelretsenseeritavates väljaannetes on ilmunud 11 publikatsiooni.

DISSERTATIONES NEUROSCIENTIAE UNIVERSITATIS TARTUENSIS

1. **Sirli Raud.** Cholecystokinin₂ receptor deficient mice: changes in function of GABA-ergic system. Tartu, 2005.
2. **Kati Koido.** Single-nucleotide polymorphism profiling of 22 candidate genes in mood and anxiety disorders. Tartu, 2005.
3. **Dzhamilja Safiulina.** The studies of mitochondria in cultured cerebellar granule neurons: characterization of mitochondrial function, volume homeostasis and interaction with neurosteroids. Tartu, 2006.
4. **Tarmo Areda.** Behavioural and neurogenetic study of mechanisms related to cat odour induced anxiety in rodents. Tartu, 2006.
5. **Aleksei Nelovkov.** Behavioural and neurogenetic study of molecular mechanisms involved in regulation of exploratory behaviour in rodents. Tartu, 2006.